Effect of Specimen Size and Shape on Strength of Concrete

Niloufar Zabihi

Submitted to the
Institute of Graduate Studies and Research
In Partial Fulfilment of the Requirements for the Degree of

Master of Science
in
Civil Engineering

Eastern Mediterranean University
January 2012
Gazimağusa, North Cyprus

Approval of the Institute of Graduate Studies and Research

Prof. Dr. Elvan Yılmaz
Director

I certify that this thesis satisfies the requirements as a thesis for the degree of Master of Science in Civil Engineering.

Assist. Prof. Dr. Murude Çelikağ
Chair, Department of Civil Engineering

We certify that we have read this thesis and that in our opinion it is fully adequate in scope and quality as a thesis for the degree of Master of Science in Civil Engineering.

Assoc. Prof. Dr. Özgür Eren
Supervisor

Examining Committee

1. Assoc. Prof. Dr. Özgür Eren _____

2. Assist. Prof. Dr. Alireza Rezaei _____

3. Assist. Prof. Dr. Serhan Şensoy _____

ABSTRACT

Testing the mechanical properties (especially compressive strength and tensile strength) of concrete is one of the most crucial stages of construction works. To control the quality of concrete, there are various moulds that are used for casting concrete samples during concreting works according to different standards at different countries. On the other hand, it is known that different shapes and sizes of concrete samples can cause variations in results of compressive strength or splitting tensile strength.

This research concentrated on the effect of specimen sizes and shapes on compressive and splitting tensile strength of concrete, cured at different conditions and tested at both early and late ages. At the end of experimental study, hardened density, non-destructive tests (i.e. rebound hammer and PUNDIT), compressive strength and splitting tensile strength for different curing conditions were performed and some analyses were done to obtain conversion factors and relations among these factors and results.

The results of analyses indicate that for all testing conditions, there is a strong influence of variation of size and shape of the specimens. In some cases, by changing the curing conditions, the change of trend of experimental results was not significant, for example the results of PUNDIT test. However, by changing testing age, there was a strong alteration in the results and their trends.

Keywords: size effect, shape effect, compressive strength, splitting tensile strength, rebound hammer, PUNDIT, curing regime, conversion factors.

ÖZ

Yapı işleri sırasında belirlenmesi gereken en önemli özellikler betonun basınç mukavemeti dayanımı ve yarmada çekme dayanımıdır. Kalite kontrolu için ise alınması gereken numune boyutu ve şekli ise standartlara ve ülkelere göre farklılıklar göstermektedir. Diğer taraftan ise, deneye tabii tutulan numune boyutu ve şekilinin betonun basınç mukavemeti ve yarmada çekme dayanımı sonuçlarında farklılıklar yaratacağı bilinmektedir.

Bu çalışmada esas olarak aynı beton karışımından yapılan farklı numune boyutları ve şekillerinin betonun özelliklerine olan etkileri araştırılmıştır. Bu beton numuneler iki farklı ortamlarda kür (hava, su) edilmiş ve iki değişik yaşlarda (yedi gün, yirmisekiz gün) deneylere tabii tutulmuşlardır.

Yapılan deneylerin sonuçları kullanılarak numuneler arasındaki çevirme katsayıları bulunmuştur (basınç mukavemeti ve yarmada çekme dayanımı için). Bu çalışma sırasında yapılan deneyler ise katı yoğunluk, tahribatsız deney metodu olan beton çekiçi ve PUNDIT, basınç mukavemeti ve yarmada çekme dayanımıdır. Tüm betonlar farklı kür şartlarında bekletılmiş ve iki değişik yaşta deneylere tabii tutulmuşlardır.

Yapılan analizlere göre beton numune şekil ve boyutlarının betonun özellikleri ve numune-boyut değişim katsayıları üzerinde çok etkili olduğu görülmüştür.

Anahtar Kelimeler: boyut etkisi, şekil etkisi, basınç mukavemeti, yarmada çekme dayanımı, beton çekici, PUNDİT, kür rejimi, çevirme katsayısı.

ACKNOWLEDGMENT

I would like to express my profound gratitude to my supervisor Assoc. Prof. Dr. Özgür Eren, for his precious valuable guidance and precious supervision, during this thesis work.

My deep appreciations go to my dear family; mother, father and my dear sister, whom without their support; this step could not be achievable for me.

My appreciations also go to Mr. Ogün Kiliç, for his valuable helps and guides and Mr. Behiç Göksan for his great assist, during the experimental works of this thesis.

To my lovely grandpa and grandma,

for their endless love and encouragement.

To my dear mom, dad and sister,

who have always supported and loved me.

TABLE OF CONTENTS

LIST OF FIGURES

LIST OF TABLES

LIST OF ABBREVIATIONS

PUNDIT…….Ultrasonic Pulse Velocity Test

MPa……Mega Pascal

D10……..……Aggregates with nominal diameter of 10 mm

D14…….…… Aggregates with nominal diameter of 14 mm

D20…….…… Aggregates with nominal diameter of 20 mm

GGBS…….……. Ground Granulated Blast Furnace Slag

OPC……..……Ordinary Portland Cement

BRE……...…Building Research Establishment

SSD…….……Saturated Surface Dry

Chapter 1

INTRODUCTION

1.1 General

Concrete, has become one of the most important construction materials for centuries because of its ability to withstand different loads on structures.

Like other construction materials, for controlling the quality of concrete, there are lots of experiments, each one designated to specify different properties of concrete. Among these experiments, the ones which are designated to evaluate the resistance of concrete against loads are more common.

Compressive strength test and splitting tensile strength test are two of the most important experiments. There are also some other experiments, including rebound hammer and Ultrasonic Pulse Velocity Test (PUNDIT), by which mechanical properties of concrete samples can be determined, without any destruction on concrete samples.

Although all the mentioned experiments are considered to determine different mechanical properties of concrete samples, results can be affected by many factors such as environmental conditions, shape and size of concrete samples.

Many previous studies and experimental investigations have been conducted in order to find out how changing specimen shape and size could influence the results. For example, a formula has been proposed for the size effect indicating that by increasing the specimen size, compressive strength decreases. In addition, there have

been conversion factors that are proposed to convert the compressive strength results of different specimens.

Moreover, previous researches have also examined the effect of curing conditions on conversion factors.

The significance of this study is to determine the conversion factors of concretes cured in air and water at 7 days and 28 days of ages. The conversion factors are obtained for compressive strength and for splitting tensile strengths of three different mix designs. The results of compressive strength, splitting tensile, PUNDIT and rebound hammer tests on the concrete samples were utilized to calculate conversion factors. Totally 225 concrete samples were made and tested.

1.2 Objectives and works done

Objective of this study is to determine the conversion factors for compressive strength and splitting tensile strength among specimens having different shape and sizes. The works done are listed below:

1. As the literature review section, several previous works on this topic were collected and studied. The results have been summarized in literature review section.
2. The required standards of experiments were collected according to the experimental work's plan. Mostly BS-EN and ASTM were used as standards.
3. Experiments of sieve analysis and trial mix designs were performed.
4. Sample of different mix designs were casted and cured according to their predetermined curing conditions and tested at different ages.

1.3 Achievements

The following analyses were done and their respective conclusions were taken from the results of experiments:

1. Hardened density, compressive strength, splitting tensile strength and the results of non-destructive tests of each of the specimens were determined.
2. By means of the above results, comparisons were made between the different results of different specimens.
3. Conversion factors were determined in order to make conversion between different specimens and sizes of concretes.
4. The conversion factors were evaluated for air curing and water curing conditions and three different mix designs separately.
5. Moreover, it was investigated that how by changing concrete mix design, conversion factors change.
6. Stress strain curves had been plotted and the area under the curve was calculated.
7. The calculated area under the curves was compared between different curing conditions, mix designs and different sizes and shapes of the specimens.

1.4 Thesis outline

In chapter 2 (literature review), the previous significant works have been mentioned. Each research has been briefly explained.

Chapter 3 (experimental works) includes complete details about the experiments, which were performed together with their respective standards.

Chapter 4 (results and discussions) contains the results of experiments and the analyses of them. Explanations and discussions about each of them are done, based on the obtained results and the previous achievements of the researchers.

In chapter 5 (conclusions), conclusions of the study are listed briefly.

Chapter 2

LITERATURE REVIEW

Testing of hardened concrete, in order to determine its compressive strength, is one of the most important and necessary experiments performed widely nowadays.

One of the usual methods of the experiments is casting concrete samples and crushing them in laboratory, by using relevant testing machine.

On the other hand, results of the experiment can be affected by diverse factors, such as specimens' sizes, their shapes, the moulds used for casting, curing conditions and rate of load application (Neville, 2002).

Two types of specimens, utilized for testing hardened concrete, are cubes and cylinders which, despite having various differences, both are used widely. While cylindrical specimens (150mm×300mm) are used mostly in Australia, Canada, France, New Zealand and the United States, cube specimens (150 mm and 100 mm) are used mostly in European region including Great Britain and Germany (Elwet & Fu, 1995). Of course, in each region, regarding to the specimens types, there are codes, explaining how to perform the experiment, like British Code test and ASTM.

One of the differences between cylinder and cube specimens is that before being loaded, cylinder specimens need capping. The specimens have to be capped by Sulphur mortar or cement paste in order to have plain loading surfaces. Unlike the cylinders, cubes do not require capping as they are turned over on their sides, when being loaded.

On the other hand, cubes show higher compressive strength that requires higher capacity testing machine and about the cylinders they are tested in the direction of casting, which is considered as an advantage for them (Elwet and Fu, 1995).

Various researches have been conducted previously, to understand and clarify the so-called size and shape effect of concrete specimens on the compressive strength test results. According to Bažant and Planas (1998) , size effect can be seen when by altering the size of a concrete member, its nominal strength also gets changed, even though their shape is similar to each other. The same definition can be proposed for shape effect as well, when nominal strength of concrete members is dependent on their shape.

Apart from the parameter of nominal strength, some other properties also differ in their results, caused by using specimens with different shapes and sizes, properties like cracking or fracture pattern and trends of stress-strain curves.

To overcome the effects of size and shape, conversion factors have been proposed regarding different conditions.

One of the first investigations about size effect was carried out in 1925 by Gonnerman, using standard cubes of 6" and 8" and different sizes of cylinders. Testing different specimens at different ages, the average cylinder/cube ratio of 0.85 to 0.88 was obtained (Gonnerman, 1925; Elwet and Fu, 1995).

Different curing condition's effect on conversion factors (cylinder/cubes) was investigated by Plowman et al. (1974).

Another investigation about shape and size effect on compressive strength of high strength concrete has been carried out, proposing different conversion factors of 0.8 for cylinder 150×300/cube 150mm, 0.93 for cylinder 100×200/cube 150mm and 0.86

for cylinder 150×300/ cylinder 100×200. It was also found out that mix design parameters, also change the strength ratio of cylinder/ cubes (Malaikah, 2009).

Shape and size effect has been also investigated about high-strength concrete, showing that size effect is stronger in cubes than cylinders.

One of the factors, which change the conversion factors, is aggregates grading that shows itself through “wall effect”. This effect indicates that the amount of mortar required to fill the space between concrete’s aggregates is less than the amount of mortar needed to fill the space between aggregates and the mould’s wall (see Figure 2.1) (Neville, 2002).

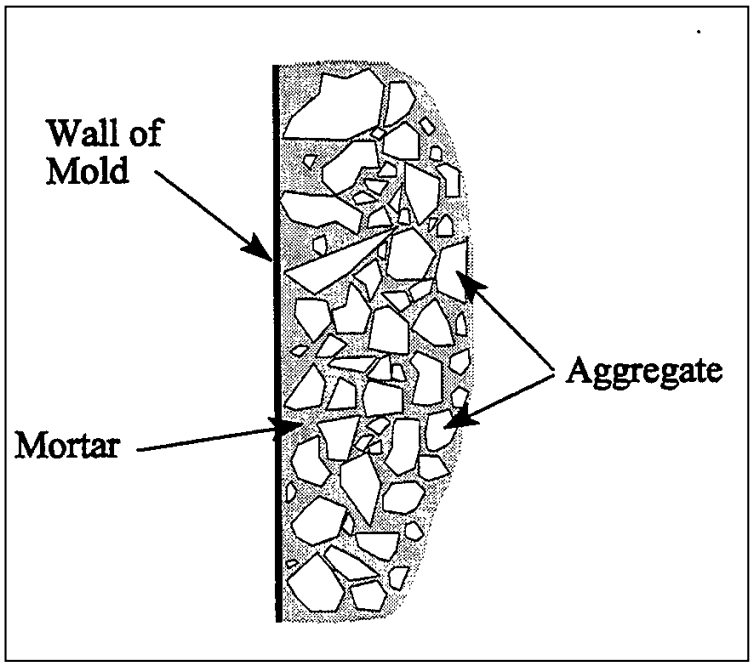

Figure 2.1: Wall effect (Neville, 2002)

The extra mortar between aggregates and wall of moulds causes an increase in compressive strength of specimens. It is also more remarkable in specimens which have larger ratio of surface/ volume and causes changes cylinder/cube conversion factor (Elwet and Fu, 1995; Tokyay and Ozdemir, 1997).

Wall effect has also been vastly investigated. One of the researches was carried out by Zheng and Li (2002). In their research, a three-dimensional model was proposed in order to simulate aggregates density inside of concrete specimens.

The corresponding graph of the model is in a way that by moving from sides to inner zone of a concrete specimen, aggregate's density, firstly has a growing trend up to a specific peak (which is a near-surface section), then after a slight decrease, the density reaches to a constant amount. Also, the peak point of the graphs rises by having more aggregates' fraction.

To eliminate the influence of wall effect, during an investigation, Turkel and Ozkul (2010), sawed concrete specimens from casted specimens. In the research, it was found that size effect is more pronounced in concrete samples of higher compressive strengths, which can be attributed to more brittle characteristics of these grades. Also, it was found that size effect depends on maximum aggregates size of concrete, for both medium and high compressive strengths, in the same manner.

Some studies have been done in order to suggest equations for converting compressive strength of different specimens to each other. For example:

L'Hermite's equation (Neville, 2002):

[1]

Where , is compressive strength of cube in psi.

Another famous law and formula, with regard to size effect, has been proposed by Bažant. The size effect rule briefly explains that by increasing the specimens' size, compressive strength of the specimens of the same mix design decreases. The formula of this law is (Bažant and Planas, 1998):

[2]

In which is the tensile strength of concrete, B and are constants and d is characteristics dimension (size of specimen).

A similar theory has also been proposed by Weinbul (1951). The weakest link theory, states that, larger specimens are more willing to contain defects and anomalies in themselves, which can cause them to fail at lower stresses (Arioz, Ramyar, Tuncan, Tuncan, & Cil, 2007).

On the contrary, according to the summation theory by Tuckers, the strength of a specimen, instead of the least strength particle, is equal to the summation of the strength of each of its individual parts (Arioz, Ramyar, Tuncan, Tuncan, & Cil, 2007).

To sum up, it can be said that the results of different sized concrete specimens, in different situations are governed by different factors, including their different particles' strength and the defects inside of them.

There is also a difference between cubes' and cylinders' fracture patterns. In cylinders a main fracture surface is nucleated, while in cubes lateral sides get broken and that there is destruction due to crushing. This shape effect can also be noticed in $\sigma-\varepsilon$ curves (Del Viso, Carmona, & Ruiz, 2008).

Effect of size and shapes of the specimens have also been investigated about tensile strength of concrete samples (especially on the results of splitting tensile strength test).

During an investigation by Kadleček et al. (2002), the splitting tensile strengths of various concrete samples of cubes, cylinders and prisms were determined. In the research a general function has been proposed, which relates fracture area of each specimen to the specimen's relative splitting tensile strength (depending on a specimen of basic size). The proposed formula is:

[3]

Where, is the relative splitting tensile strength (%) and A is the fracture area (cm^2).

In addition, in another research, it has also been found that up to a specific value, by increasing the specimens' size, splitting tensile strength decreases, but after the point the trend gets deviated from the size effect law trend. The reason of this result can be both, due to not increasing of splitting fracture length by increasing diameter or also due to change of failure mechanism by increasing of specimens' size (Bažant, Kazemi, Hasegawa, & Mazers, 1991).

Chapter 3

EXPERIMENTAL WORK

3.1 Introduction

The main goal of this study is to find out the effect of different factors, on conversion ratios for different concrete specimens' compressive strength. During the experimental study, different concrete specimens of different concrete mix designs were tested at different ages, with different curing conditions.

For casting concrete specimens, GGBS (Ground Granulated Blast Furnace Slag) cement, class of 42.5, was used. Crushed limestone aggregates from Beşparmak Mountains Cyprus (both fine and coarse), potable water and for one concrete mix design, superplasticizer (Glenium) was also utilized.

Before beginning of casting, sieve analysis was done and moisture conditions for all the aggregates were determined (Table 3.1 to Table 3.4).

Table 3.1: Sieve analysis of aggregate with 20 mm maximum size

Sieve (mm)	Weight (kg)	% Retained	Cumulative % retained	Cumulative % Passing
28	0.00	0.00	0.00	100.00
20	0.75	19.04	19.04	80.96
14	2.69	68.27	87.31	12.69
10	0.40	10.15	97.46	2.54
6.3	0.10	2.54	100.00	0.00
5	0.00	0.00	100.00	0.00
3.35	0.00	0.00	100.00	0.00
Pan		0.00	100.00	0.00
	3.94			

Table 3.2: Sieve analysis of aggregate with 14 mm maximum size

Sieve (mm)	Weight (kg)	% Retained	Cumulative % retained	Cumulative % Passing
28	0.00	0.00	0.00	100.00
20	0.05	1.26	1.26	98.74
14	0.30	7.57	8.83	91.17
10	2.39	60.15	68.98	31.02
6.3	1.17	29.51	98.49	1.51
5	0.04	0.88	99.37	0.63
3.35	0.03	0.63	100.00	0.00
Pan	0.00	0.00	100.00	0.00
	3.97			

Table 3.3: Sieve analysis of aggregate with 10 mm maximum size

Sieve (mm)	Weight (kg)	% Retained	Cumulative % retained	Cumulative % Passing
28	0.00	0.00	0.00	100.00
20	0.00	0.00	0.00	100.00
14	0.00	0.00	0.00	100.00
10	0.05	2.01	2.01	97.99
6.3	1.17	47.08	49.09	50.91
5	0.54	21.53	70.62	29.38
3.35	0.49	19.72	90.34	9.66
Pan	0.24	9.66	100.00	0.00
	2.49			

Table 3.4: Sieve analysis of fine aggregates

Sieve (mm)	Weight (g)	% Retained	Cumulative % retained	Cumulative % Passing
4.75	0.00	0.00	0.00	100.00
2.36	140	14.00	14.00	86.00
1.19	310	30.50	44.50	55.50
0.59	220	21.50	66.00	34.00
0.297	130	12.50	78.50	21.50
0.149	90	8.50	87.00	13.00
Pan	130	13.00	100.00	0.00
	1000			

Sieve analysis test's curves are shown in Figure 3.1.

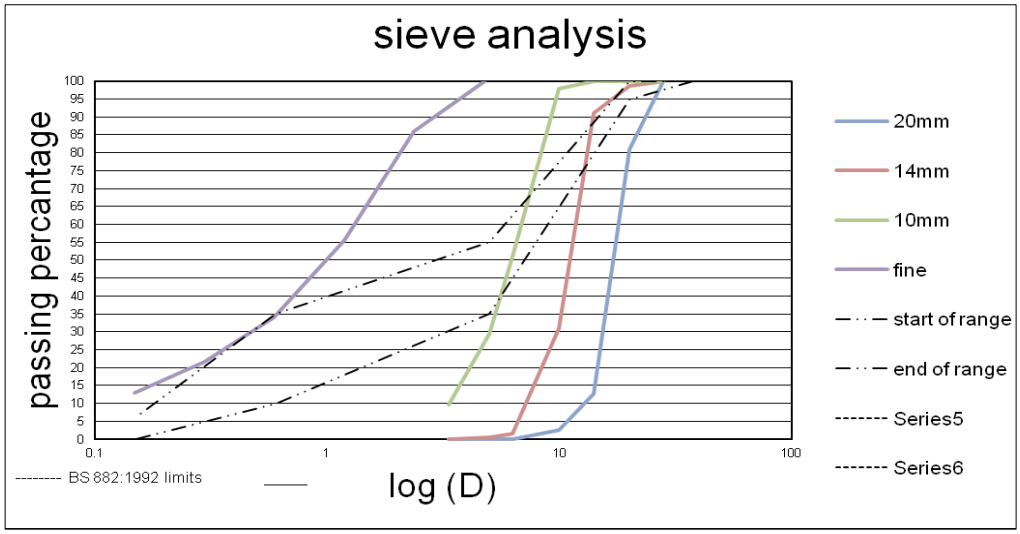

Figure 3.1: Sieve analysis

Three mix designs were chosen for this study. The mix designs were decided to be different in cement content and water/cement ratio.

For each mix design, before casting, trial mix-designs were done in order to make sure that each mix satisfies the requirements. Table 3.5 to Table 3.7 show the proportioning of materials and results of trial mixes for each concrete mix.

Table 3.5: Mix design A

Cement (kg/m^3)	Water (kg/m^3)	Fine aggregates (kg/m^3)	D10 (kg/m^3)	D14 (kg/m^3)	D20 (kg/m^3)
357	225	808	180	270	539

Table 3.6: Mix design B

Cement (kg/m^3)	Water (kg/m^3)	Fine aggregates (kg/m^3)	D10 (kg/m^3)	D14 (kg/m^3)	D20 (kg/m^3)
402	225	815	167	251	501

Table 3.7: Mix design C

Cement (kg/m^3)	Water (kg/m^3)	Fine aggregates (kg/m^3)	D10 (kg/m^3)	D14 (kg/m^3)	D20 (kg/m^3)
486	170	628	212	318	630
superplasticizer: Glenium , 0.6% by weight of cement					

Water to cement ratio of mix design A, B and C are kept constant to be equal to 0.63, 0.56 and 0.35, respectively.

On fresh concrete, for each mix design, test of workability and on hardened concrete, compressive strength tests, and splitting tensile strength test were performed. Also, non-destructive tests, including ultrasonic pulse velocity and rebound hammer tests, were executed.

Two types of curing conditions (water and air) and testing ages (7 and 28 days) were considered for the test specimens.

3.2 Materials used

3.2.1 Cement

For casting all the specimens, GGBS cement with the class of 42.5 was used. Chemical compositions and physical properties of the cement are shown in Table 3.8 and Table 3.9.

Table 3.8: Chemical compositions of GGBS cement

Chemical compositions (%)									Loss on ignition	Insoluble material
SiO_2	Al_2O_3	Fe_2O_3	CaO	MgO	SO_3	Na_2O	K_2O	Cl^-		
39.18	10.18	2.02	32.82	8.52	–	1.14	0.3	–	1	0.88

Table 3.9: Physical properties of GGBS cement

Physical properties of GGBS cement	Specific gravity (g/cm^3)	Fineness: specific surface (cm^2/g)	Fineness (retained on 90 μm sieve)	Fineness (retained on 45 μm sieve)
	2.87	4250	0	0.8

3.2.2 Aggregates

Both coarse and fine aggregates used for this study were crushed limestone. As mentioned before, prior to casting, tests were done to determine the aggregates properties. Sieve analysis results were shown in previous section and in Table 3.10

and Table 3.11. It should be added here that, in the following tables, Fine, D20, D14 and D10 stand for fine aggregates and aggregates with the maximum nominal size of 20 mm, 14 mm and 10 mm, respectively.

Table 3.10: Water absorption of aggregates (SSD based)

Aggregates	Water absorption %
Fine	1.00
D10	1.60
D14	0.94
D20	0.64

Table 3.11: Results of aggregates' specific gravity

aggregates	Bulk specific gravity		Apparent specific gravity
	Dry	SSD	
Fine	2.60	2.66	2.78
D10	2.51	2.54	2.60
D14	2.66	2.68	2.71
D20	2.65	2.67	2.71

3.2.3 Water

Tap water was used for casting all specimens (BS5328: Part 1, 2000).

3.2.4 Glenium

For only one mix design, mix design C, Glenium, manufactured by BASF, was used as the superplasticizing admixture.

Glenium helps in producing concrete mixes with higher strength and more durability (GLENIUM).

3.3 Methodology

Three different concrete mixes were designed according to BRE for designing normal concrete (Teychenné, 1997). Following the method of weight batching, trial mixes were designed, casted and after some repetitions, mix design A, B, and C were accepted (see Table 3.5 to Table 3.7).

3.3.1 Casting concrete

The process of batching, weighting and mixing of necessary materials were performed according to British Standards. By using a pan mixer, first aggregates and cement were mixed for 30 seconds, then water was added to the blended materials and mixed for approximately 3 minutes. When a test on fresh concrete (i.e. slump or vebe time test) had to be performed, necessary sample was taken from fresh concrete, test was executed and then, the utilized amount of concrete was poured back to the source, blended once again to make homogeneous mix and then concrete was poured into the moulds (BS 1881 : Part 125: 1986, 2009).

3.3.2 Compacting and curing

Two types of vibration tables were used in order to vibrate and compact the filled concrete moulds. One was an ordinary vibrating table and another one was the vibrating table on which the concrete moulds could be fixed. The later one was used especially for heavy metal cubic moulds size of 200 mm (see Figure 3.2 and Figure 3.3).

Concrete specimens, were carried to curing room after being casted and compacted, in which the humidity percentage is over 90% and the temperature was kept equal to 21°C. After being kept for approximately 24 hours, the specimens were taken to water tank or air room, regarding to their specified curing conditions, and kept there until their testing age.

Figure 3.2: Vibrating table type I

Figure 3.3: Vibrating table type II

3.4 Tests on fresh concrete

3.4.1 Workability test

The only tests, performed on fresh concrete mixes, were Vebe and slump test. Both of the experiments were performed according to BS EN 12350-3:2009 and BS EN 12350-2:2009, respectively. Figure 3.4 and Figure 3.5 show performance of slump and Vebe tests.

Figure 3.4: Slump test

Figure 3.5: VeBe test

3.5 Tests on hardened concrete

Totally five experiments were carried out on hardened concrete specimens, namely compressive strength, splitting tensile strength, PUNDIT, rebound hammer and density.

3.5.1 Compressive strength

In this research, as concrete specimens were chosen from different sizes and shapes, for executing compressive strength test, different standards were followed. For measurement of compressive strength of cubes, BS EN 12390-3:2009 was used.

Compressive strength test of cylindrical specimens were carried out according to ASTM C39/C39M – 11. Testing cylinders in compressive strength has an additional stage of capping. In Figure 3.6, capped samples of cylinder 150×300 mm are shown.

Loading speed was adjusted to be 0.6 ± 0.2 MPa/s (BS EN 12390-3:2009, 2009). In this investigation, the loading speed was 0.4 MPa/s or sometimes 0.5 MPa/s for all specimens during compressive strength test. It should be mentioned that, some of concrete specimens were also chosen for plotting load-deformation curve, for which the speed of loading had to be 0.05 MPa/s.

Figure 3.6: Capped cylindrical specimens

Figure 3.7, shows the testing machine used for compressive strength test.

Figure 3.7: Compressive strength testing machine

3.5.2 Splitting tensile strength test

Splitting test was also carried out on both cubes and cylinders at the age of 28 days. At the time of testing, specimens were removed from curing tank and a line was drawn on specimens to make sure that the load was applied axially. Specimens were properly placed into the machine to be tested (See Figure 3.8 and Figure 3.9).

Figure 3.8:Cylinder specimen under splitting tension

Figure 3.9: Cubic specimen setup before splitting tension

3.5.3 Determination of concrete density

For density measurement of concrete specimens, BS EN 12390-7, 2009 was followed.

3.5.4 Ultrasonic Pulse Velocity Test (PUNDIT)

Ultrasonic pulse velocity test is one of the non-destructive experiments, performed to estimate compressive strength of concrete specimens.

The experiment's specific equipment determines the travel time of an ultrasonic wave through the concrete specimen between the transmitter and receiver placed on two opposite sides of the sample. By means of the determined travel time, the wave's velocity can be determined (BS 1881 : Part 201, 2009). This test was only done on cubic specimens at the age of 28 days, both for air and water cured samples.

In Figure 3.10, the performance of PUNDIT test is shown.

Figure 3.10: Ultrasonic Pulse Velocity Test (PUNDIT) for a cubic sample

Each time, the relevant equipment had to be calibrated before the test. After that, for each specimen, the center points of 2 opposite sides of cube were spotted. Center points surroundings and the equipment's probe were covered with a greasy material, and then the probes were placed on each side's centers. The number which is shown on the equipment's screen is the travel time of ultrasonic pulse in microseconds.

3.5.5 Rebound hammer test

Rebound hammer or Schmidt hammer test is categorized as surface hardness test. It is another famous non-destructive test, which is performed for estimating concrete specimen's compressive strength. During the process of experiment ten impacts are stroke to the surface of concrete specimen. For each specimen, the test should be repeated about 10 times on the same side (BS 1881 : Part 201, 2009). The performance of rebound hammer test is shown in Figure 3.11.

Results of this test can be affected by some factors including moisture condition of testing surface and cement type.

Figure 3.11: Rebound hammer test

According to ASTM C 805/C 805M (2008), for calculating the true number of rebound hammer through approximately 10 replicates, first the average of all 10 results is calculated, then those replicates, which have more than 6 units of difference with the average amount are discarded. At the next stage, average of the remained replicates is calculated and reported as the specimen's rebound number.

Chapter 4

RESULTS AND DISCUSSIONS

4.1 Introduction

In the previous chapter, the performed experiments were briefly explained. In this chapter, the outcomes of those mentioned experiments will be shown; graphs and findings from analyses will be presented, followed by discussions about each of the results.

The experiments carried out were included slump and Vebe test (for fresh concrete), hardened density, ultrasonic pulse velocity test (PUNDIT), rebound hammer (non-destructive tests on hardened concrete) and finally, compressive strength and splitting tensile strength test (destructive tests on hardened concrete). For each test, results will be presented and discussed.

4.2 Tests on fresh concrete

4.2.1 Slump test and VeBe test

For each mix design, slump and VeBe tests were performed. The results are presented in the tables below.

Table 4.1: Slump and Vebe test results

Mix Design	Workability	
	Slump (cm)	Vebe (s)
A	15.0	2.3
B	6.5	4.3
C	2.0	8.7

The results show that by decreasing water to cement ratio of mix designs, there is a reduction for slump and increase for Vebe time.

Despite the fact that for mix design C, superplasticizer was utilized, the level of workability was still low, which was caused by low water/cement ratio (i.e. 0.35).

For the mix design A, high slump value is in fact due to high water/ cement ratio. Water to cement ratio was chosen to be 0.63 during the process of mix-design. This was probably as a result of the utilized cement's strength grade (i.e. 42.5).

4.3 Experiments on hardened concrete (non-destructive)

4.3.1 Hardened density of concrete

On each mix design, hardened concrete density test was performed according to BS EN 12390-7, 2009 . Table 4.2 shows the average hardened density for each experiment's condition.

Table 4.2: Hardened density test results

Age	Mix Design	Curing Type	Average Density* (kg/m^3)
7 days	A	water	2452
		air	2355
	B	water	2427
		air	2353
	C	water	2510
		air	2453
28 days	A	water	2412
		air	2356
	B	water	2419
		air	2342
	C	water	2500
		air	2444

*This column shows the average density of 15 samples, which had the same age, mix design and curing condition

In Table 4.2, it is clear that the densities of water cured samples are higher than air cured samples. The reason of this observation is that when samples are air cured, the hydration reaction in them ceases, due to lack of moisture. When the hydration is stopped, the production of CSH (calcium silicate hydrate) gel impedes. CSH gel is the main product of cement hydration which provides strength (Safiuddin, Raman, &

Zain, 2007). Consequently, the air-cured samples will have weaker concrete bonds (lower density) and also lower strengths.

Table 4.3: Average density for each mix design

Mix Design	Average Density* (kg/m^3)
A	2394
B	2385
C	2477

*Average density of 30 samples, with the same mix design

It can be noticed that density is slightly increasing by decreasing water/cement ratio for different mix designs.

Although it is negligible but, the hardened density of mix design A is slightly higher than density of mix design B. This could again be due to utilized cement's strength grade, by which even if the water to cement ratio is high in mix A, still strong concrete bond is formed.

4.3.2 Ultrasonic pulse velocity test (PUNDIT)

This test was performed on both air cured and water cured cubic specimens at the age of 28 days. The outcomes of the experiment are given in the following sections.

Table 4.4 shows the results of PUNDIT test for different sizes of cubic specimens.

Table 4.4: PUNDIT results for each size of cubes

Specimen Size (mm)	Mix Design	Velocity (km/s)	Strength (MPa)
cube 100	A	4.67	37.56
	B	3.57	35.26
	C	5.33	53.53
cube 150	A	4.71	38.86
	B	4.44	43.20
	C	5.25	75.37
cube 200	A	4.74	39.32
	B	4.74	47.12
	C	5.30	93.42

In Table 4.4, the columns of velocity and strength are the average of results' values of different curing conditions.

In Figure 4.1, results are shown graphically.

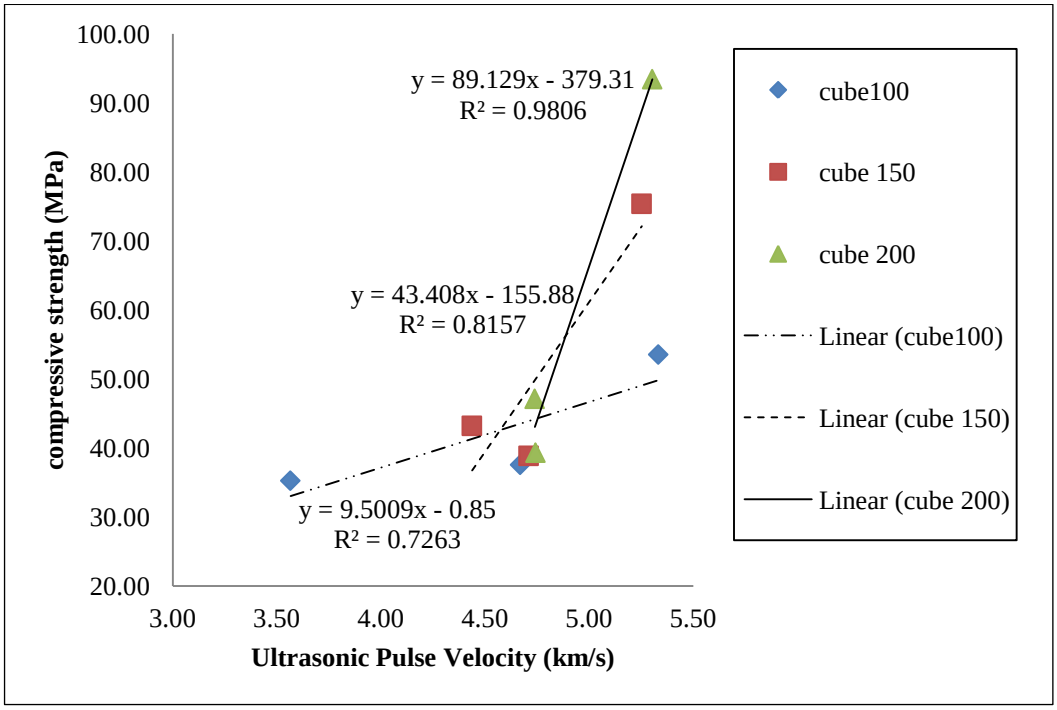

Figure 4.1: Compressive strength versus PUNDIT (the lines are trendlines connecting different strength levels for each specimen)

In Figure 4.1, different trends can be seen among different sized cubic specimens. This difference can be related to size effect, according to which, different

compressive strengths are resulted from different sized specimens. From the figure it is obvious that cubes of 200 mm, which have higher compressive strengths, are accumulated in the region of higher pulse velocities.

It is of interest to note in Figure 4.1 that for samples of cube 200, results of PUNDIT test are almost equal to each other, while for other samples the results are more varied. Also, this variation, increases by decreasing the sample size. This observation can be due to the fact that larger samples are more homogeneous than smaller ones. Being more homogeneous have caused the cubes of 200 to have better and stronger bonds, less scattered and hence, higher PUNDIT results.

As it can be observed, the cubes of 200 mm have higher PUNDIT results, only until the compressive strength of about 45 MPa. Beyond this border, up to approximately 60 MPa, the least amount of PUNDIT results are taken from cube 150, and beyond 60 MPa, cube 200 results in the lowest ultrasonic velocities.

The reason of this observation can be ascribed to two reasons. One could be the fact that as the concrete mix design changes toward stronger bonds, the fraction of coarse aggregates increases steadily. If the small cubes of 100 mm are considered, by increasing the fraction of coarse aggregates, due to smaller size, the density of large aggregates inside of them increases even more than cube 200 (as they are less homogeneous). This fact can increase the probability of passing the ultrasonic pulses through coarse aggregates. Consequently, as the coarse aggregates have more density, the PUNDIT results can get higher in small specimens than large ones. In addition, this observation can also be only a statistical observation.

In this investigation, the maximum aggregate size was kept constant and equal to 20 mm for each mix design, which especially for small moulds' sizes could cause heterogeneity in concrete mix. According to Turkel and Ozkul (2010), when

aggregates size increases, with respect to sample's size, the distribution of aggregates inside of the mould becomes less uniform and decreases the homogeneity of concrete mix.

Table 4.5 and Figure 4.2, show the results of PUNDIT test for different curing conditions of samples.

Table 4.5: Results of PUNDIT test

Curing Type	Mix Design	Velocity (km/s)	Strength (MPa)
Water	A	4.81	41.20
		4.87	42.32
		4.83	42.61
	B	2.47	37.54
		4.12	46.67
		4.88	52.05
	C	5.43	54.47
		5.19	75.81
		5.32	91.90
Air	A	4.53	33.92
		4.55	35.40
		4.65	36.02
	B	4.66	32.97
		4.76	39.74
		4.60	42.20
	C	5.24	52.59
		5.32	74.92
		5.28	94.93

It should be explained that results of PUNDIT test are affected by some factors which can cause errors. For example, in Table 4.5, few results are not in accordance with their relevant strengths; for instance, for compression result of 37.54 MPa, PUNDIT test gave a result of 2.47 km/s. This result could be due to air bubbles or some anomaly particles, which might have probably, exist in the path of ultrasonic pulse.

The following graph shows the relation between compressive strength and the PUNDIT results.

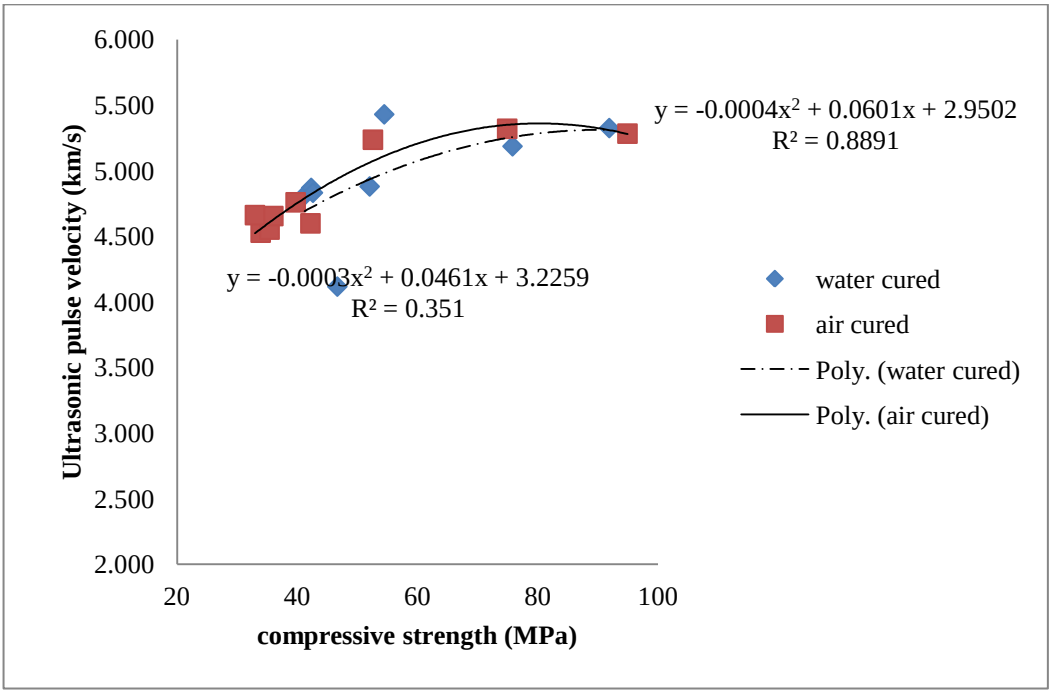

Figure 4.2: PUNDIT versus compressive strength for different curing conditions

Both graphs explicitly indicate that increasing compressive strength causes higher velocity of the ultrasonic pulse velocity through concrete samples.

Also, it is noticeable that the PUNDIT results of air cured samples are more accordant to the proposed model of trend line ($R^2 = 0.889$). This seems to be due to fewer environmental errors.

In above graphs, it can be noticed that the PUNDIT results do not alter significantly among different curing conditions, i.e. both water curing and air curing conditions result in almost the same ultrasonic pulse velocities.

4.3.3 Rebound (Schmidt) hammer test

Like PUNDIT test, rebound hammer test was also performed on both air and water cured and different cubic specimens at the age of 28 days.

The results of this test include graphs of obtained rebound number vs. compressive strength for the cubic specimens. It was tried to propose correlations between two parameters.

According to the utilized equipment's guidebook (Concrete Test Hammer Mod N, Toni Technik), a calibrated linear graph is proposed for concrete mixes made of OPC cement, while in this research, the consumed cement used was GGBS.

The following table shows the Rebound numbers of each specimen separately.

Table 4.6: Rebound Hammer results for each cubic specimen

Specimen Type/ Size (mm)	Mix Design	Rebound Number	Strength (MPa)
cube 100	A	34.41	37.56
	B	34.10	35.26
	C	42.31	53.53
cube 150	A	34.15	38.86
	B	34.68	43.20
	C	42.92	75.37
cube 200	A	34.08	39.32
	B	35.47	47.12
	C	44.42	93.42

It is needed to explain that the stress and rebound number in Table 4.6 are the average of cubic samples for both water and air curing conditions.

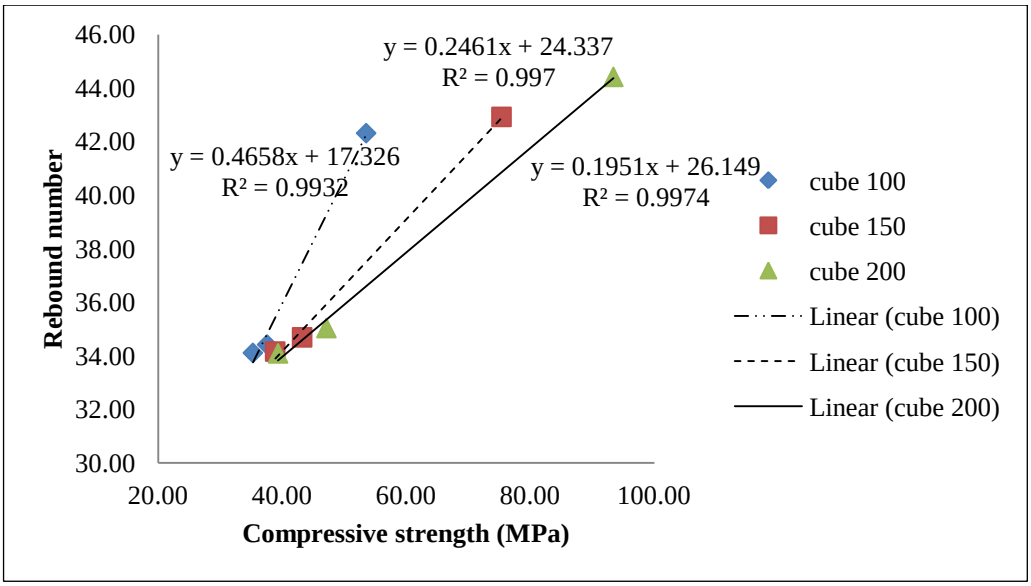

Figure 4.3: Cubic specimens' compressive strength vs. rebound number

Relations between cubic specimens' compressive strength and their respective rebound hammer numbers are fairly linear according to Figure 4.3.

Trend lines relate compressive strength levels of different specimens. It is noticeable that for all mix designs, the rebound numbers of cubes of 200 mm are averagely lower. However the points of those samples are accumulated in the region of higher compressive strengths.

Although the cubes of 200 mm have resulted in the highest compressive strength, their rebound hammer value, according to the results, are averagely lower than other cubic samples. The difference between the hammer values of cube 150 and 200 is not that significant, but there is a large gap between the results of cube 100 mm and 200 mm.

The especial results of rebound hammer can be attributed to the aggregates grading.

According to Zheng and Li (2002), in one sample, aggregate's density has a specific peak point at a near-surface section, which the peak point of aggregates density rises by having more aggregates' fraction. As a result, when by increasing the

specimens' size, the aggregates' volume fraction increases (due to having more space and better pouring), and larger cubic specimens are expected to have larger rebound number.

In addition, as it is known, rebound hammer test is affected by specimens' surface condition, on which the hammer is stroke (BS 1881 : Part 201, 2009).

In other words, the results of these experiments are not in agreement with the mentioned discussion.

As mentioned before, the reason of this contradictory observation can be explained by aggregates grading. In this investigation, the maximum aggregates size was kept constant throughout the experiments (equal to 20mm). It can be explained that by decreasing the size of specimens, from 200mm to 100mm, the probability of existence of a large aggregate of 20mm, near the specimen's surface, gets much higher. In other words, in smaller specimens, the hammer is more willing to strike to an aggregate. Consequently, the results of rebound hammer are higher in smaller cubic specimens.

This result truly shows that for cubic specimens there is a strong wall effect, which has influenced the results rebound hammer. As it was mentioned before about wall effect, the effect of walls of concrete samples' moulds causes an especial aggregates density inside the specimens.

With respect to different curing conditions, Table 4.7 has been prepared. In this table, rebound hammer results are shown for different curing conditions. Columns of rebound number and strength show the average results of specimens.

Table 4.7: Rebound hammer results for different curing conditions

Curing Type	Mix Design	Rebound num.	Strength (MPa)
water	A	33.57	41.20
		33.34	42.32
		33.30	42.61
	B	32.97	37.54
		35.00	46.67
		35.03	52.05
	C	46.38	54.47
		45.68	75.81
		48.67	91.90
air	A	35.25	33.92
		34.96	35.40
		34.87	36.02
	B	35.23	32.97
		34.37	39.74
		35.91	42.20
	C	38.94	52.59
		39.46	74.92
		40.16	94.93

Figure 4.4 shows the rebound number versus compressive strength. It can be observed that especially in the range of higher strengths, graph of water cured is equal or higher than air cured. This is due to the fact that when specimens are cured in water, hydration reaction of the specimens continues. Consequently, the water cured specimens obtain stronger bonds leading to higher rebound number.

The trend lines propose linear relations between the two parameters have R^2 of 0.7774 and 0.8295 for water and air curing conditions, respectively, showing a less scattered results for air cured samples.

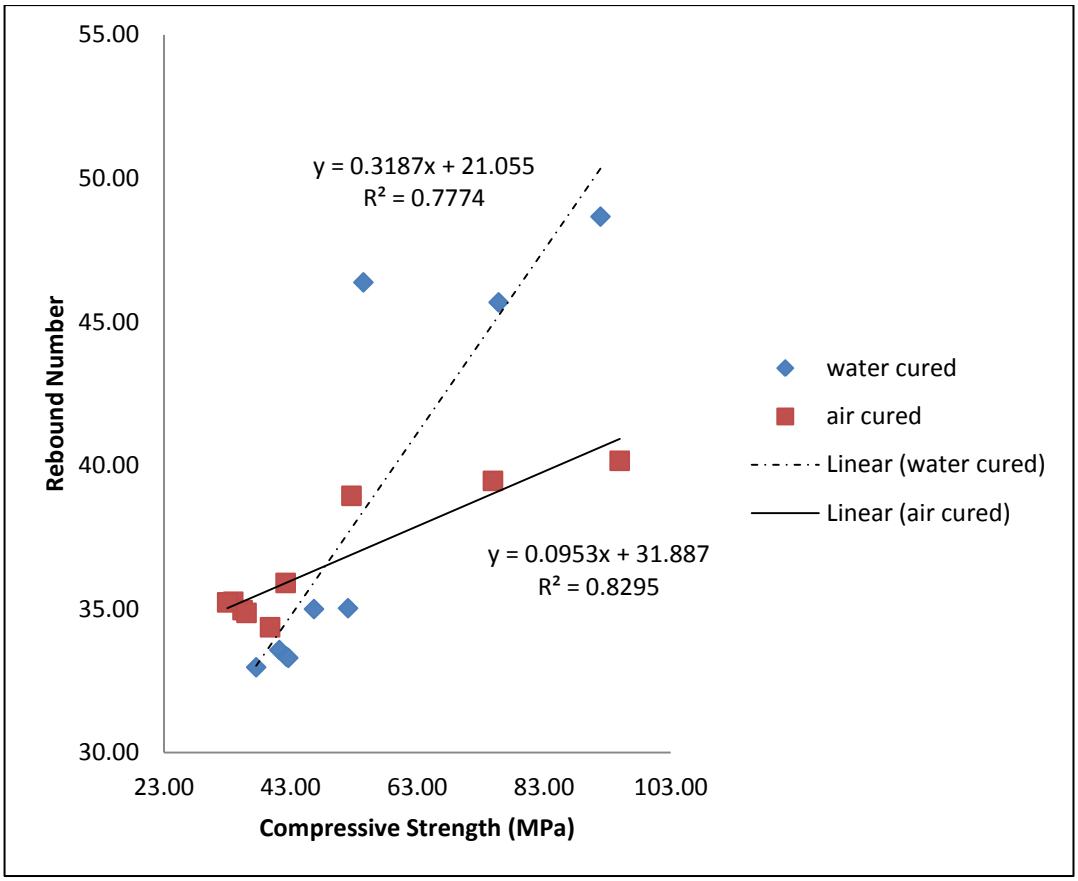

Figure 4.4: Rebound hammer vs. compressive strength for different curing conditions

4.4 Experiments on hardened concrete (destructive)

4.4.1 Splitting tensile strength test

In this experimental investigation, splitting tensile strength test was performed on both cubic and cylindrical samples, cured in water, at the age of 28 days.

Outcomes of the experiment are shown in Table 4.8. The table has two sections, the left side indicates the results of splitting test and the right section shows the compressive strength results of specimens.

Table 4.8: Splitting tensile strength test results

Samples	Splitting Tensile test results (MPa)	Mix Design A	Mix Design B	Mix Design C	Compressive Strength Test results (MPa) – water cured, 28 days	Mix Design A	Mix Design B	Mix Design C
Cyl.100×200 (1)		4.28	4.41	6.04		35.59	38.88	62.40
Cyl.100×200 (2)		4.47	4.47	5.31		38.10	36.44	82.70
Cyl.100×200 (3)		3.95	3.81	6.91		17.30	18.10	53.72
Cyl.150×300 (1)		3.72	4.67	5.84		35.70	48.10	71.60
Cyl.150×300 (2)		3.83	4.60	5.60		29.00	47.10	68.20
Cyl.150×300 (3)		3.65	4.49	6.08		29.90	38.60	63.60
Cu. 100 (1)		3.75	1.69	1.59		40.50	41.80	56.42
Cube 100 (2)		3.47	1.55	1.45		39.80	45.91	54.80
Cube 100 (3)		2.53	1.60	2.69		43.30	24.92	52.20
Cube 150 (1)		3.38	3.59	5.48		47.90	50.10	72.24
Cube 150 (2)		3.15	3.59	4.84		43.40	51.60	74.30
Cube 150 (3)		3.40	3.52	4.63		35.66	38.31	80.90
Cube 200 (1)		3.54	3.70	9.31		47.08	53.53	90.81
Cub 200 (2)		3.48	4.04	10.05		46.77	55.14	91.21
Cube 200 (3)		3.53	3.83	9.65		33.99	47.48	93.69

In the following figures (Figure 4.5 to Figure 4.9), splitting tensile strength vs. compressive strength is shown for different conditions.

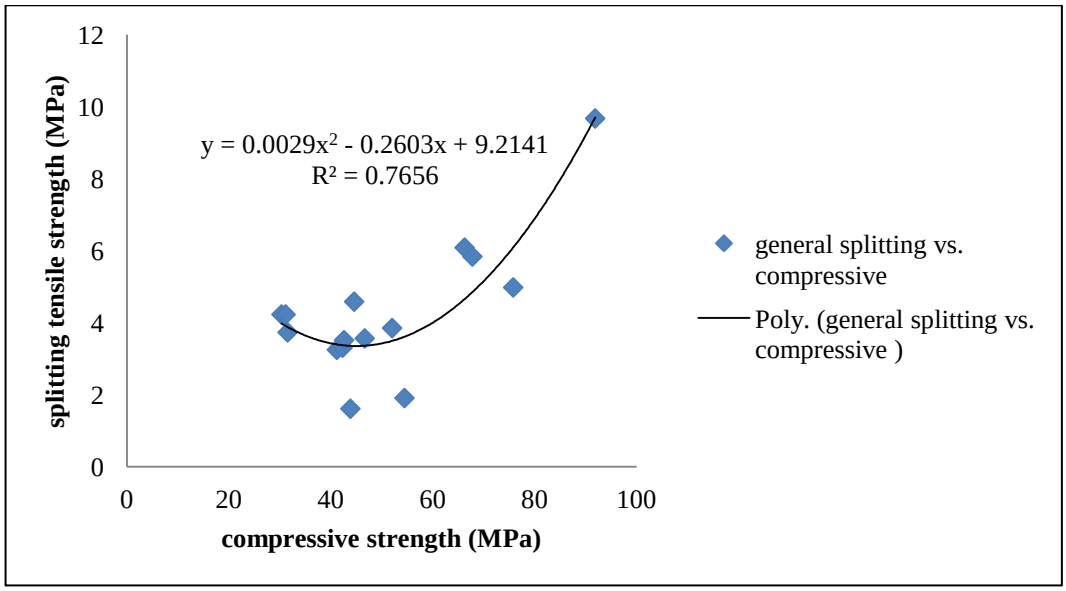

Figure 4.5: Splitting tensile strength vs. compressive strength for all the specimens

In Figure 4.5, the points represent the tested experiments' compressive strengths and their obtained splitting tensile strength.

In Figure 4.5, it is noticeable that the concavity of graph of splitting tensile strength vs. compressive strength is positive, meaning that the coefficient which converts compressive strength to splitting (slope of the graph) increases by increasing compressive strength.

On the opposite, in previous researches, it has been shown that at low strengths, splitting tensile strength can be as much as 10 percent of compressive strength, but in higher strengths, this coefficient decreases to 5 percent (Caldarone, 2009). In other words, by increasing compressive strength, the coefficient which converts compressive strength to splitting, decreases.

The reason of this observation can also be attributed to the different shapes of specimens. In order to find out the relation, splitting versus compressive strength graphs of all the specimens have been plotted separately in the following section.

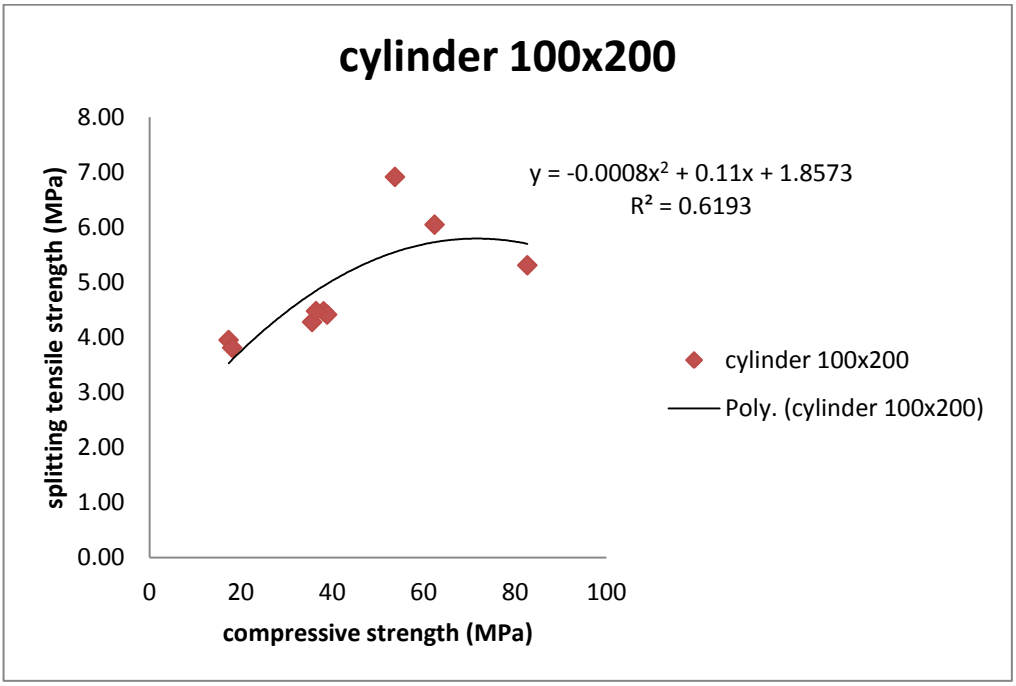

Figure 4.6: Splitting tensile strength vs. compressive strength of cylinder 100 mm × 200 mm

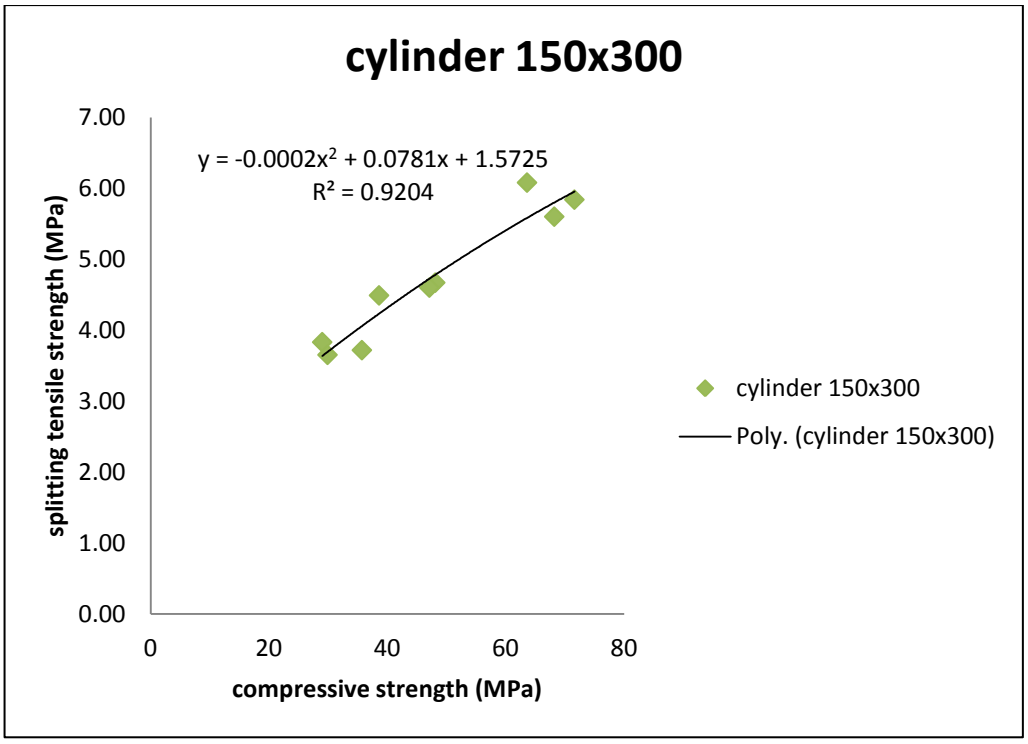

Figure 4.7: Splitting tensile strength vs. compressive strength of cylinder 150 mm × 300 mm

In the trend lines of Figure 4.6 and 4.7, the negative concavity of the graphs can be observed.

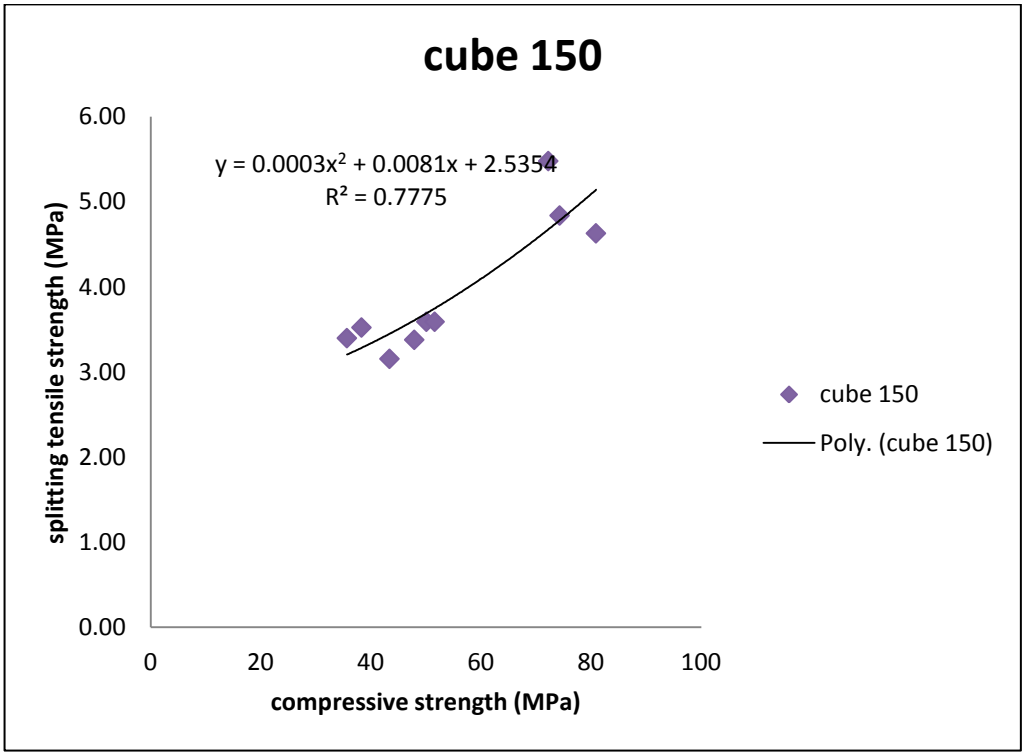

Figure 4.8: Splitting tensile strength vs. compressive strength of cubes 150 mm

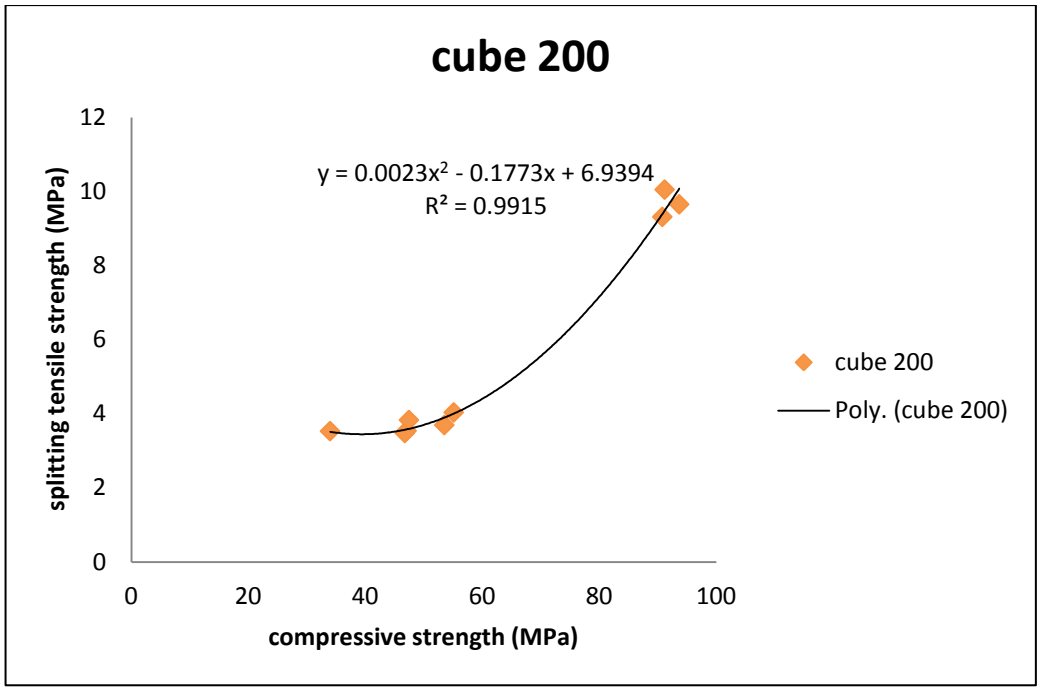

Figure 4.9: Splitting vs. compressive strength of cube 200

In Figure 4.8 and Figure 4.9, splitting tensile strength increases with an increasing slope, i.e. the concavity of both of the graphs are positive.

It can be explained that the mild declining slope (negative concavity) of cylinders' splitting tensile strength -compressive strength graphs are predominated by cubes' sharply increasing trend (positive concavity). Consequently, the general curve of splitting tensile strength vs. compressive strength of the entire samples has a sharp raising trend with a positive concavity.

Apart from the difference between the curves of cubes and cylinders, differences can also be noticed among the cubes and cylinders. In cylinders, growing trend of the bigger specimen cylinder 150×300 mm (by increase of compressive strength), is milder than the smaller one, cylinder 100×200 mm. While in cubes, unlike the cylinders, the smaller cube (150mm) has milder increasing tendency than the larger cubes of size 200 mm.

Figure 4.10 shows the splitting tensile strength of samples for each mix design, with respect to their shape and size.

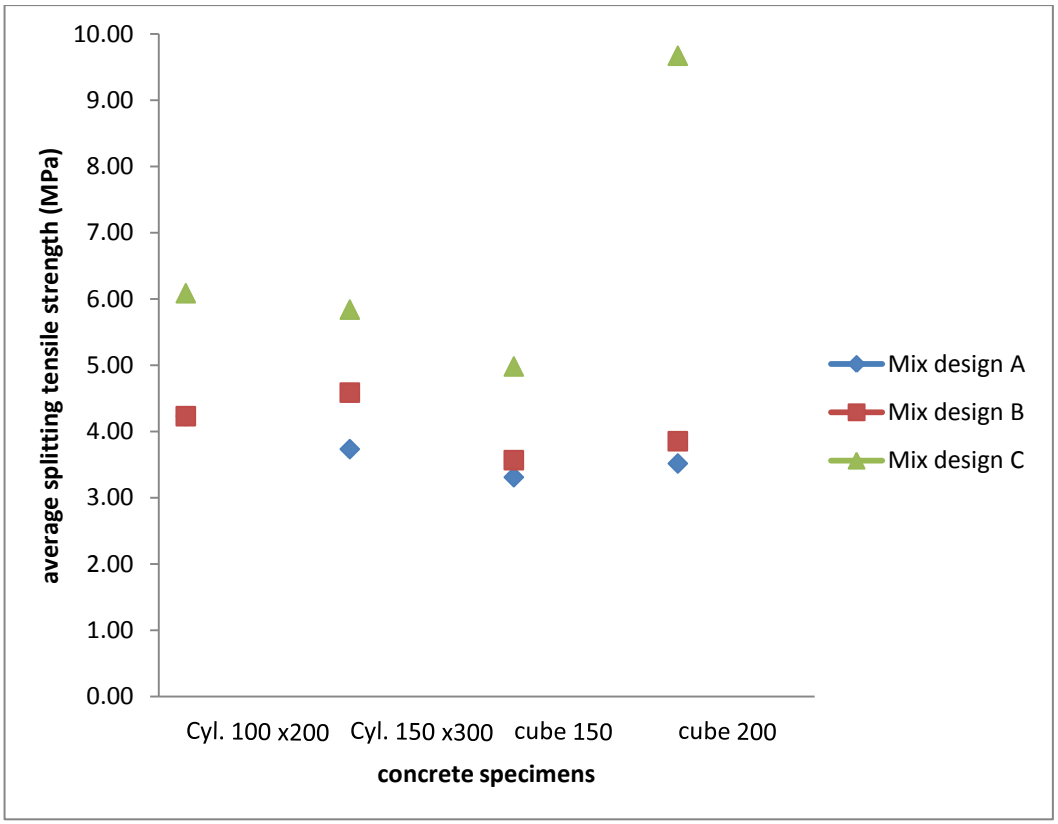

Figure 4.10: Splitting tensile strength of concrete specimens

In each graph of Figure 4.10, it can be seen that generally, by changing the specimens' size and shape, the amount of splitting tensile strength remains constant. The only contradictory result about this conclusion is cubic specimen of 200 mm for concrete mix design C. The result of this sample can be attributed to the big size of this specimen. The big size of the specimen together with using Glenium superplasticizer has resulted in a very uniform homogeneous concrete bond, which could withstand a high splitting tensile strength and result in the highest amount of splitting tensile strength.

In Figure 4.10, the tendency of increasing splitting strength together with compressive strength can be clearly observed.

It should be added here that, these results of splitting tensile strength test are in agreement with the results of Bažant et al. (1991). If the specimens' diameters (widths) are considered, by increasing the diameter (width) up to 150 mm, splitting

tensile strength decreases in general and after this level, the strength tends to increase.

To find out more about the different results of specimens' splitting tensile strength, conversion factors of the strengths have been defined as the division of different specimens' strengths by each other.

It can be explained that if the splitting tensile strength results of different specimens are plotted against each other, the slopes of the curves show the conversion factors of different specimens' strengths to each other.

In order to explore how these conversion factors change by changing strength level, the mentioned graphs are plotted in the following section to show the general changing trend of conversion factors.

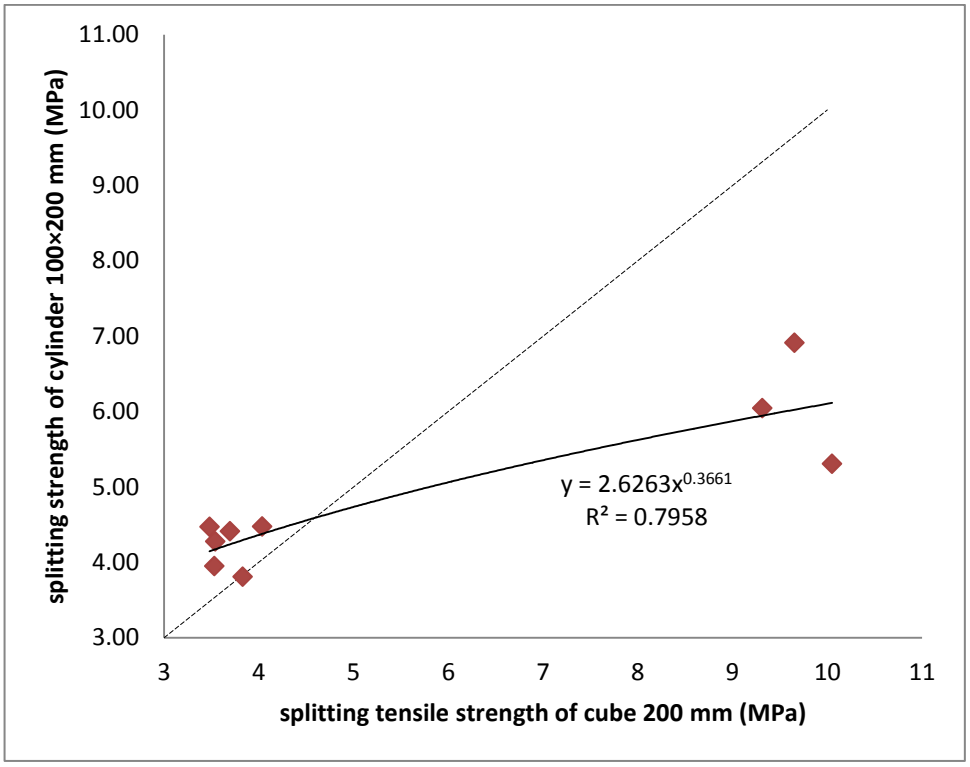

Figure 4.11: Splitting tensile strength of cylinder 100×200 mm vs. cube 200 mm

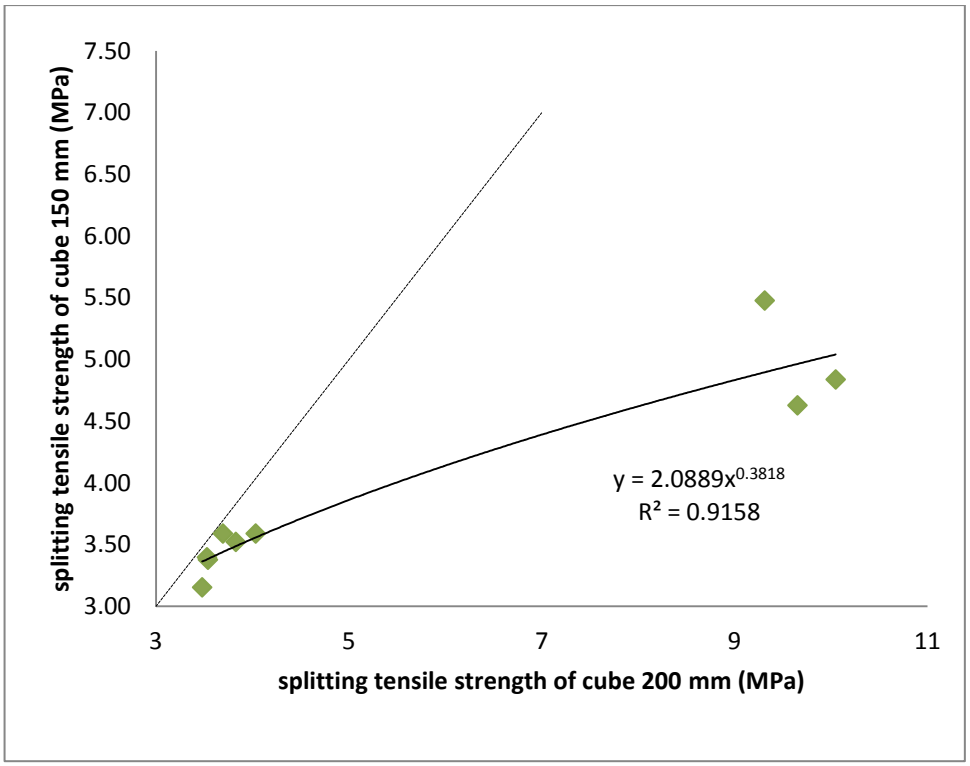

Figure 4.12: Splitting tensile strength of cube 150 vs. cube 200

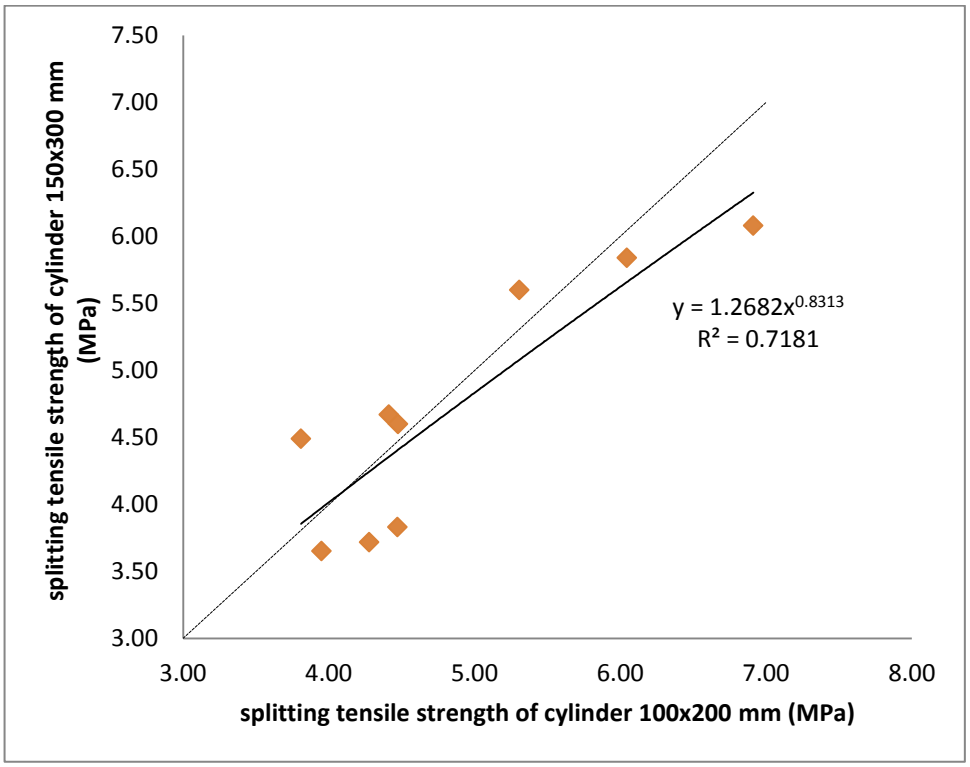

Figure 4.13: Splitting tensile strength of cylinder 150×300 mm vs. cylinder 100×200 mm

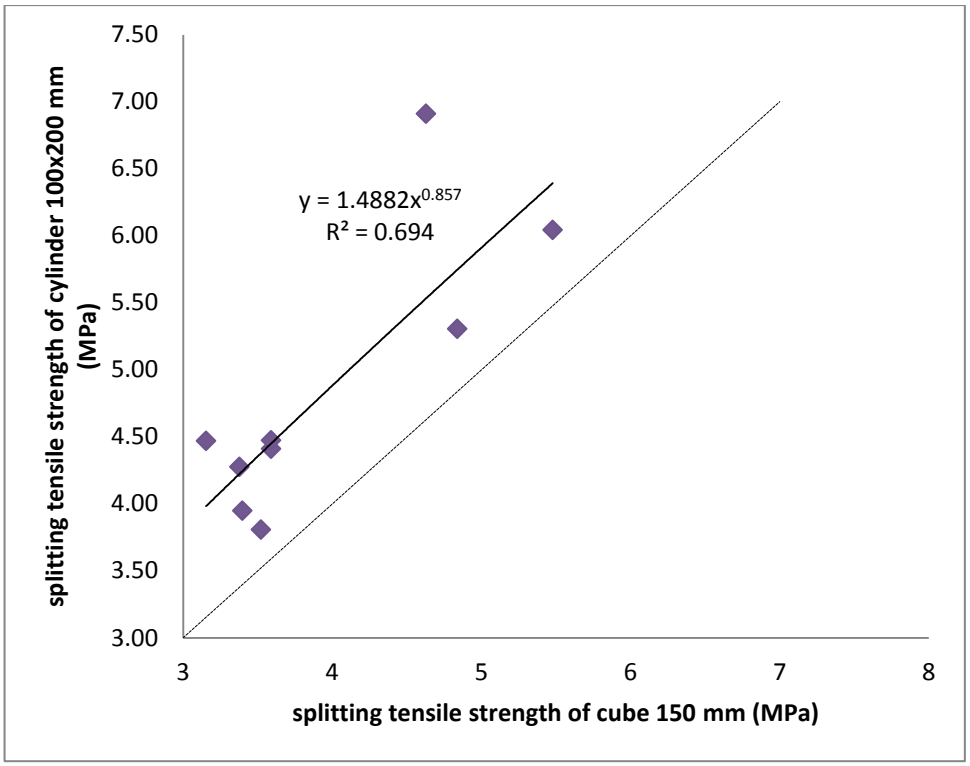

Figure 4.14: Splitting tensile strength of cylinder 100×200 mm vs. cube 150 mm

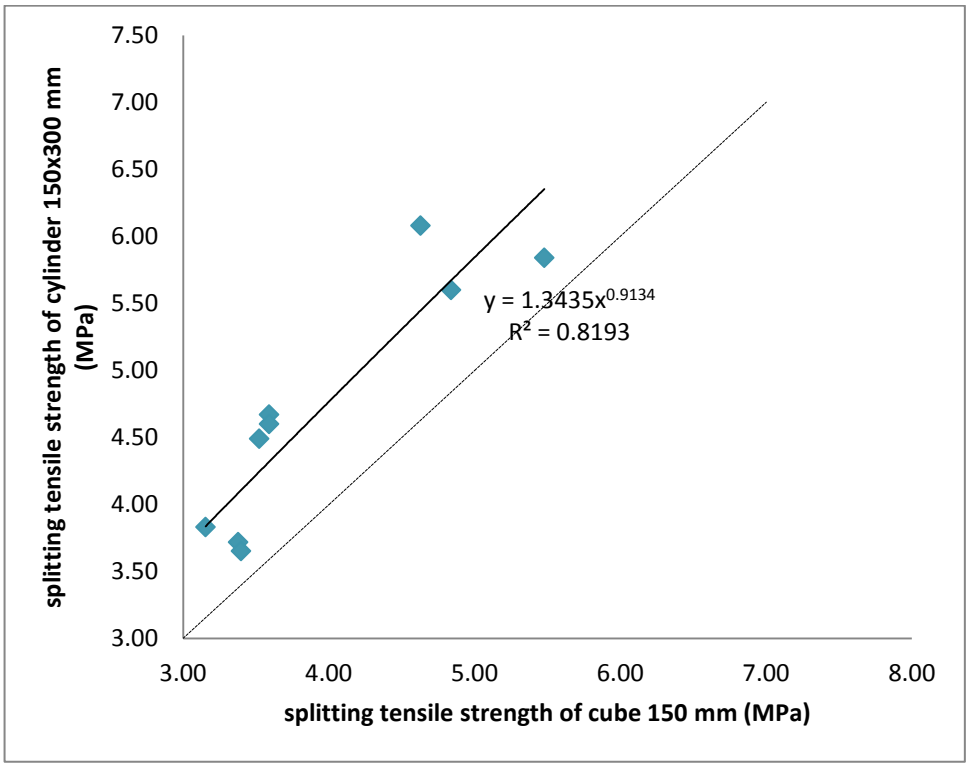

Figure 4.15: Splitting tensile strength of cylinder 150×300 mm vs. cube 150 mm

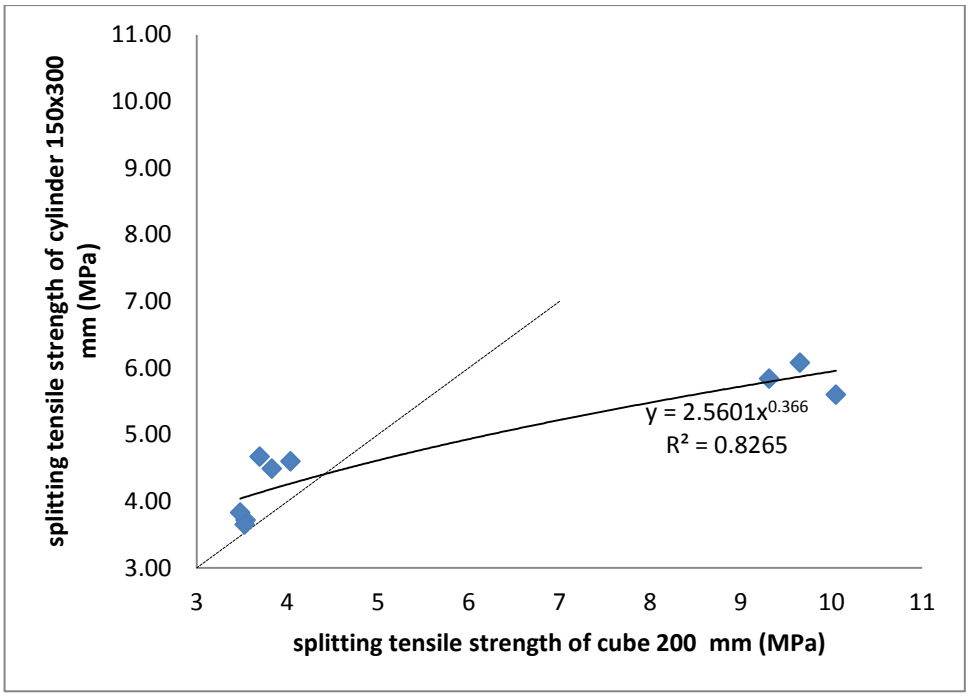

Figure 4.16: Splitting tensile strength of cylinder 150×300 mm vs. cube 200 mm

As explained before, the changing of slope of the trend lines of Figure 4.11 to Figure 4.16 are in fact indicate splitting tensile strength conversion factors' changing trend.

The dashed lines in each figure are the line with the equation of y=x, having the slope of 45°. The line has been plotted in order to compare different trend lines with each other.

It can be noticed that, approximately, the same pattern can be observed in all the graphs. In three of the figures (Figure 4.13, Figure 4.14 and Figure 4.15) the changing trends are much milder than other ones.

Each trend line which is approximately parallel with the dashed line shows that the increasing trend of splitting results of their corresponding specimens does not change significantly by changing the mix design. Such cases can be observed in Figure 4.15 and Figure 4.14 which convert splitting tensile strength of cylinder 100×200 mm and cylinder 150×300 mm to cube 150 mm.

Another noticeable point in each of the graphs is that in all figures (except Figure 4.15 and Figure 4.14), by increasing splitting tensile strength, the deviation from the line of x=y increases (for instance in Figure 4.13, in lower strengths, tensile strength of cylinder 150×300 mm and cylinder 100×200 mm are almost equal but at higher strengths, the strength of cylinder 100×200 mm is obviously higher than the strength of cylinder 150×300 mm). It means that at higher splitting strengths, splitting tensile strengths of the specimens are more scattered and the specimens have resulted more differently. In other words, in this investigation, size effect phenomenon for splitting tensile strength showed itself more at higher strength levels.

In addition to the figures, tables of conversion factors can also be helpful to convert results of different specimens and mix designs.

The following three tables show the results of splitting tensile strength conversion factors, for different concrete mix designs, separately.

Table 4.9: Conversion factors of splitting tensile strength- Mix design A

Mix design A Specimen type/size (mm)	Cyl.100×200	Cyl.150×300	Cube 150	Cube 200
Cyl.100×200	1.00	0.88	0.78	0.83
Cyl.150×300	1.13	1.00	0.89	0.94
Cube 150	1.28	1.13	1.00	1.06
Cube 200	1.20	1.06	0.94	1.00

Table 4.10: Conversion factors of splitting tensile strength- Mix design B

Mix design B Specimen type/size (mm)	Cyl.100×200	Cyl.150×300	Cube 150	Cube 200
Cyl.100×200	1.00	1.08	0.84	0.91
Cyl.150×300	0.92	1.00	0.78	0.84
Cube 150	1.19	1.29	1.00	1.08
Cube 200	1.10	1.19	0.93	1.00

Table 4.11: Conversion factors of splitting tensile strength- Mix design C

Mix design C Specimen type/size (mm)	Cyl.100×200	Cyl.150×300	Cube 150	Cube 200
Cyl.100×200	1.00	0.96	0.82	1.59
Cyl.150×300	1.04	1.00	0.85	1.66
Cube 150	1.22	1.17	1.00	1.94
Cube 200	0.63	0.60	0.52	1.00

For obtaining conversion factors, the average results of splitting tensile strengths of specimens were used.

Variations in the mix design and water/cement ratio change the slope of lines. Lower water/cement ratio causes the slopes of graphs to get milder and this means that the splitting strength ratios of different specimens have more deviation. So, their corresponding conversion factors will be more scattered from 1. This fact is in accordance with the average of conversion factors of each mix design. Average conversion factor of specimens in mix design C is 0.86, while for mixes of B and A, they are equal to 1.10.

There is a difference between Table 4.9 to Table 4.11 and Figure 4.11 to Figure 4.16, which is for calculating the tables' conversion factors, average amounts of three specimens have been used, while for plotting the graphs, raw results of all the specimens have been used (without calculating the average amount).

It should be added here that, instead of plotting all specimens' splitting tensile strength graphs against each other, only half of the graphs (totally 6 graphs) have been plotted. This is because the tables are like symmetric matrices, so the rest of graphs are simply the inverse of these functions.

In addition, the results of splitting tensile test of cubes of 100 mm were withdrawn from analyses as their results were highly scattered due to some induced errors, during casting. Errors were due to dimensional variations of the moulds.

As the conclusion, it can be said that in these experiments, size effect was observed in splitting tensile strength test results, and the results tend to be scattered and size dependant in higher strengths (as they were more deviated in the results of mix design C).

4.4.2 Compressive strength test

The most extensive experiment was compressive strength test during this study.

Totally four different factors were investigated to find out their influence on concrete compressive strength test results. The factors are two different ages, two different curing conditions, three different concrete mix designs and finally, moulds' shapes and sizes. The employed moulds were 3 different cubes (100, 150 and 200 mm) and two different cylinders (100×200 mm and 150×300 mm). Three samples were casted for each case of testing in order to minimize scatters and errors in results and analyses.

In addition, for one sample from each three samples of different testing cases, stress- strain curves are plotted by using strain rate controlled testing machine ToniNorm.

4.4.2.1 Results of compressive strength test and the conversion factors

4.4.2.1.1 Specimens of mix design A

The results of concrete sample of mix design A are shown in Table 4.12. Conversion factors, obtained from compressive strength of these specimens are shown in the following sections.

Table 4.12: Compressive strength results for mix design A.

Samples (specimen number) units in mm	7 days (MPa)		28 days (MPa)	
	Water Cured	Air Cured	Water Cured	Air Cured
Cyl.100×200 (1)	28.87	*1.20**	35.59	24.27
Cyl.100×200 (2)	26.06	12.23	38.10	26.84
Cyl.100×200 (3)	*17.00**	16.44	*17.30**	*8.24**
Cyl.150×300 (1)	29.30	*16.59**	35.70	30.60
Cyl.150×300 (2)	26.10	17.50	29.00	*28.15**
Cyl.150×300 (3)	*22.73**	17.90	*29.90**	31.40
Cube 100 (1)	25.88	21.26	40.50	36.90
Cube 100 (2)	24.19	21.17	39.80	35.20
Cube 100 (3)	*16.76**	*5.95**	43.30	*29.65**
Cube 150 (1)	31.10	21.20	47.90	37.30
Cube 150 (2)	30.80	20.70	43.40	37.30
Cube 150 (3)	*26.20**	*14.41**	*35.66**	*31.59**
Cube 200 (1)	26.52	21.87	47.08	36.14
Cube 200 (2)	27.18	22.14	46.77	37.94
Cube 200 (3)	*24.11**	*18.28**	*33.99**	*33.98**

*Italic cells are the specimens used for drawing stress-strain curves

In Tables 4.13 to 4.16, compressive strength conversion factors are shown. These factors convert the average strength of each of the specimens (average of three samples).

The factors are calculated by dividing the strength of specimens in the 1st row to the specimen in the 1st column.

Table 4.13: Conversion factors of samples- water cured, 7days, mix design A

7 days- water cured	Cyl.100×200	Cyl.150×300	Cube 100	Cube 150	Cube 200
Cyl.100×200	1.00	1.09	0.93	1.22	1.08
Cyl.150×300	0.92	1.00	0.86	1.13	1.00
Cube 100	1.08	1.17	1.00	1.32	1.16
Cube 150	0.82	0.89	0.76	1.00	0.88
Cube 200	0.92	1.00	0.86	1.13	1.00

Table 4.14: Conversion factors of samples- air cured, 7days, mix design A

7 days- air cured	Cyl.100×200	Cyl.150×300	Cube 100	Cube 150	Cube 200
Cyl.100×200	1.00	1.21	1.48	1.31	1.45
Cyl.150×300	0.83	1.00	1.22	1.08	1.20
Cube 100	0.68	0.82	1.00	0.88	0.98
Cube 150	0.76	0.92	1.13	1.00	1.11
Cube 200	0.69	0.83	1.02	0.90	1.00

Table 4.15: Conversion factors of samples- water cured, 28 days, mix design A

28 days- water cured	Cyl.100×200	Cyl.150×300	Cube 100	Cube 150	Cube 200
Cyl.100×200	1.00	0.86	1.12	1.15	1.16
Cyl.150×300	1.17	1.00	1.31	1.34	1.35
Cube 100	0.89	0.77	1.00	1.03	1.03
Cube 150	0.87	0.75	0.97	1.00	1.01
Cube 200	0.86	0.74	0.97	0.99	1.00

Table 4.16: Conversion factors of samples- air cured, 28 days, mix design A

28 days- air cured	Cyl.100×200	Cyl.150×300	Cube 100	Cube 150	Cube 200
Cyl.100×200	1.00	1.18	1.33	1.39	1.41
Cyl.150×300	0.85	1.00	1.13	1.18	1.20
Cube 100	0.75	0.89	1.00	1.04	1.06
Cube 150	0.72	0.85	0.96	1.00	1.02
Cube 200	0.71	0.83	0.94	0.98	1.00

4.4.2.1.2 Specimens of mix design B

In Table 4.17, the results of compressive strength of samples of mix design B are shown.

By using the results of the table, corresponding conversion factors have been calculated. The factors are shown in Tables 4.18 to 4.21.

Table 4.17: Compressive strength results for mix design B

Samples (specimen number) units in mm	7 days (MPa)		28 days (MPa)	
	Water Cured	Air Cured	Water Cured	Air Cured
Cyl.100×200 (1)	*18.79**	*13.89**	38.88	31.02
Cyl.100×200 (2)	29.42	23.28	36.44	*28.80*
Cyl.100×200 (3)	29.94	22.05	*18.10**	wrong
Cyl.150×300 (1)	*27.03**	*21.18**	48.10	35.40
Cyl.150×300 (2)	28.60	23.70	47.10	34.00
Cyl.150×300 (3)	28.60	25.70	*38.60**	*28.24**
Cube 100 (1)	33.70	*21.46**	41.80	*34.69**
Cube 100 (2)	32.90	24.09	45.91	29.32
Cube 100 (3)	*16.02**	23.47	*24.92**	34.90
Cube 150 (1)	33.60	*21.70**	50.10	40.20
Cube 150 (2)	31.33	25.00	51.60	42.10
Cube 150 (3)	*26.76**	24.80	*38.31**	*36.91**
Cube 200 (1)	34.43	26.66	53.53	43.00
Cube 200 (2)	33.02	28.10	55.14	42.95
Cube 200 (3)	*27.48**	*22.90**	*47.48**	*40.64**

*Italic cells are the specimens tested for drawing stress-strain curves

Table 4.18: Conversion factors of samples- water cured, 7 days,mix design B

7 days- Water Cured	Cyl.100×200	Cyl.150×300	Cube 100	Cube 150	Cube 200
Cyl.100×200	1.00	1.08	1.28	1.17	1.21
Cyl.150×300	0.93	1.00	1.19	1.09	1.13
Cube 100	0.78	0.84	1.00	0.92	0.95
Cube 150	0.85	0.92	1.09	1.00	1.04
Cube 200	0.82	0.89	1.05	0.97	1.00

Table 4.19: Conversion factors of samples- air cured, 7 days, mix design B

7 days- Air Cured	Cyl.100×200	Cyl.150×300	Cube 100	Cube 150	Cube 200
Cyl.100×200	1.00	1.04	1.02	1.05	1.14
Cyl.150×300	0.96	1.00	0.98	1.01	1.10
Cube 100	0.99	1.02	1.00	1.04	1.13
Cube 150	0.95	0.99	0.97	1.00	1.09
Cube 200	0.88	0.91	0.89	0.92	1.00

Table 4.20: Conversion factors of samples- water cured, 28 days, mix design B

28 days- Water Cured	Cyl.100×200	Cyl.150×300	Cube 100	Cube 150	Cube 200
Cyl.100×200	1.00	1.18	1.16	1.35	1.38
Cyl.150×300	0.84	1.00	0.98	1.14	1.17
Cube 100	0.86	1.02	1.00	1.16	1.19
Cube 150	0.74	0.88	0.86	1.00	1.02
Cube 200	0.72	0.86	0.84	0.98	1.00

Table 4.21: Conversion factors of samples- air cured, 28 days, mix design B

28 days- Air Cured	Cyl.100×200	Cyl.150×300	Cube 100	Cube 150	Cube 200
Cyl.100×200	1.00	1.09	1.10	1.33	1.41
Cyl.150×300	0.92	1.00	1.01	1.22	1.30
Cube 100	0.91	0.99	1.00	1.21	1.28
Cube 150	0.75	0.82	0.83	1.00	1.06
Cube 200	0.71	0.77	0.78	0.94	1.00

4.4.2.1.3 Specimens of mix design C

For this mix design, the raw results of compressive strength are shown in Table 4.22.

An explanation here has to be added about compressive strength results of cube 200 mm having mix design C. The cubes of 200 mm have the largest volume between the utilized samples. Having a high volume together with utilization of superplasticizer has resulted in a high compressive strength (due to the fact that larger specimens result in more homogeneous concrete bonds (Turkel and Ozkul, 2010).

High compressive strength of the specimens in cooperation with large surface area, caused the specimens' ultimate bearing load to be much higher than loading capacity of the testing machine. As a result, during experiments, the testing procedure of the cubes of 200 mm were stopped in the middle of the process.

For doing the analyses, as the compressive strength results of those samples were essentially needed, the required data were extrapolated linearly by using MS Excel software. The extrapolation was done by using the surface area and corresponding compressive strength results of other specimens. The shadowed cells in Table 4.22 are those data which have been extrapolated.

Table 4.22: Compressive strength results for mix design C

Samples (specimen number) units in mm	7 days (MPa)		28 days (MPa)	
	water cured	Air cured	water cured	Air cured
Cyl.100×200 (1)	*61.62**	53.00	62.40	*55.11**
Cyl.100×200 (2)	57.00	47.30	82.70	62.10
Cyl.100×200 (3)	61.30	*43.43**	*53.72**	58.30
Cyl.150×300 (1)	*57.49**	*45.10**	71.60	*61.25**
Cyl.150×300 (2)	52.30	52.60	68.20	65.20
Cyl.150×300 (3)	60.10	52.30	*63.60**	64.70
Cube 100 (1)	*51.66**	57.00	*56.42**	38.80
Cube 100 (2)	57.80	51.50	54.80	*55.97**
Cube 100 (3)	58.90	*49.19**	52.20	63.00
Cube 150 (1)	*58.06**	60.40	*72.24**	*73.57**
Cube 150 (2)	66.20	62.40	74.30	73.60
Cube 150 (3)	65.10	*58.56**	80.90	77.60
Cube 200 (1)	*60.56**	65.32	90.81	94.54
Cube 200 (2)	63.79	65.22	91.21	94.69
Cube 200 (3)	66.37	*56.98**	93.69	95.56

*Italic cells are the specimens used for drawing stress-strain curves

Conversion factors of specimens of mix design C are shown in the following Tables.

Table 4.23: Conversion factors of samples- water cured, 7 day, mix design C

7 days- Water Cured	Cyl.100×200	Cyl.150×300	Cube 100	Cube 150	Cube 200
Cyl.100×200	1.00	0.94	0.94	1.05	1.06
Cyl.150×300	1.06	1.00	0.99	1.11	1.12
Cube 100	1.07	1.01	1.00	1.12	1.13
Cube 150	0.95	0.90	0.89	1.00	1.01
Cube 200	0.94	0.89	0.88	0.99	1.00

Table 4.24: Conversion factors of samples- air cured, 7 day, mix design C

7 days- Air Cured	Cyl.100×200	Cyl.150×300	Cube 100	Cube 150	Cube 200
Cyl.100×200	1.00	1.04	1.10	1.26	1.30
Cyl.150×300	0.96	1.00	1.05	1.21	1.25
Cube 100	0.91	0.95	1.00	1.15	1.19
Cube 150	0.79	0.83	0.87	1.00	1.03
Cube 200	0.77	0.80	0.84	0.97	1.00

Table 4.25: Conversion factors of samples- water cured, 28 days, mix design C

28 days- Water Cured	Cyl.100×200	Cyl.150×300	Cube 100	Cube 150	Cube 200
Cyl.100×200	1.00	1.02	0.82	1.14	1.39
Cyl.150×300	0.98	1.00	0.80	1.12	1.36
Cube 100	1.22	1.24	1.00	1.39	1.69
Cube 150	0.87	0.89	0.72	1.00	1.21
Cube 200	0.72	0.74	0.59	0.82	1.00

Table 4.26: Conversion factors of samples- air cured, 28 days. mix design C

28 days- Air Cured	Cyl.100×200	Cyl.150×300	Cube 100	Cube 150	Cube 200
Cyl.100×200	1.00	1.09	1.02	1.28	1.62
Cyl.150×300	0.92	1.00	0.93	1.18	1.49
Cube 100	0.98	1.07	1.00	1.26	1.60
Cube 150	0.78	0.85	0.79	1.00	1.27
Cube 200	0.62	0.67	0.63	0.79	1.00

4.4.2.2 Discussions on compressive strength results

To show the changing trends of compressive strength between different specimen sizes, the following linear graphs (Figure 4.17 to Figure 4.20) have been drawn. Each graph shows the specimens' obtained compressive strength for different curing conditions and different ages.

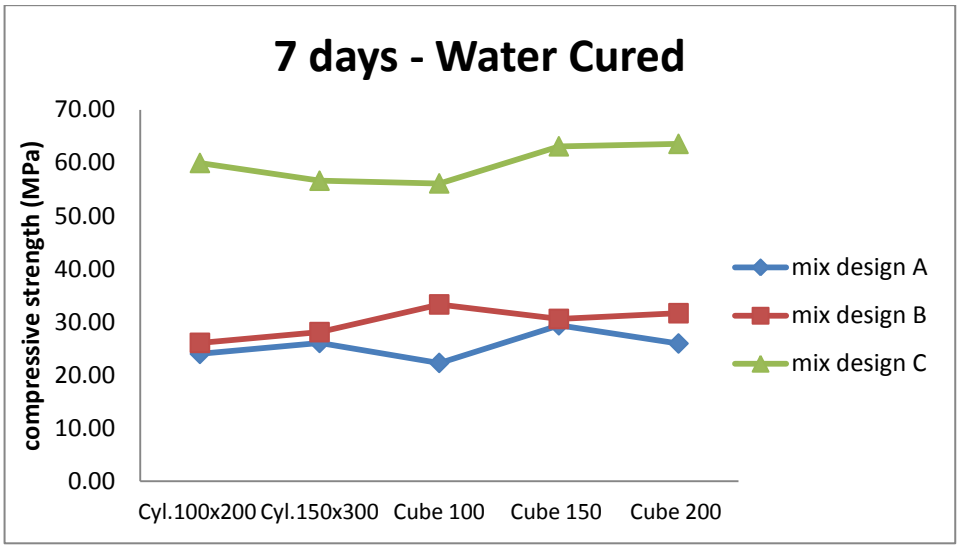

Figure 4.17: Compressive strength of specimens at 7 days cured in water

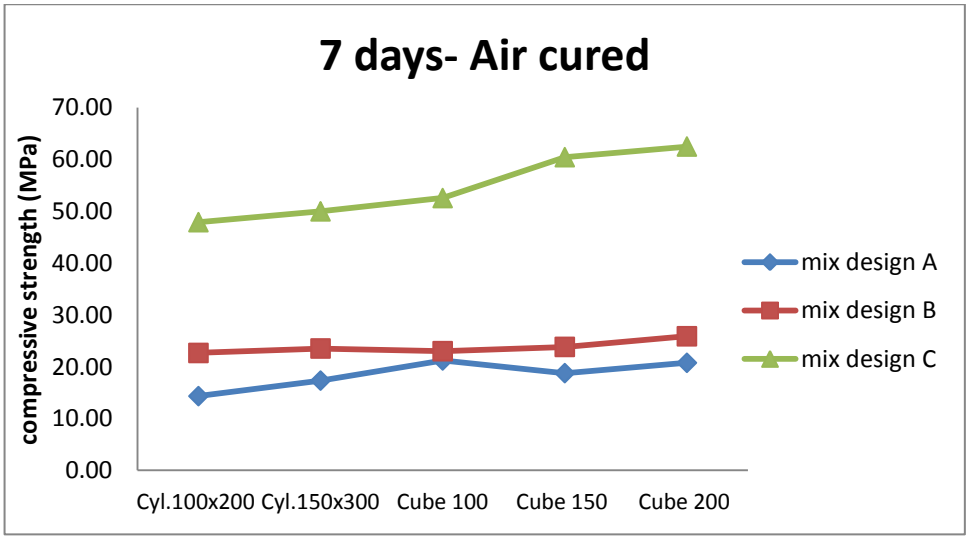

Figure 4.18: Compressive strength of specimens at 7 days cured in air

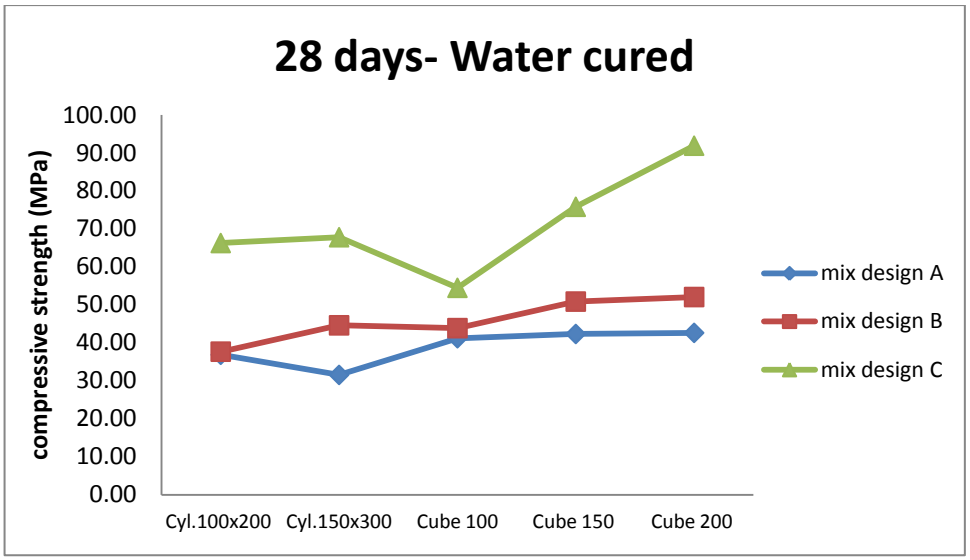

Figure 4.19: Compressive strength of specimens at 28 days cured in water

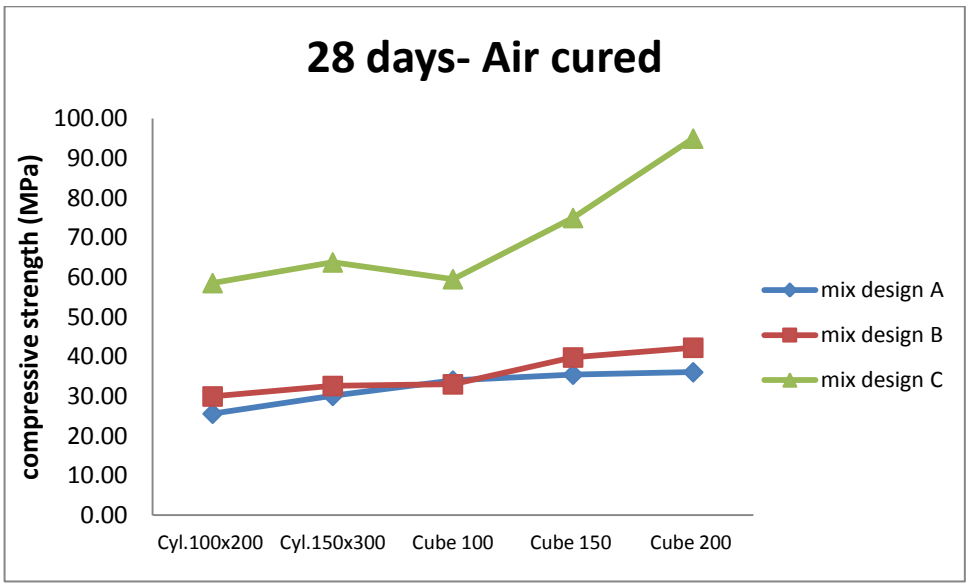

Figure 4.20: Compressive strength of specimens at 28 days cured in air

According to these figures, it can be noticed that the least size and shape effect can be observed in specimens having air cured and tested on the 7th day (the graphs of 7 days specimens are comparably more uniform). This result can especially be noticed for concrete specimens of lower compressive strength, i.e. mix design A and B. The most uniform compressive strength results were obtained from samples of mix design B, cured in air and tested on the 7th day after casting.

The reason of this observation could be due to weaker strength of concrete specimens at the early age. As it was mentioned before, the utilized cement for these experiments was GGBS cement which gains strength slowly. It is known that the concrete samples of these cements will have lower strength gain rate (Dongxu, et al 2000; and GGBS and concrete properties, 2007). As the result, all the specimens, at 7 days age, fracture (especially in lower strength concretes) before the load reaches to the aggregates. In other words, while in size effect and wall effect phenomena (especially wall effects), the aggregates of specimens are playing the main roles (Zheng and Li, 2002), in these samples' failures, the cement paste controls the failure at the early age of concrete samples.

The graphs of samples tested at 28 days are alike each other according to the Figures 4.19 and 4.20. This observation also can be due to developed strength of concrete bonds, at the age of 28 days which causes the size effect and wall effect, influence on compressive strength.

The same results can be observed for samples tested at 7days age. Both of the graphs have mild changes in compressive strength.

Size effect can be said to be lower among the cylinders while it is more noticeable amongst cubic specimens. This can especially be observed for higher concrete strengths (mix design C), while for lower strengths, it is not that much clear.

The influence of changing the size and shape of specimens is more obvious for samples of mix design C. Especially size effect is more noticeable among cubes (for this mix design).

It can be observed from nearly all figures that the compressive strength of cubes of 200 mm is higher than the other specimen sizes' compressive strengths. This observation is more significant for specimens of mix design C, tested at 28 days.

As an additional explanation, it is widely accepted that the most common testing age of concrete samples is 28 days and the most accepted type of curing is water curing. If the samples' results in the mentioned conditions are investigated (Figure 4.19), it can be seen that the sample of cylinder 150×300 mm has given out the most trustable results for different mix designs (the compressive strength of about 30 MPa for mix design A, more than 40 MPa for mix design B and above 60 MPa for mix design C).

4.4.2.3 Investigating the wall effect

As it has been explained previously in this chapter as well as chapter of literature review, the moulds' walls have significant influence on the concrete samples' aggregates density. According to a model proposed by Zheng and Li (2002), the density in the surface of the specimens are the least amount and by moving toward the inner regions, the density increases and after one decrease, it reaches to a constant amount. This deviation in aggregates density causes variations in compressive strength results. Aggregates' grading influences through wall effect (Elwet and Fu, 1995).

To study the wall effect, although aggregates grading was constant during the investigation, compressive strength results of different specimens have been plotted against surface/volume ratio of samples. Table 4.27 shows the ratio of surface/volume for each of the specimens. Values of Table 4.27 have been plotted against compressive strength for different conditions in Figures 4.21 to 4.24.

Table 4.27: Lateral surface/volume ratio for different specimens

Sample types size in mm	Lateral surface/volume ratio (mm^{-1})
Cyl.100×200	0.050
Cyl.150×300	0.033
Cube 100	0.060
Cube 150	0.040
Cube 200	0.030

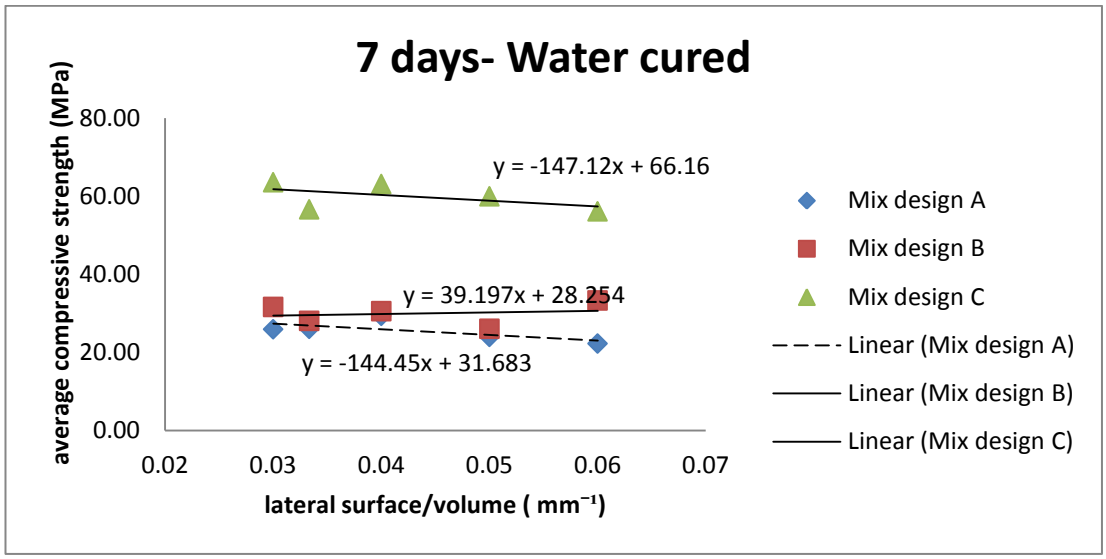

Figure 4.21: Investigating wall effect for water cured samples, tested at 7 days

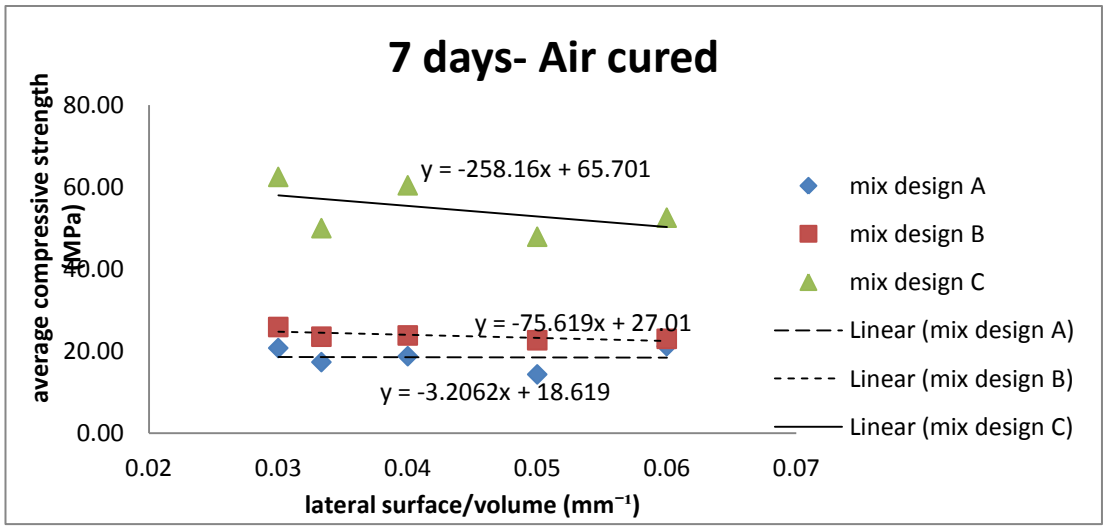

Figure 4.22: Investigating wall effect for air cured samples, tested at 7 days

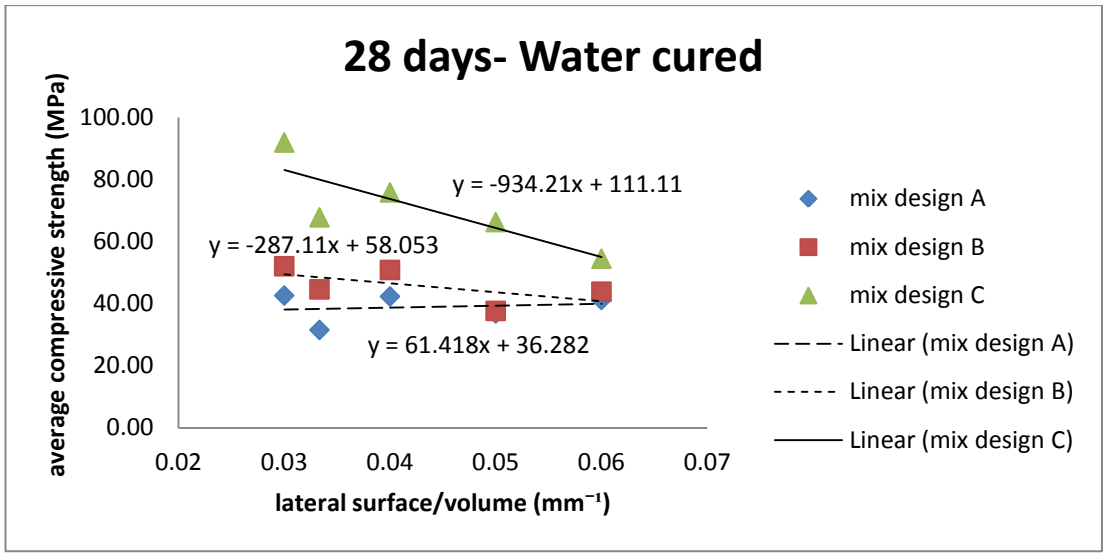

Figure 4.23: Investigating wall effect for water cured samples, tested at 28 days

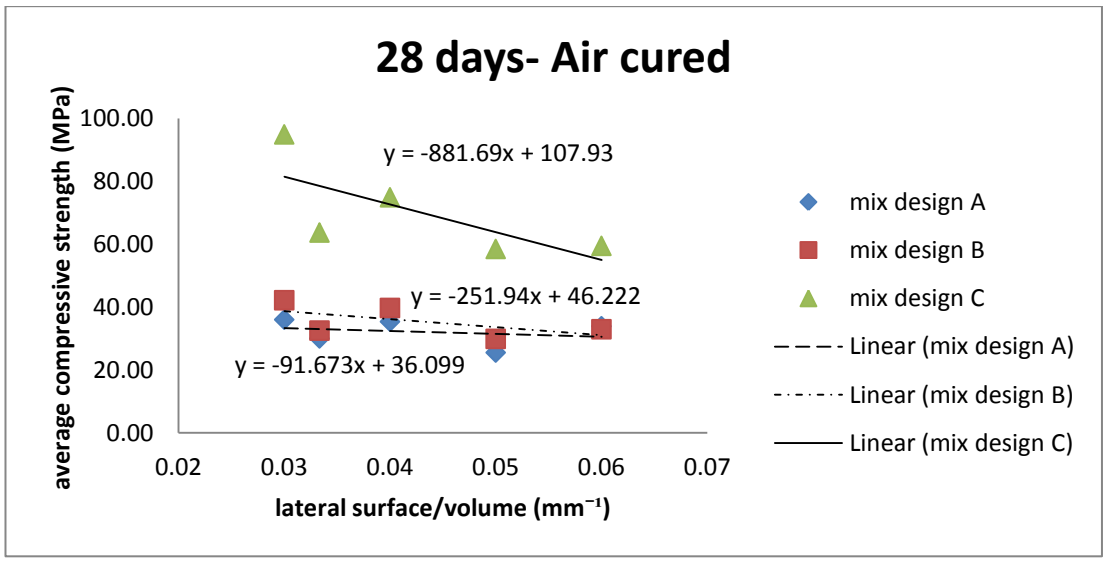

Figure 4.24: Investigating wall effect for air cured samples, tested at 28 days

The point which is quite clear from all these graphs is that by increasing the ratio of lateral surface to volume, compressive strength has a steady decreasing trend.

Increasing the ratio of surface/volume, in fact means that for each cubic meter of the specimens, there is an increasing amount of surface area. When the maximum size of the aggregates is constant, the extra provided surface area is more willing to be filled with mortar instead of aggregates. Consequently, concrete in the boundary zones gets less uniform. In addition, it is known that mortars have some properties which can affect compressive strength of samples, including porosity which can

deteriorate the compressive strength. As a result, specimens with higher ratio of surface area/volume are willing to have less compressive strength.

Figure 4.21 to Figure 4.24 show that the cubes of 200 mm, which have the least ratio of surface to volume, show the highest amount of compressive strength. Also, according to the data, almost for all cases, when the ratio of lateral surface to volume was approximately equal (i.e. cylinder 150×300 mm and cube 200 mm), the higher compressive strength was allocated to the cubic specimen. This observation might be due to more uniform concrete, caused by a better compaction.

It should be added that the trend lines in the mentioned figures are only drawn to clearly show the decreasing trend.

Compressive strength vs. lateral surface area/volume has been plotted for different curing conditions in figures 4.25 and Figure 4.26.

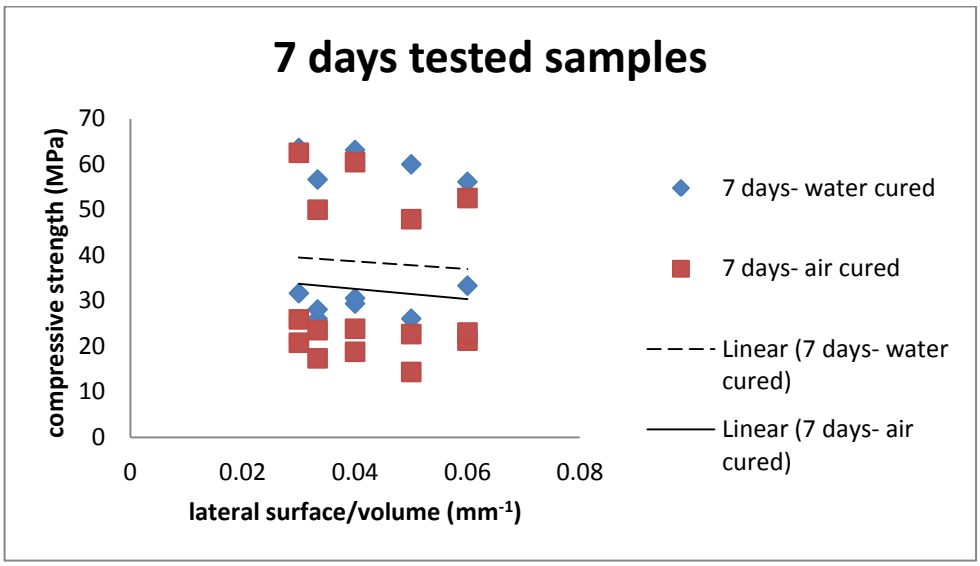

Figure 4.25: Compressive strength vs. lateral surface/volume for different mix designs tested at 7 days age.

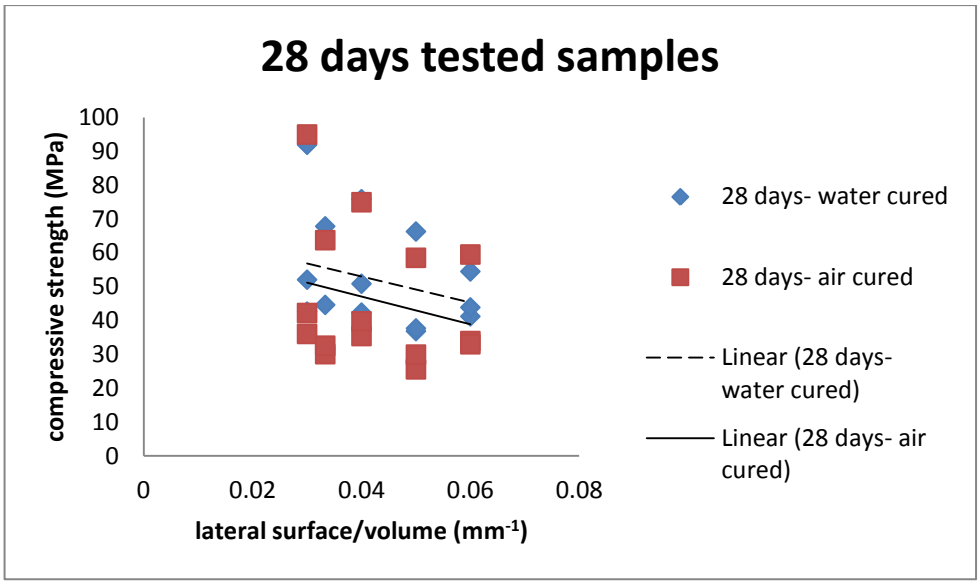

Figure 4.26: Compressive strength vs. lateral surface/volume for different mix designs tested at 28 days age.

Figure 4.25 and Figure 4.26 have been plotted according to results of same size specimens having various concrete strength grades. The resulting points do not show a clear obvious trending. In spite of this fact, for each of the series, a linear trend line have been plotted to only show the overall decreasing tendency of the points.

4.4.2.4 Investigation about conversion factors

To discuss about changing trend of concrete samples' conversion factors (which were calculated in section 4.4.2.1), figures 4.27 to 4.29 have been plotted.

It should be explained that each of the graphs show the conversion factors of only one of the samples (the one which the vertical axis is named), converting the sample's compressive strength to the specimens which are shown in the horizontal axis. The values on the vertical axis are the result of division of compressive strength of the vertical axis by the compressive strength of horizontal axis.

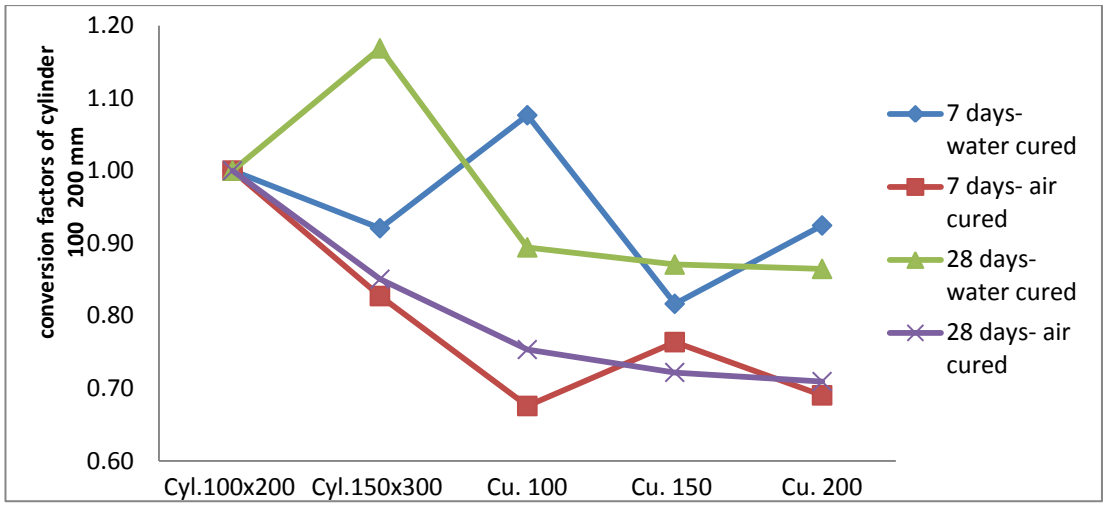

Figure 4.27: Conversion factors of cylinder 100×200 mm for mix design A

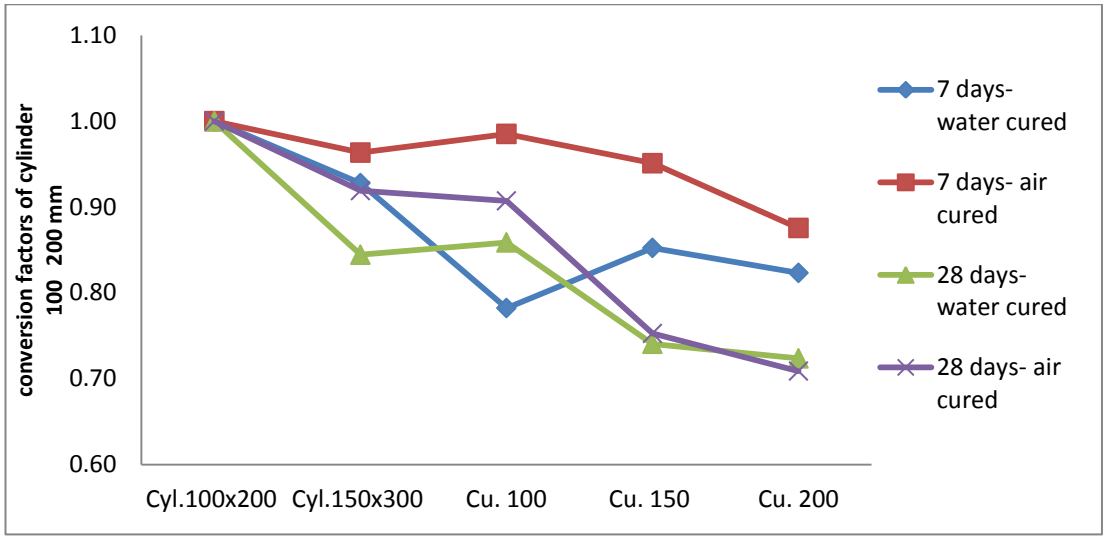

Figure 4.28: Conversion factors of cylinder 100×200 mm for mix design B

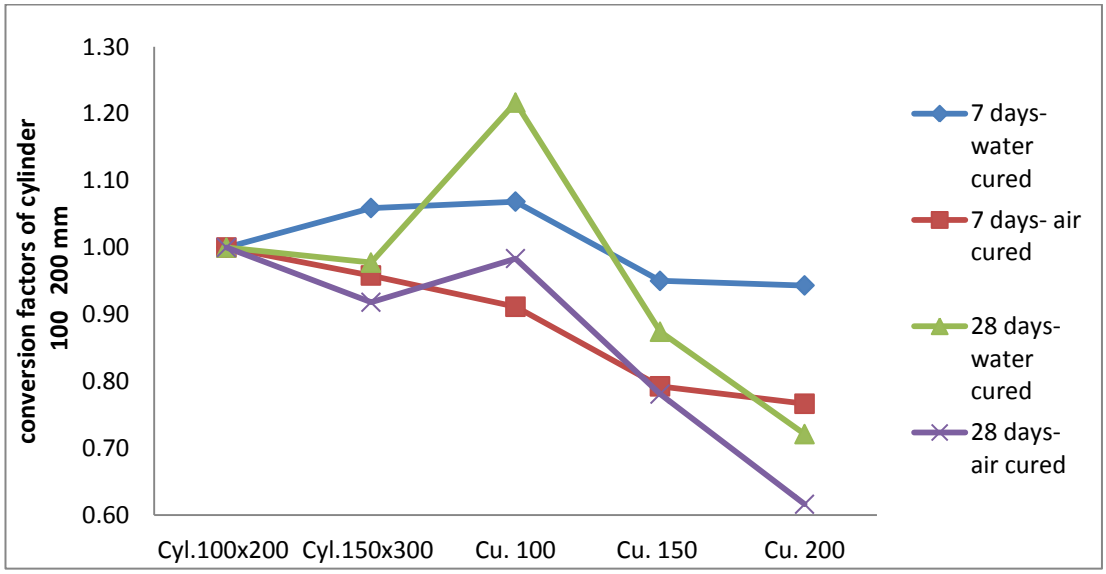

Figure 4.29: Conversion factors of cylinder 100×200 mm for mix design C

Each of these figures shows the conversion factors of cylindrical specimens of 100×200 mm. As an example, in order to convert compressive strength of cylinder 100×200 mm to cube 100 mm, for mix design C, air cured and tested at 7 days, the cylinder's compressive strength should be divided by 0.91 (Figure 4.29).

As an explanation for figures 4.27 to 4.29, it can be said that for mix design C, with the lowest w/c ratio and highest expected compressive strength, the tendencies of samples at the same age are identical to each other. For 7 days conversion factors, there is a mild decreasing trend generally, while for conversion factors at 28 days, after a mild decrease in the beginning, there is a sharp increase at the point of cube 100 mm, and then again a decreasing trend begins for both of them.

For mix design B, the same explanation can be said for only one testing age, which is 28 days. Both of the graphs have identical graphs and also overall decreasing trend. On the other hand, for testing age of 7 days, there are different growing trends. However, both of them still have decreasing trend.

For mix design A, although there is still a noticeable trend of declining, none of the graphs are identical to each other.

Decreasing trend of these figures is obvious because of cubes of 200 mm, which have higher compressive strength than other specimens.

The reason of these similarities and differences might be attributed to the strength of concrete bonds. As it is shown for mix design C, which possesses the strongest bond among all, for both of the testing ages, changing trend of the conversion factors are similar. The same explanation is valid for mix design B (medium strength bond), at the testing age of 28 days in which the concrete strength is higher than testing age of 7 days. Finally for mix design A, which has the least expected strength, none of changing trends of 28 days or 7 days are similar to each other.

For investigating cylindrical specimen of 150×300 mm, figures 4.30 to 4.32 are plotted.

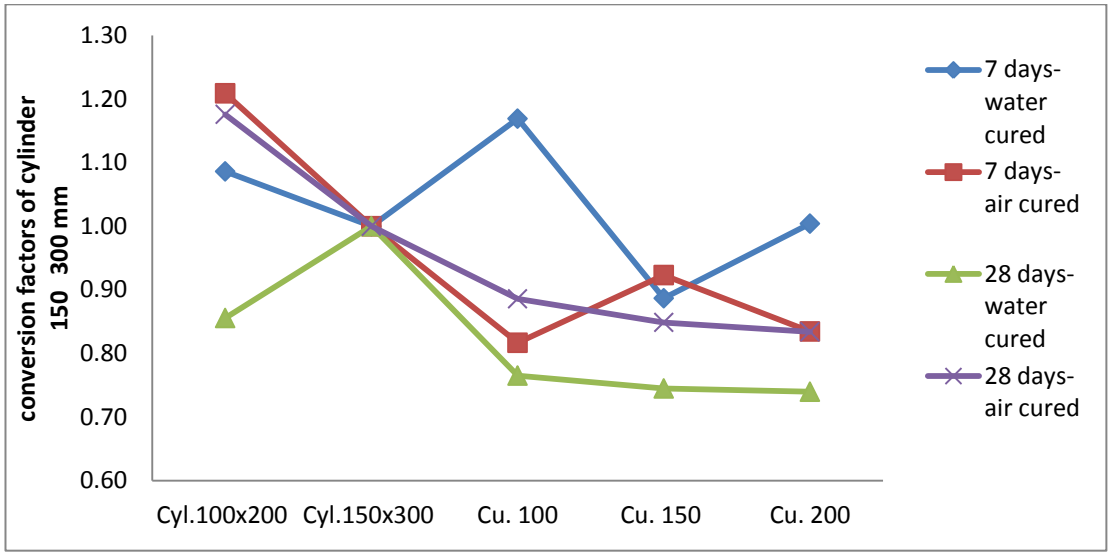

Figure 4.30: Conversion factors of cylinder 150×300 mm for mix design A

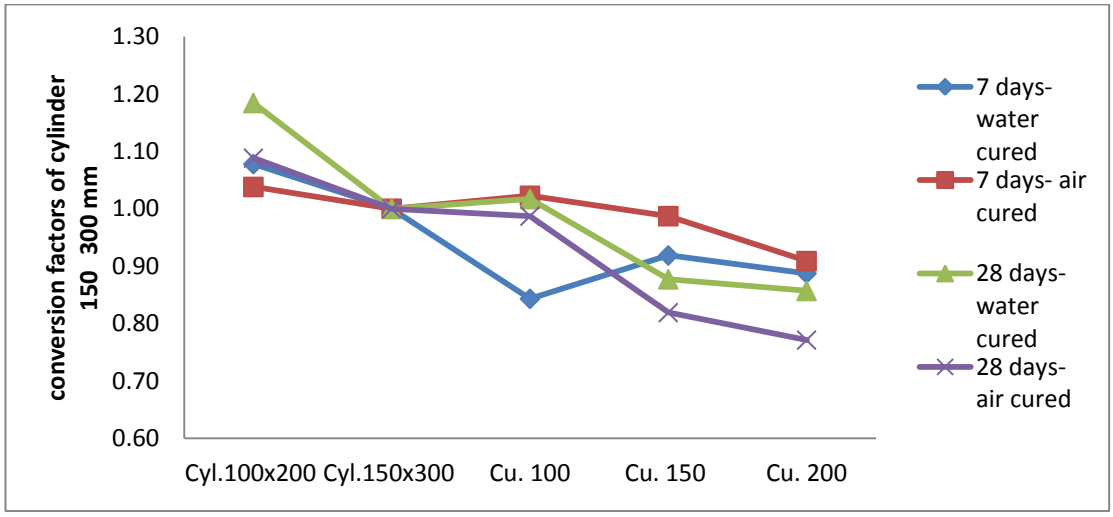

Figure 4.31: Conversion factors of cylinder 150×300 mm for mix design B

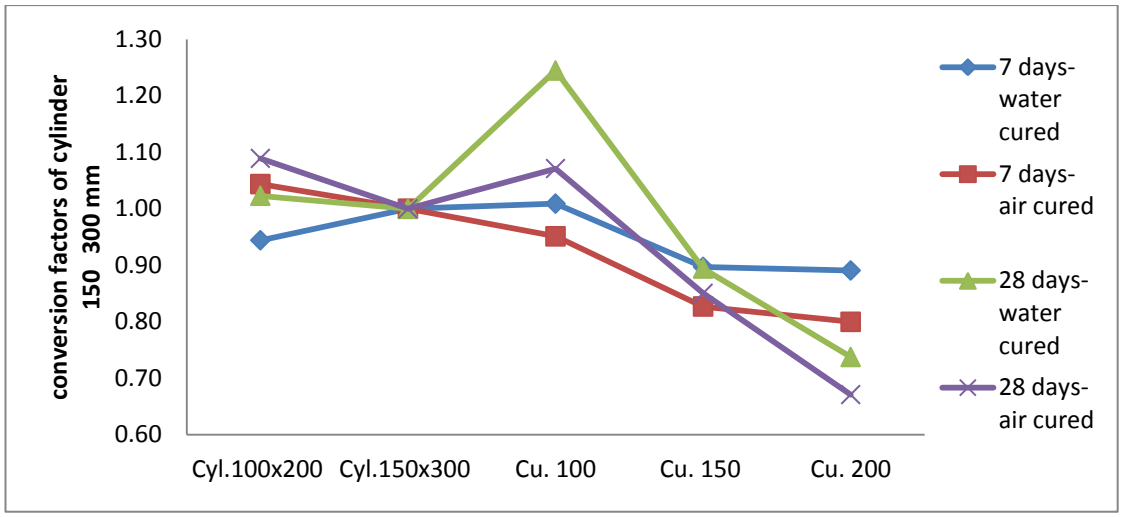

Figure 4.32: Conversion factors of cylinder 150×300 for mix design C

For cylinders 150×300 mm, the similarities of the graphs are similar to the graphs of cylinder 100×200. In mix design C, graphs of testing age at 7 and 28 days are identical to each other. In mix design B, only the graphs of 28 days are like each other and in mix design A, none of the trends are similar to each other.

It can be claimed that, the similarities are due to strength of bonds of specimens (as was explained for graphs of cylinder 100×200), in a way that the strength of the bonds governs the changing trend of conversion factors of the specimens.

Conversion factors' graphs of cubes of 100 mm are shown in figures 4.33 to 4.35.

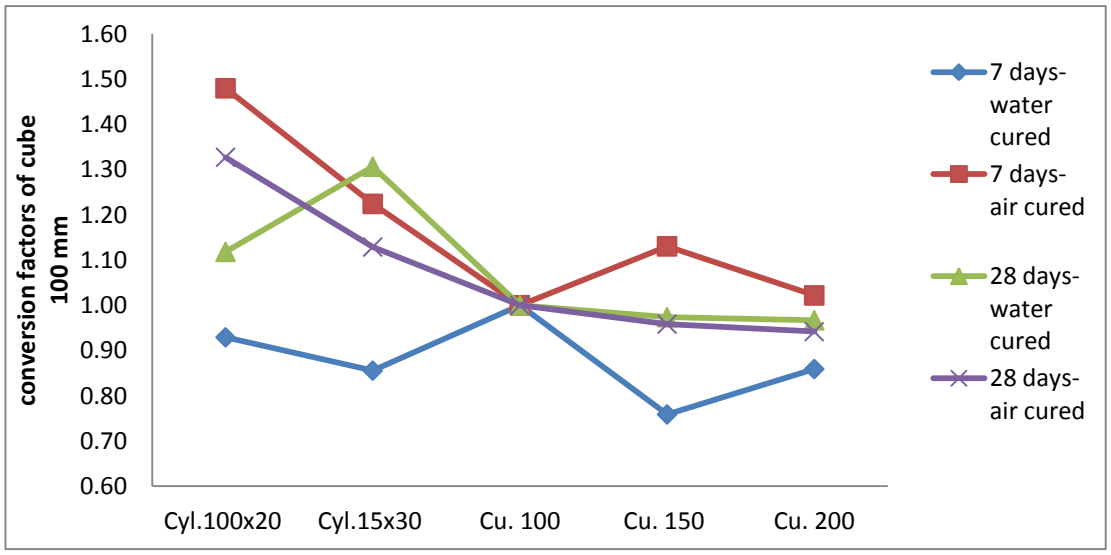

Figure 4.33: Conversion factors of cube 100 mm for mix design A

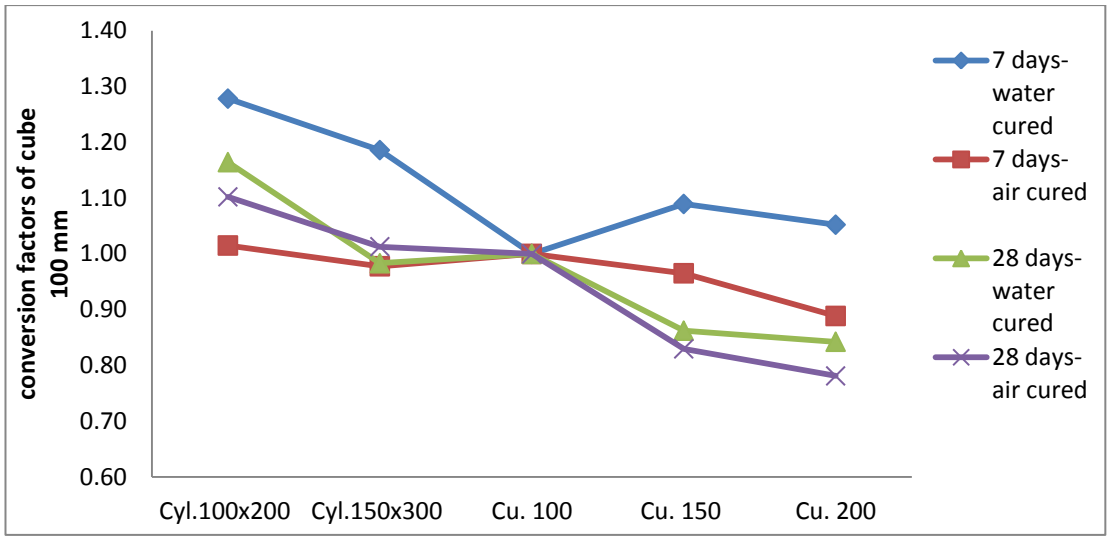

Figure 4.34: Conversion factors of cube 100 mm for mix design B

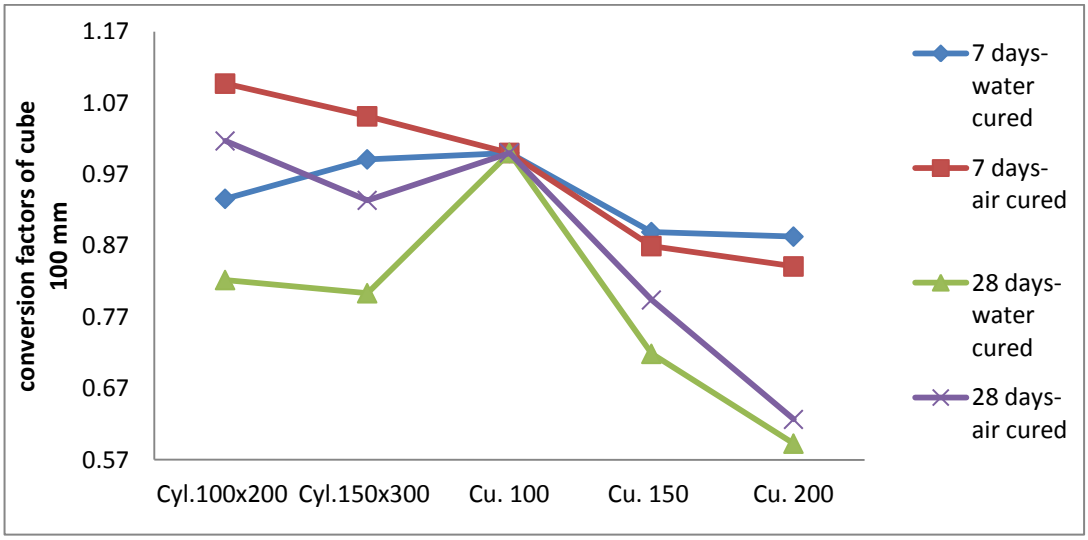

Figure 4.35: Conversion factors of cube 100 mm for mix design C

In Figure 4.33, no identical trend can be noticed among the graphs of conversion factors, while in Figure 4.34, only graphs, which convert samples tested at 28th day are alike each other, by having the same breaking points. In Figure 4.35, for mix design C, the samples with the same testing age are identical to each other.

It is again possible to refer these changing trends to strength of concrete bonds.

To investigate about specimens of cube 150, figures 4.36 to 4.38 have been plotted.

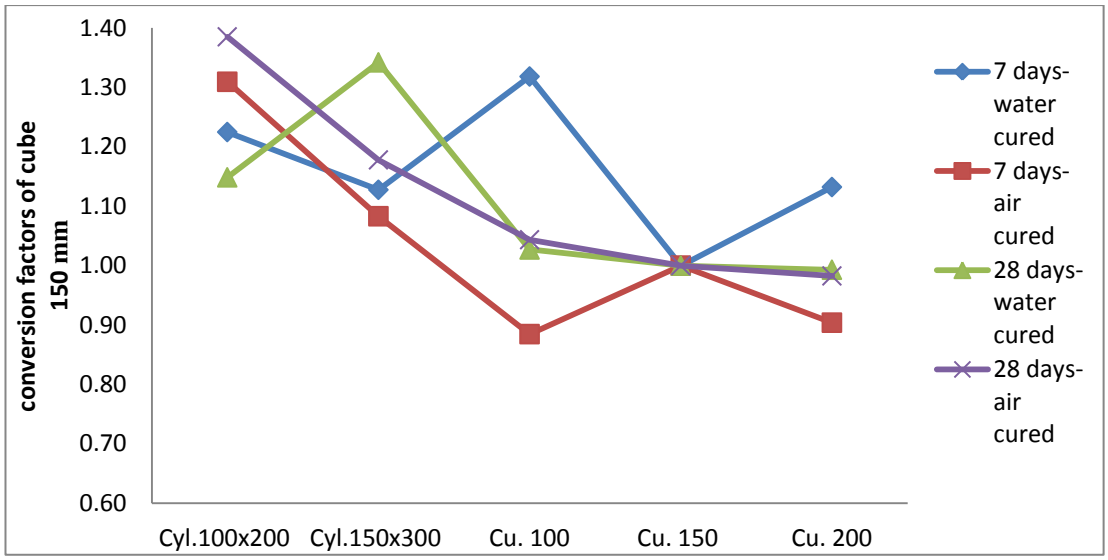

Figure 4.36: Conversion factors of cube 150 mm for mix design A

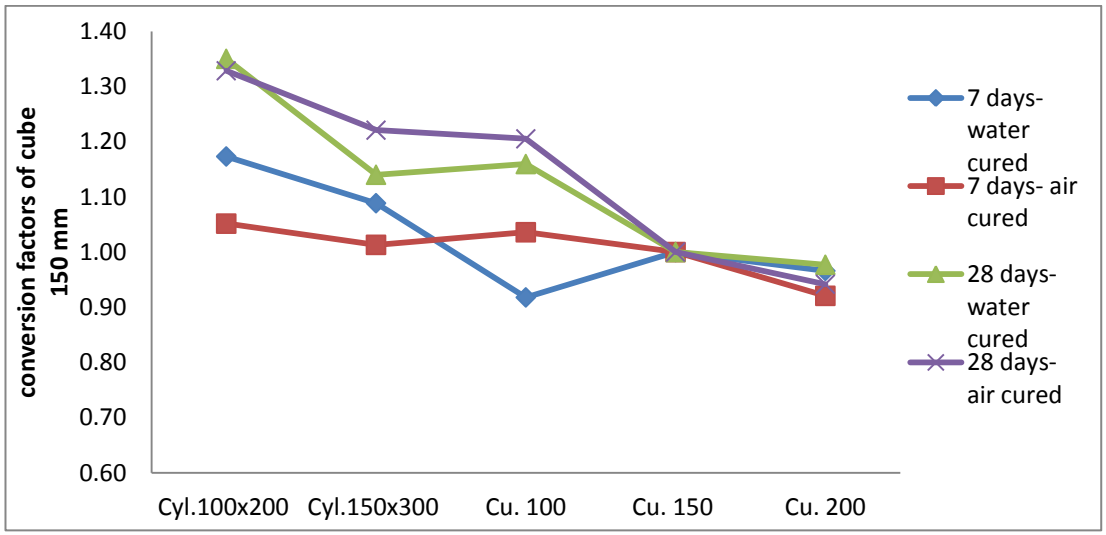

Figure 4.37: Conversion factors of cube 150 mm for mix design B

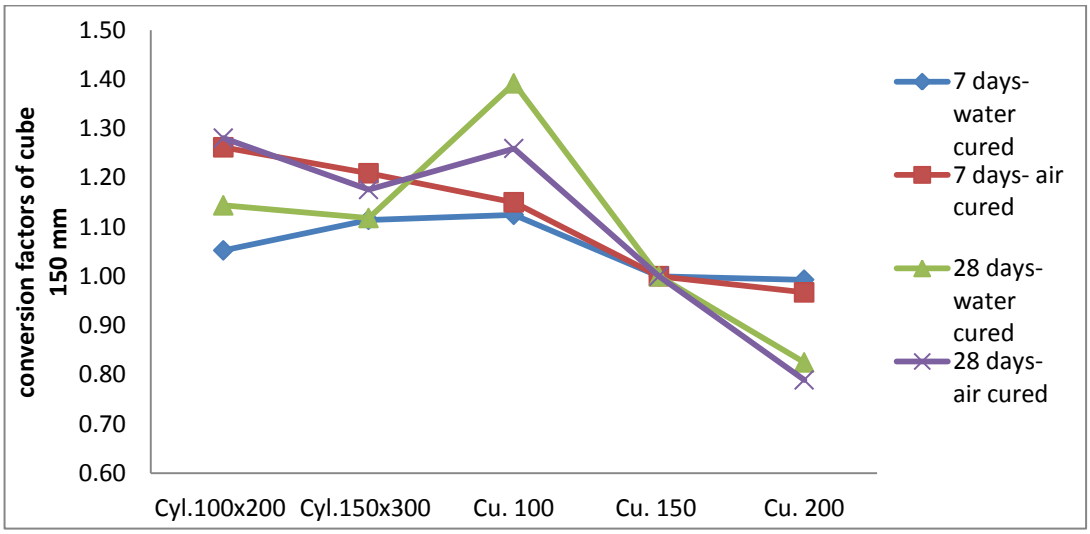

Figure 4.38: Conversion factors of cube 150 mm for mix design C

In the changing trends of the graphs of cube 150 in mix design C, graphs of testing age at 28 days and 7 days are similar to each other. In mix design B, only the graphs of 28 days are identical and in mix design A, none of the graphs are similar.

As from the samples of mix design A, testing age of 7 days, to samples of mix design C, testing age of 28 days, a steady growth of concrete bond's strength is expected, the similarities' changing trends can be ascribed to the concrete bonds' strength (as it has been again explained for previous specimens).

In the following section, the respective graphs of cubes of 200 mm are plotted.

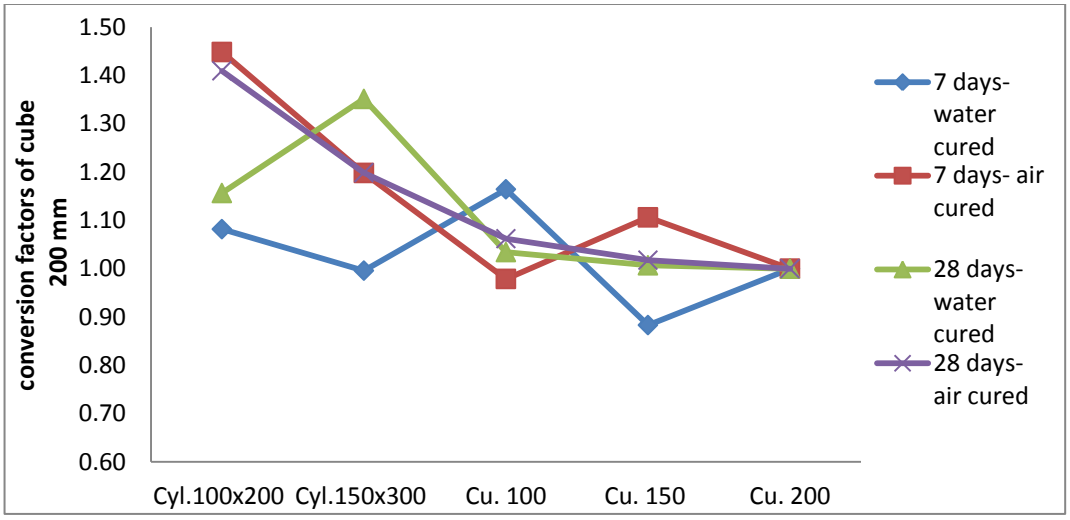

Figure 4.39: Conversion factors of cube 200 mm for mix design A

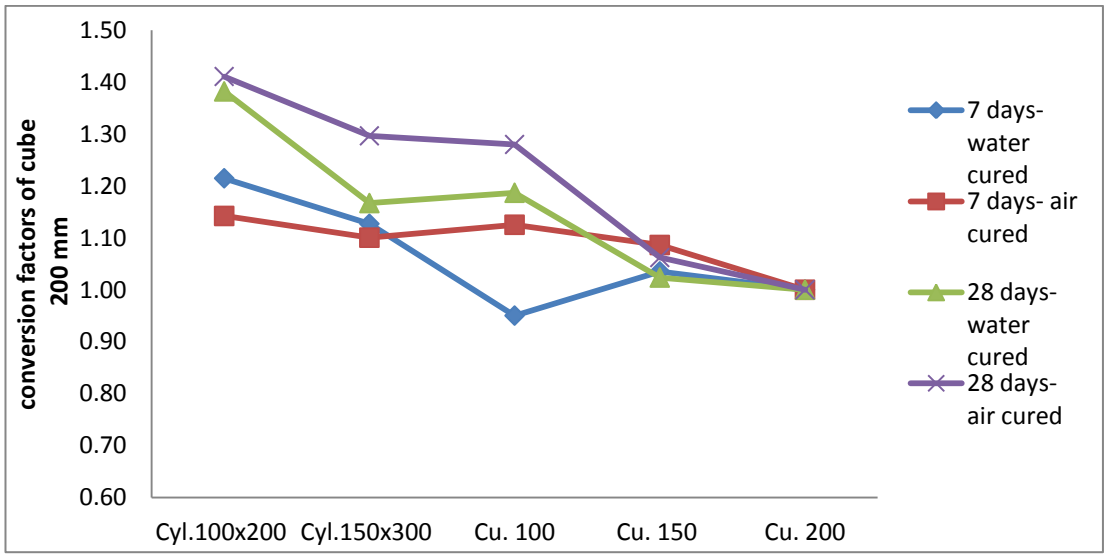

Figure 4.40: Conversion factors of cube 200 mm for mix design B

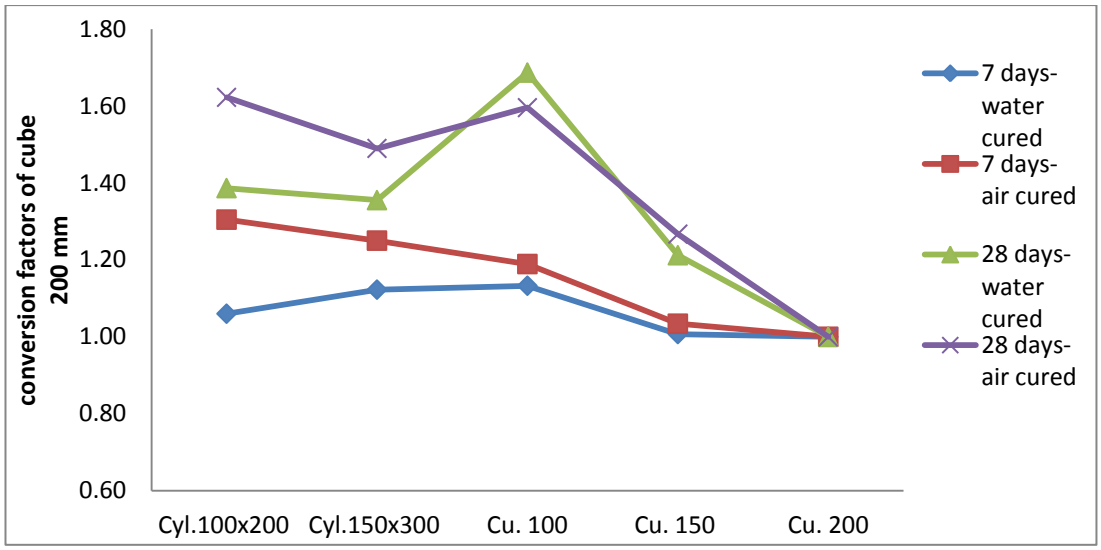

Figure 4.41: Conversion factors of cube 200 mm for mix design C

The similarities between graphs of testing age of 28 days and graphs of 7 days are observed for mix design C, in Figure 4.41. In mix design B, the identical graphs of testing age of 28 days are noticeable. Finally, for mix design A, no similarity between samples can be observed. In other words, the same resemblances, as the previous figures with a good approximation, are again repeated for cubic specimens of 200 mm size.

These observations can again certify the reason of bond strength of concrete specimens for formation of similar conversion factors' changing trends.

In other words, according to these observations, if the concrete's bond's strength is beyond a specific level, the concrete's samples of different shape and size will have similar changing trends at the same testing age.

According to Arioz et al. (2007), it was proposed that the conversion factors possibly decrease by age, although, in this investigation, the hypothesis was not observed in all the graphs.

Common trend of all the specimens is their decreasing movement toward the last point. This is due to high strength of cube 200 mm. This means that compressive strength of cubes having size of 200 mm is higher than the compressive strength of

other specimens. As a result, when other samples' compressive strengths are divided by the strength of 200 mm cubic specimen, the least value is given out. As in the horizontal axis, the last specimen is cube 200 mm; the trends of graphs are the decreasing one. In the case when cube 200 mm is investigated (Figures 4.39 to 4.41), the least amount of conversion factors is 1, which is allocated to cube 200 mm; hence, the decreasing trend is still kept.

4.4.2.5 Investigation of different curing condition

This section of the research was performed in order to see the variation of conversion factors of compressive strength by changing curing conditions. This analysis has been only performed on samples which have been tested at the age of 28 days.

A total amount of 10 figures have been plotted, which are shown in the following pages.

The points of figures are compressive strength vs. compressive strength of samples. Consequently, the slopes of graphs' trend lines approximately indicate the average value of conversion factors of specimens. Moreover, the figures are only plotted for half of the conversion factors; the value of other half is just equal to inverse of these values.

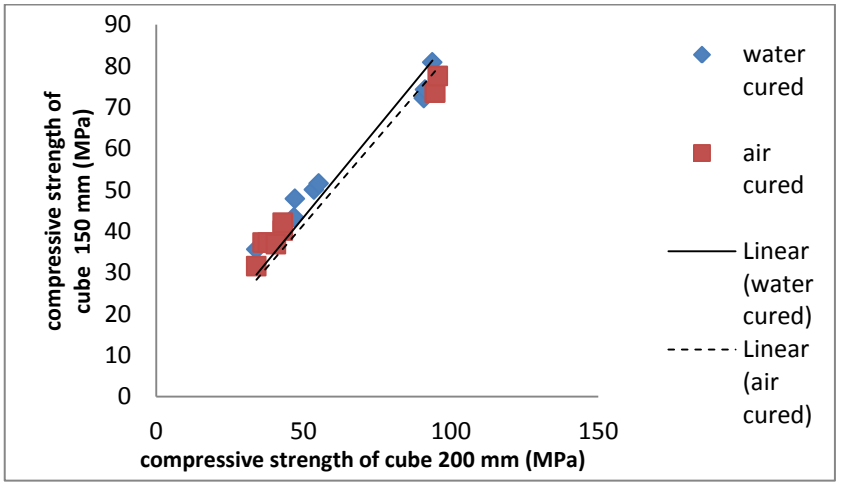

Figure 4.42: Compressive strength of cube 150 mm vs. cube 200 mm

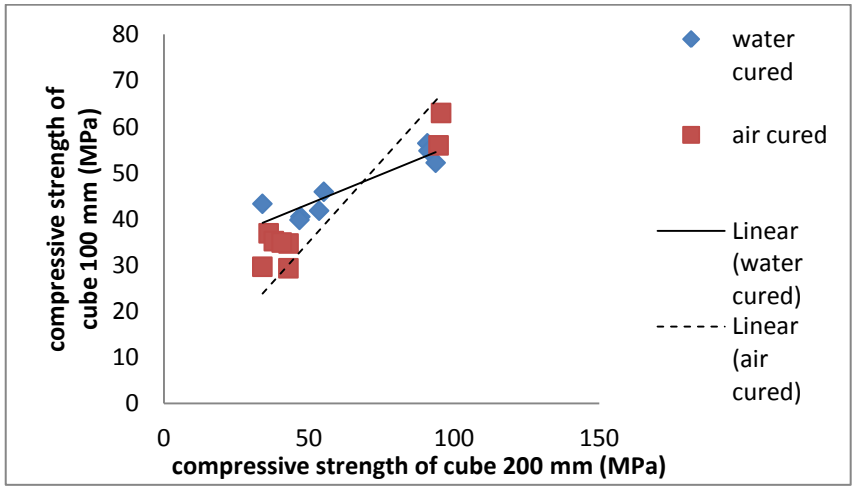

Figure 4.43: Compressive strength of cube 100mm vs. cube 200mm

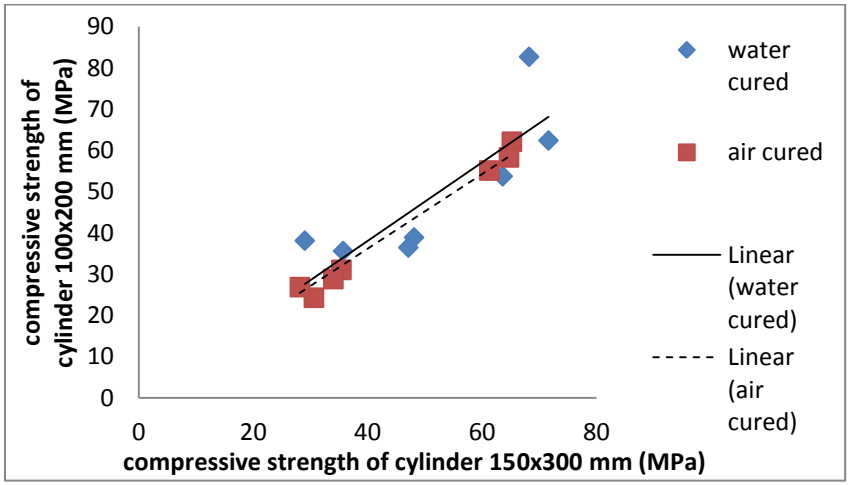

Figure 4.44: Compressive strength of cyl.100×200 mm vs. cyl.150×300 mm

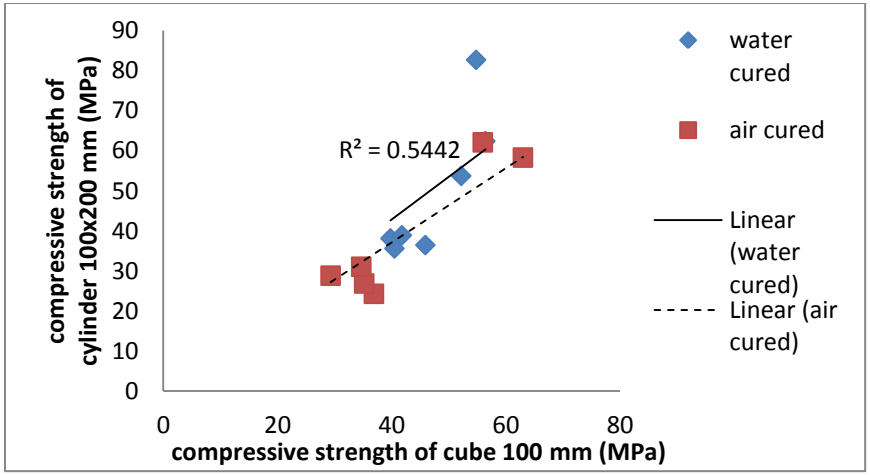

Figure 4.45: Compressive strength of cyl.100×200mm vs. cube100 mm

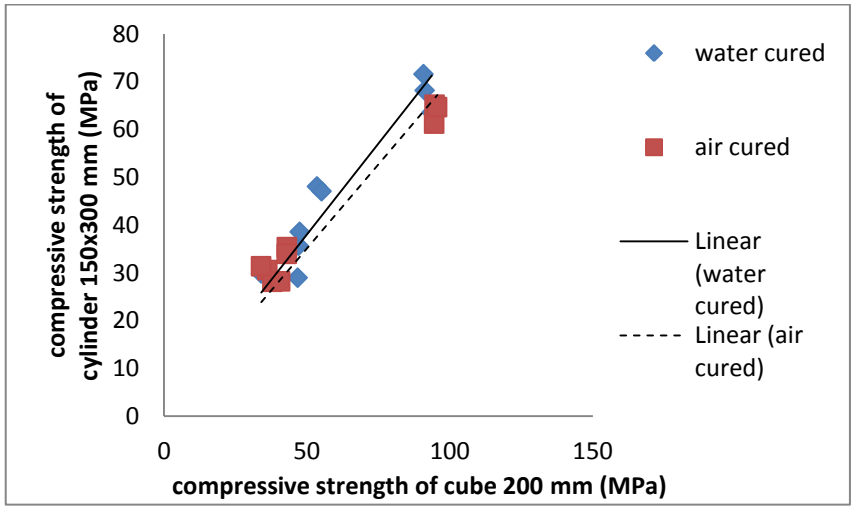

Figure 4.46: Compressive strength of cyl.150×300 mm vs. cube 200 mm

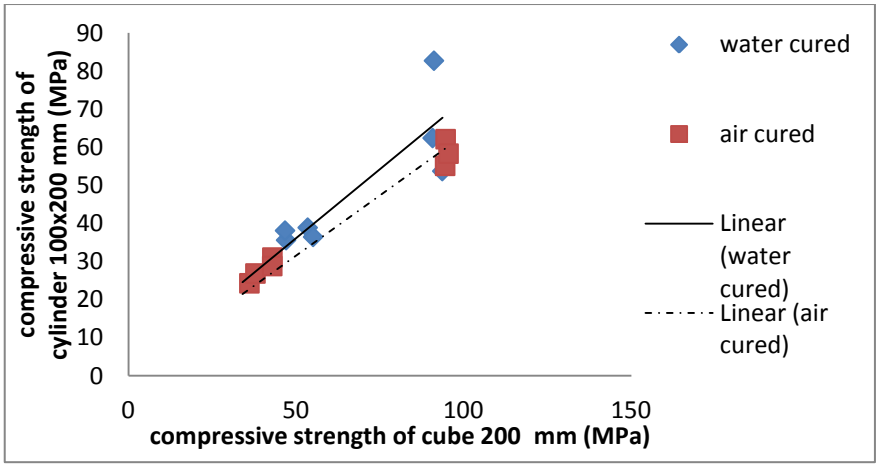

Figure 4.47: Compressive strength of cyl.100×200mm vs. cube 200 mm

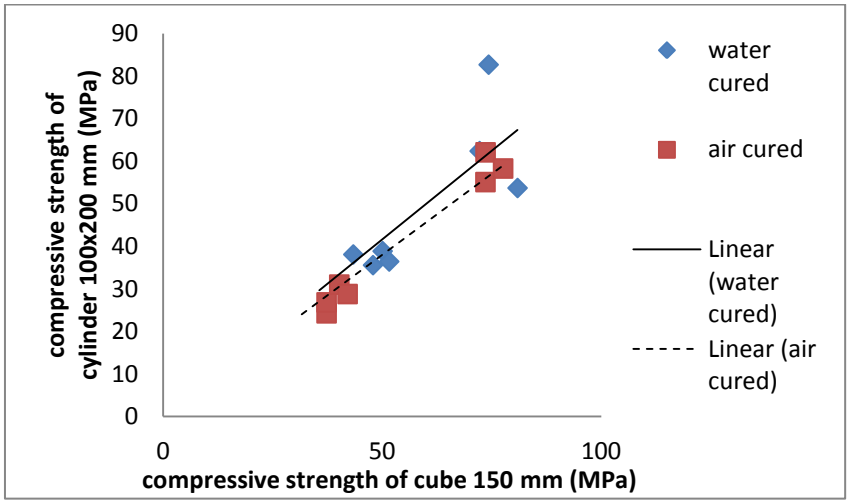

Figure 4.48: Compressive strength of cyl.100×200mm vs. cube 150 mm

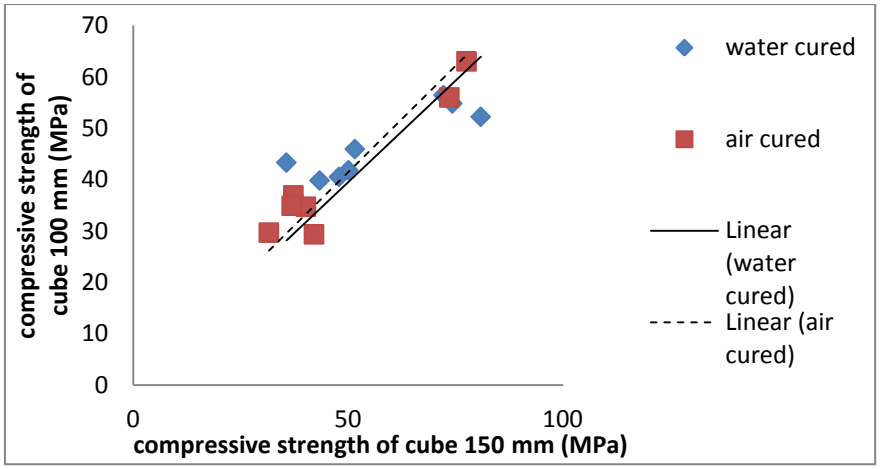

Figure 4.49: Compressive strength of cube 100 mm vs. cube 150 mm

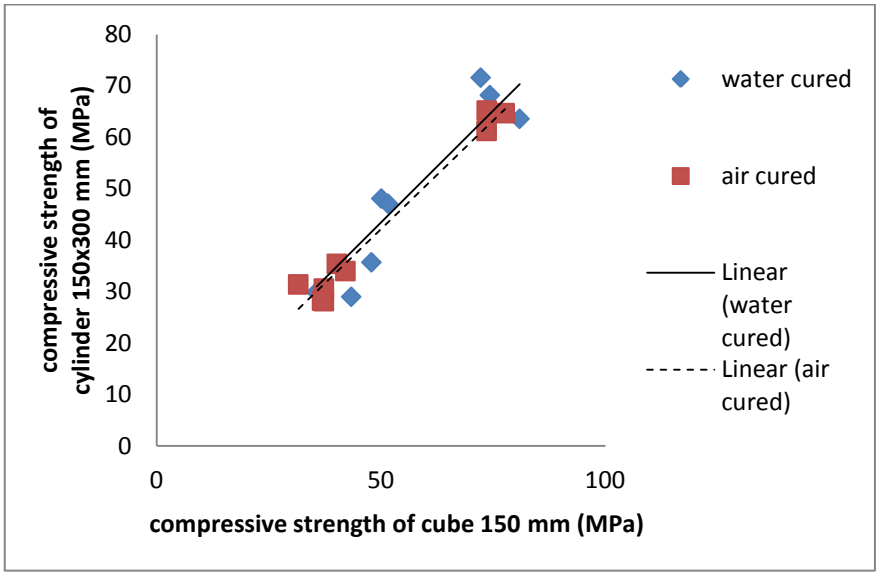

Figure 4.50: Compressive strength of cyl.150×300 mm vs. cube 150 mm

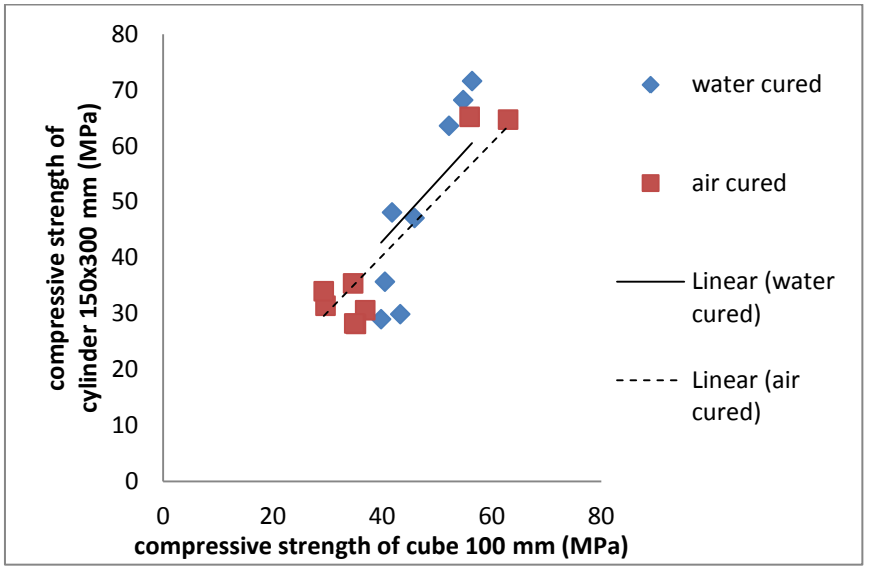

Figure 4.51: Compressive strength of cyl.150×300 mm vs. cube 100 mm

From most of these figures, it can be seen that the trend line of graphs of water cured sample are sharper in slope. In other words, the value of conversion factors for water cured samples is higher than that of air cured samples.

In the case of converting cube 150 mm to cube 200 mm, cylinder 100×200 mm to cylinder 150×300 mm and cylinder 150×300 mm to cube 150 mm, the difference between slopes is lower. However, generally, the differences are especially significant when converting cubes to cylinders or the opposite.

4.4.2.6 Investigating stress-strain curves

Another analysis which was performed was the stress-strain behavior of specimens having different shapes and sizes.

Among each three samples, one of the samples was chosen for plotting stress strain curve by using the strain-rate controlled testing machine.

The area under the load- deformation curves which have been calculated by using DataFit V.9.0.59 software is shown in Table 4.28.

In this section, typically, stress- strain curves of concrete specimens, with mix design B, air cured and tested on 28 days, have been shown.

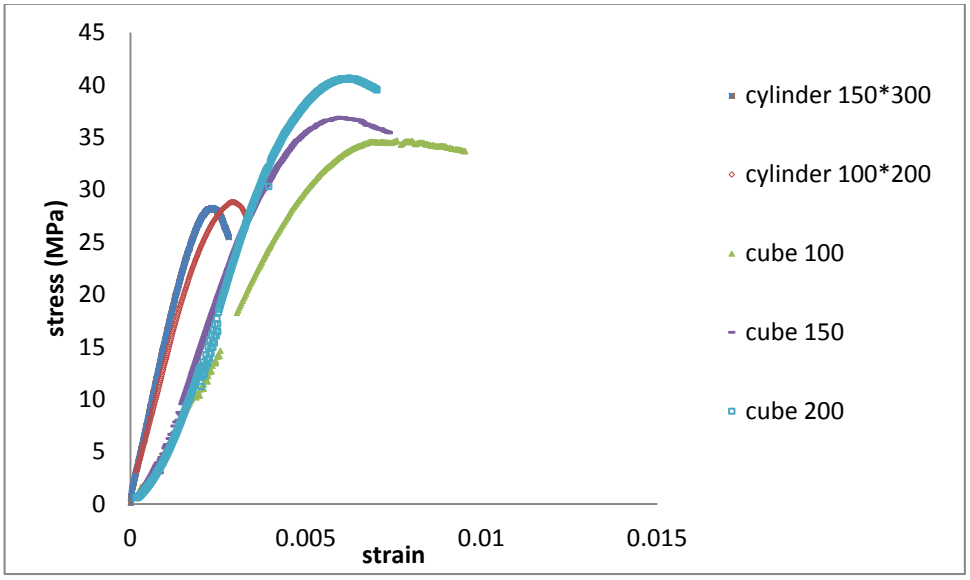

Figure 4.52: Stress- strain curves of mix design B at 28 days cured in air

According to Figure 4.52, it is obvious that cubic specimens, especially cube 200 mm, reach to higher compressive strengths.

It can also be observed that cubic and cylindrical specimens' trend is alike each other but there are differences between cubes and cylinders.

In addition to higher stress, it can be noticed that at their ultimate point, cubic specimens have also reached to larger strains.

The post-peak behaviors of the graphs of different shaped specimens are different as well. Cubic specimens mostly have mild decreasing trend after the peak point, while the cylinder specimens' graphs mostly decrease sharply, after their ultimate loading.

Mild post-peak decreasing trend of cubic specimens' graphs indicates large energy dissipation after fracture. In addition, for cylinders, as they have sharper stress-strain curves, more brittle behavior can be considered for these specimens. The reason of these observations can be attributed to the fracture pattern of the different shaped specimens (Del Viso, Carmona, & Ruiz, 2008). The large energy dissipations for cubic samples are in accordance with the fracture pattern of the specimens. In normal conditions, the fracture pattern of cubic samples, begin from their external edges and continues to a final shape of hour-glass failure form. In contrast, for cylinders, the fracture starts with internal structural failures, which suddenly triggers and a main fracture surface is formed, i.e. the behavior of cylinders, in fracture is more brittle than cubes (Del Viso, Carmona, & Ruiz, 2008). Having different fracture pattern, it is expectable that they have different stress-strain curves. In figures 4.53 and 4.54 typically two fractures specimens of cylinders and cubes are shown, respectively.

Figure 4.53: fractured cylinder specimen

Figure 4.54: Fractured cubic specimen

In addition to these explanations, it should also be noted that for both shapes of cubes and cylinders, by decreasing the specimen's size, their ultimate points' strain decreases, i.e., maximum strain of cube 200 mm (equal to 0.006217) is less than that

of cube 100 mm (equal to 0.0086346), and the same for cylinders. In other words, by increasing the size of cubic specimens, their behavior tends to be more brittle. However, this is more pronounced in cubic specimens.

The results of this section of analyses were in accordance with results of (Del Viso, Carmona, & Ruiz, 2008).

It should be explained here that the missing region in cube of 200 mm was a machine error in recording the data; however, the trending costume of the graph is not disturbed.

In Table 4.28, the results of area under the curves of stress strain diagram are shown. The values have been calculated by using Data fit software.

Table 4.28: Area under stress-strain diagram (N.m)

testing age	28 days					
Mix design	A		B		C	
curing condition	water	Air	Water	Air	Water	Air
Cyl.100×200	55.60	29.04	47.50	99.27	180.34	159.98
Cyl.150×300	278.04	393.57	375.14	277.27	613.46	632.78
Cu. 100	234.61	360.23	105.97	226.30	361.42	427.27
Cu. 150	410.45	747.66	432.33	606.14	445.24	952.64
Cu. 200	1188.13	2058.10	1538.34	1385.80	1434.08*	1560.05*
testing age	7 days					
Mix design	A		B		C	
curing condition	Water	Air	Water	Air	Water	Air
Cyl.100×200	41.02	52.49	61.84	60.28	176.61	160.65
Cyl.150×300	237.21	193.39	251.26	266.94	518.31	430.10
Cu. 100	140.77	35.63	118.10	170.25	296.10	232.41
Cu. 150	351.27	269.86	358.92	394.68	494.28	529.88
Cu. 200	736.58	855.14	932.34	829.01	1729.37	1558.25

* The amounts show area under load-deformation curve up to the maximum measured load.

In both of the testing ages, by increasing compressive strength and increasing the specimens' size, the area under the load- deformation curve increases.

Figure 4.55 to 4.58 of the next page show the area under load- deformation curves.

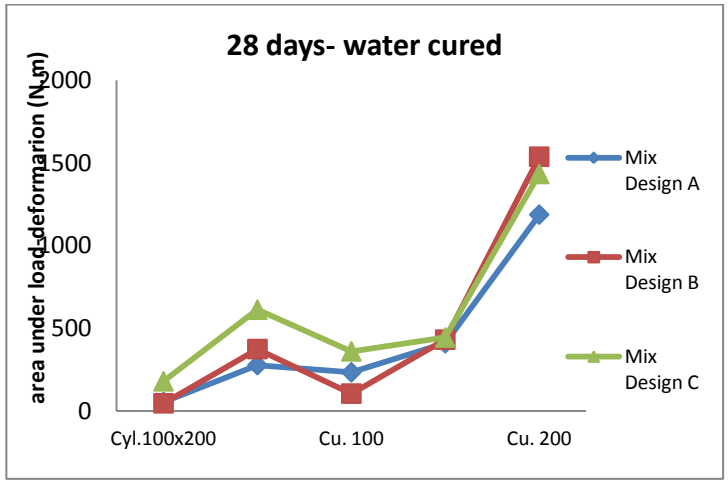

Figure 4.55: Area under load-deformation curve of samples at 28 days cured in water

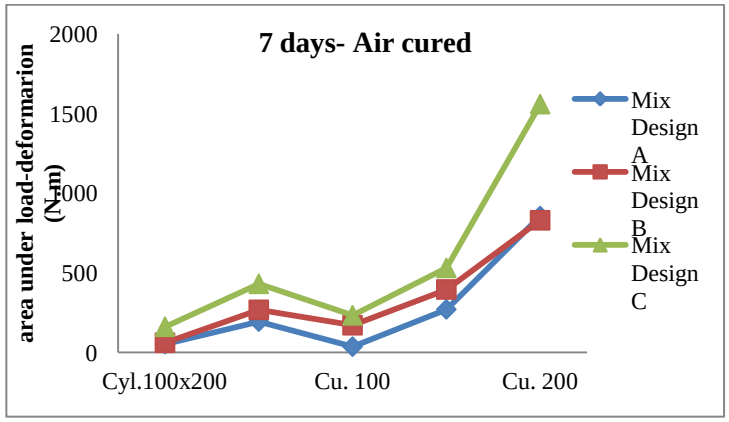

Figure 4.56: Area under load-deformation curve of samples at 7 days cured in air

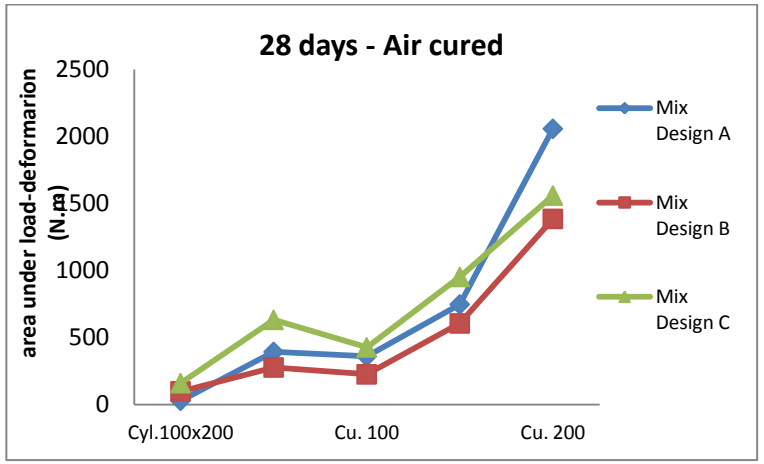

Figure 4.57: Area under load-deformation curve of samples at 28 days cured in air

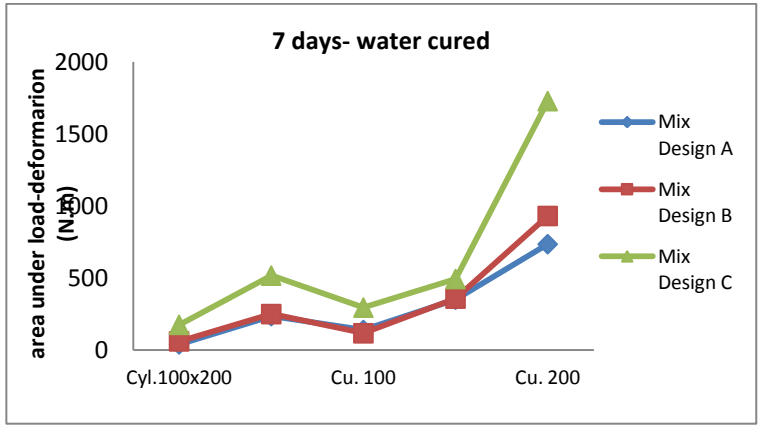

Figure 4.58: Area under load-deformation curve of samples at 7 days cured in water

If the graphs of each of the figures are investigated, similarities can be observed among the figures. In all the graphs, the area under load-deformation curve for cylinder 150×300 mm is larger than that of cylinder 100×200 mm.

Also for cubic specimens, increasing the size causes an increase in the area under stress-strain diagram.

Increasing the area by size, in fact means that the specimens absorb more energy until their fracture point. In other words, in this investigation, increasing the size has caused specimens to have stronger bonds, so that when loaded, a large amount of energy should be consumed until their fracture point.

It should be added that as mentioned before, the testing procedure for the cubic specimens of 200 mm, water and air cured, 28 days tested, was stopped due to exceeding the loading capacity of the machine. As a result, their corresponding amounts in Figure 4.53 and Figure 4.55 are the area under their load deformation curves until the last recorded stress-strain data.

The discussions about stress-strain behavior of the specimens here are only about the selected curves which have been shown in this section. The rest of the curves also have identical trends and the results can be also valid for them. The stress-strain curves of samples of other conditions are given out in the appendix 1.

Chapter 5

CONCLUSIONS

Investigating the effect of specimens' shapes and their sizes on the outcomes of different experiments was the main goal of this research. Different specimens' size effect and shape effect were studied on the results of non-destructive tests (rebound hammer and PUNDIT) as well as destructive tests of compressive and splitting tensile strength. Through the analyses, conversion factors for converting compressive or splitting tensile strength of different specimens to each other were calculated and it was tried to understand how these factors change by changing curing type, testing age and mix design.

The complete experimental section of this research included various experiments such as slump and VeBe time, hardened concrete density, ultrasonic pulse velocity (PUNDIT), rebound hammer, splitting tensile strength, and compressive strength.

The following conclusions can be done from this study:

1. By decreasing the water/cement ratio, workability of concrete matrices decreases.

2. By changing mix design, and reducing the water/cement ratio, hardened density of concrete samples increases due to having stronger bonds. However, using high grade cement can cause disruptions in the increasing trend.

3. Changing curing type causes the average density changes. The average density of concrete samples is lower for the ones cured in air.

4. As the cubic specimens size increases, the specimens resulted in higher ultrasonic pulse velocity (i.e. faster pulse speeds). The observations can be due to stronger (more homogeneous) bonds and higher maximum aggregate density in larger specimens.

5. As the fraction of coarse aggregates increases, if the maximum aggregates size is kept constant, smaller concrete samples might result in higher ultrasonic pulse velocities than biggest samples (cube 200 mm).

6. The results of PUNDIT tests are less scattered for larger specimens which indicate more homogeny of larger specimens.

7. The rebound hammer results against compressive strengths of samples are fairly linear for GGBS cement concrete.

8. The rebound hammer results of larger specimens were observed to be lower than smaller specimens. Due to having the same maximum aggregate size, the hammer is more willing to be stroke on aggregates than cement paste.

9. The effect of curing type in rebound hammer test results is also noticeable. Water curing causes samples to have stronger surface concrete. Therefore, water cured samples have higher rebound hammer results.

10. If the tensile strengths of all shapes of specimens are considered, the slope of the graph of splitting tensile strength vs. compressive strength will have an increasing trend.

11. Growing trend of splitting tensile strength by compressive strength for cubes and cylinders are different. Cubes' graphs increase sharply while cylinders have mild increasing trend.

12. Splitting tensile strength of concrete samples tends to have a changing trend by changing the specimen size. Up to a specific width, gradually by increasing in

width of specimens, the splitting strength decreases. After the specific point, the splitting tensile strength starts to increase.

13. Effect of size and shape of specimens on splitting tensile strength are more pronounced at higher strengths.

14. Compressive strength results were strongly influenced by their specimen sizes and wall effect.

15. When the concrete bonds are weaker, the results of compressive strengths seem to be more uniform, since the compressive strength of the samples are controlled by their bonds' strength.

16. If the testing ages of concrete specimens (for different sizes and shapes) are equal and if they are categorized as moderate or high strength concretes, the conversion factors of different specimens will have similar trends.

17. For testing concrete samples for quality control of concreting works, cylinder specimens of 150×300 mm seem to be the most reliable samples.

18. By decreasing the ratio of lateral surface/volume of specimens, the compressive strength increases.

19. When concrete samples are 28 days old, the average conversion factor of compressive strengths of water cured and air cured samples are equal to each other or have slight differences.

20. After the ultimate point of the stress-strain curves, cylinders have sharp decreasing trend while cubes' decreasing trend is milder.

21. Cubic specimens have higher ultimate strain compared to cylinders.

22. Fracture patterns of the specimens of different shapes are also different. Cylinders have a main fracture surface which causes a sharp fracture. Cubes have cracks in their surface which gradually grow and forms a glass-hour pattern.

23. The formats of stress-strain curves are in agreement with the fracture models of the samples. Cylinders release a large amount of energy suddenly (sharp decrease), while cubes release the energy gradually (mild decrease).

24. In all mix designs by enlarging the specimens' size, area under load deformation curves increases since the specimens can absorb more energy until their fracture.

REFERENCES

Arioz, O., Ramyar, K., Tuncan, M., Tuncan, A., & Cil, I. (2007). Some factors influencing effect of core diameter on measured concrete compressive strength. *ACI Materials Journal* , 291-296.

ASTM C 805/C 805M. (2008). *Standard Test Method for Rebound Number of Hardened Concrete.*

ASTM C 805/C 805M. (2008). *Standard Test Method for Rebound Number of Hardened Concrete* .

ASTM C39/C39M. (2011). *Standard Test Method for Compressive Strength of Cylindrical Concrete Specimens* .

Bažant, Z. P., & Planas, J. (1998). *fracture and size effect in concrete and other quasibrittle materials.* CRC Press.

Bažant, Z. P., Kazemi, M. T., Hasegawa, T., & Mazers, J. (1991). Size effect in Brazilian split-cylinder tests: Measurements and fracture analysis. *ACI Materials Journal* , 325-332.

British Standards Institution. (1986). BS 1881 : Part 1125 . *Methods for mixing and sampling fresh concrete in the laboratory* .

BS 146:2002. (2002, March). *Specification for blastfurnace cements with strength properties outside the scope of BS EN 197-1* . British Standards Institution.

BS 1881 : Part 114. (1983). *Testing concrete. Methods for determination of density of hardened concrete* .

BS 1881 : Part 116 : 1983. (1983). *Method for determination of compressive strength of concrete cubes* . British Standards Institution.

BS 1881 : Part 125: 1986. (1986). *Methods for mixing and sampling fresh concrete in the laboratory* . British Standards Institution.

BS 1881 : Part 125: 1986. (2009). *Methods for mixing and sampling fresh concrete in the laboratory* . British Standards Institution.

BS 1881 : Part 201. (2009). *Guide tc the use of nondestructive methods of test for hardened concrete* .

BS EN 12390-3:2009. (2009). *Compressive strength of test specimens* . British Standards Institution.

BS EN 12390-7. (2009). *Density of hardened concrete* .

BS5328 : Part 1 : 1997. (2000, December). *BRITISH STANDARD* . British Standards Institution.

Caldarone, M. A. (2009). *High-Strength Concrete: A Practical Guide.* Taylor & Francis.

Del Viso, J., Carmona, J., & Ruiz, G. (2008). Shape and size effects on the compressive strength of high-strength concrete. *Cement and Concrete Research* , 386–395.

Dongxu, L., Xuequan, W., Jinlin, S., & Yujiang, W. (2000). The influence of compound admixtures on the properties of high-content slag cement. *Cement and Concrete Research* , 45-50.

Elwet, D. J., & Fu, G. (1995). *Compression Testing of Concrete: Cylinders vs. Cubes.* New York: New York State Department of Transportation.

GGBS and concrete properties. (2007, June). Retrieved December 2011, from HeidelbergCement Group: http://www.heidelbergcement.com/NR/rdonlyres/B9870ADD-3C7C-4C3B-8501-74C3B0F2DAC2/0/GGBS..

GLENIUM. (n.d.). Retrieved October 2011, from BASF - The Chemical Company - Corporate Website: http://www.basf.com/group/corporate/en/brand/GLENIUM

GLENIUM. (n.d.). Retrieved October 2011, from BASF - The Chemical Company - Corporate Website: http://www.basf.com/group/corporate/en/brand/GLENIUM

Gonnerman, H. F. (1925). Effect of Size and Shape of Test Specimen on Compressive Strength of Concretes. *Structural Materials Resaearch Laboratory* , 1-21.

India Cements. (n.d.). Retrieved 2011, from India Cements: http://www.indiacements.co.in/asktheconcreteman.htm

Kadleček, S. V., Modrý, S., & Kadleček, J. V. (2002). Size effect of test specimens on tensile splitting strength of concrete: general relation. *MATERIALS AND STRUCTURES* , 28-34.

Malaikah, A. S. (2009). Effect of Specimen Size and Shape on the Compressive Strength of High Strength Concrete. *Pertanika Journal of Science & Technology* , 87-96.

Neville, A. M. (2002). *Properties of concrete.* John Wiley & Sons.

Plowman, J., Smith, W., & Sheriff, T. (1974). Cores, Cubes and the Specific Strength of Concrete. *The Structural Engineer* , 421-426.

Safiuddin, M., Raman, S., & Zain, M. (2007). Effect of Different Curing Methods on the Properties of Microsilica Concrete. *Australian Journal of Basic and Applied Sciences* , 87-95.

Teychenné, F. E. (1997). *Design of normal concrete mixes.* Construction Research Communications Ltd.

Tokyay, M., & Ozdemir, M. (1997). Specimen Shape and Size Effect on the Compressive Strength of Higher Strength Concrete. *Cement and Concrete Research* , 1281-1288.

Turkel, A., & Ozkul, M. H. (2010). size and wall effects on compressive strength of concrete. *ACI Materials Journal* , 372-379.

Turkel, A., & Ozkul, M. H. (2010). Size and Wall Effects on Compressive Strength of Concretes. *ACI Materials Journal* , 372- 379.

Zheng, J. J., & Li, C. Q. (2002). Three-dimensional aggregate density in concrete with wall effect. *ACI Materials Journal* , 568-575.

APPENDIX

Appendix 1: Stress-strain curves

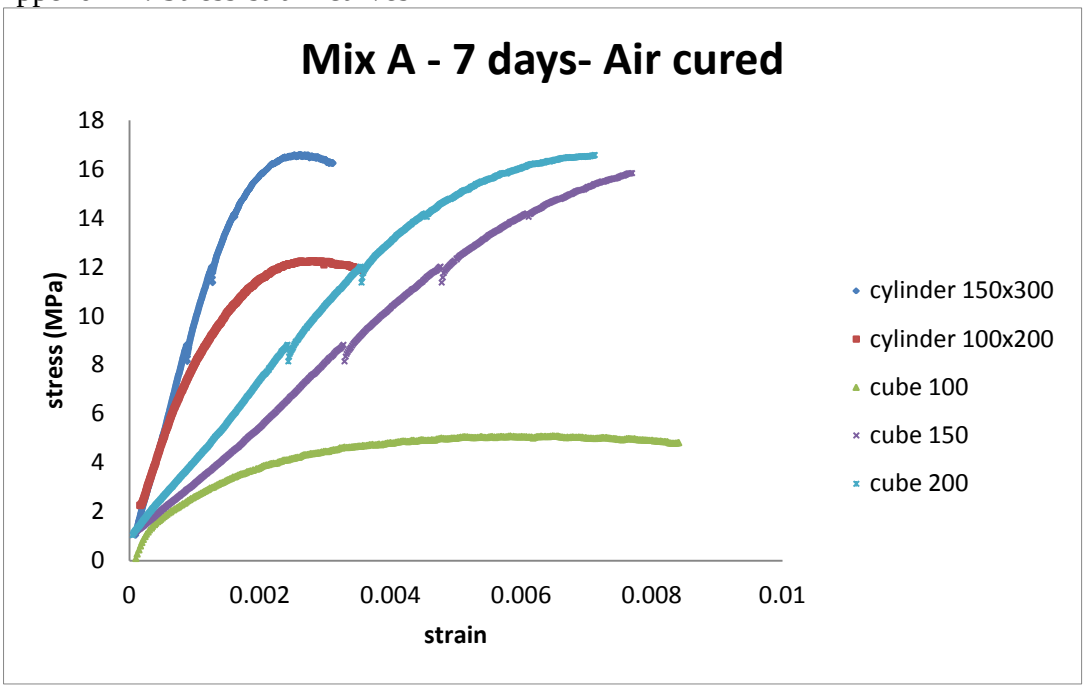

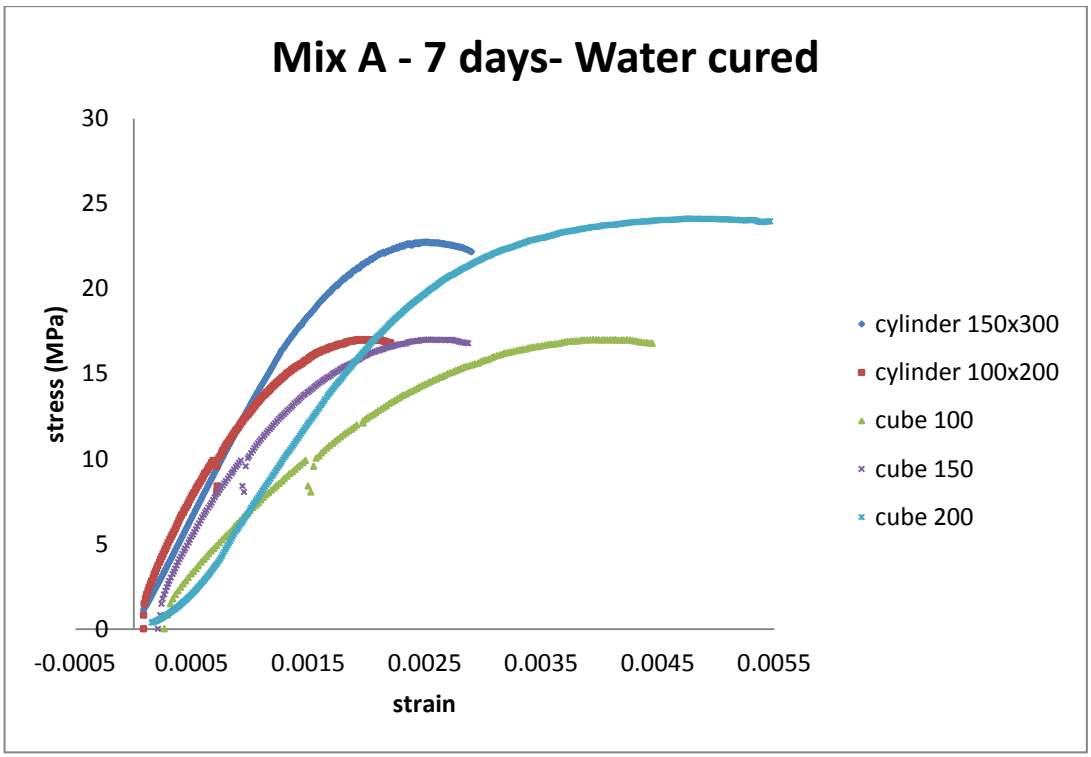

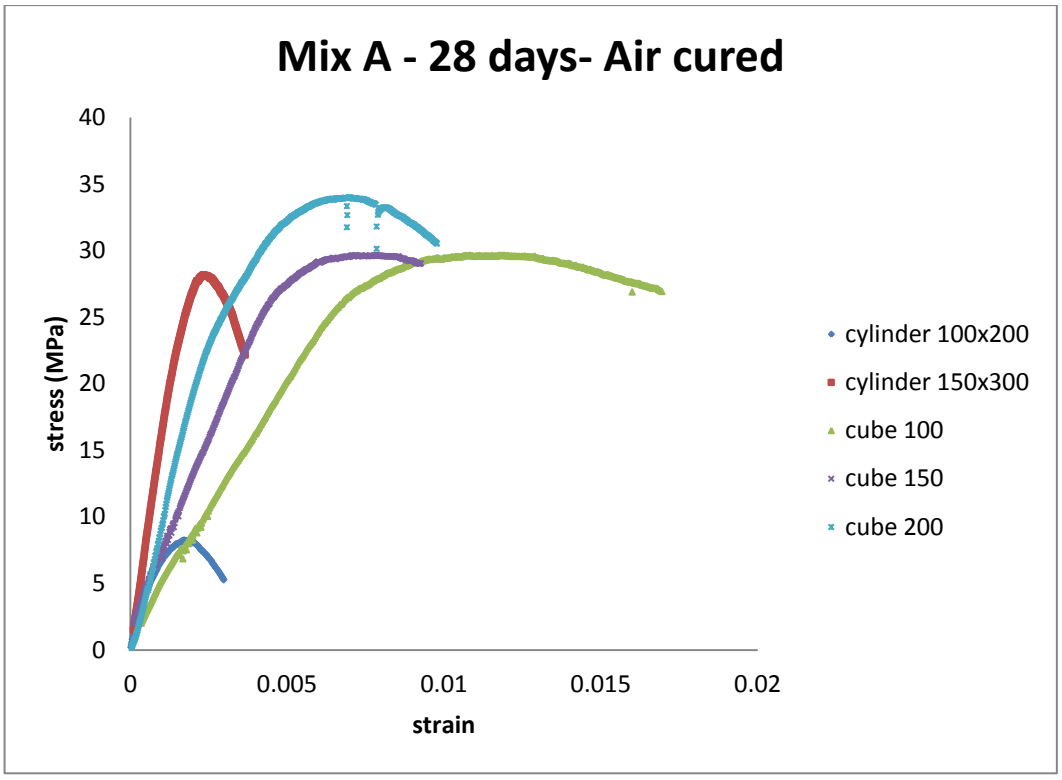
Mix A - 28 days- Air cured
stress (MPa)
strain
0
5
10
15
20
25
30
35
40
0
0.005
0.01
0.015
0.02
cylinder 100x200
cylinder 150x300
cube 100
cube 150
cube 200

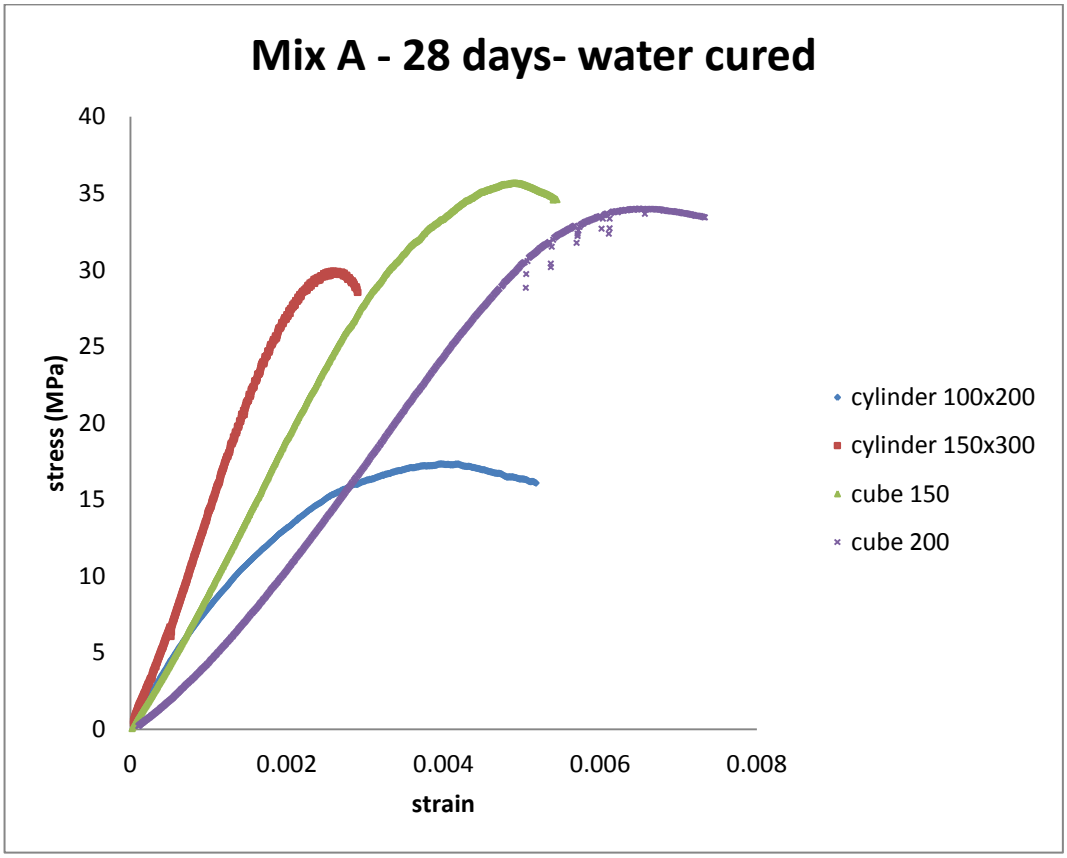
Mix A - 28 days- water cured
stress (MPa)
strain
0
5
10
15
20
25
30
35
40
0
0.002
0.004
0.006
0.008
cylinder 100x200
cylinder 150x300
cube 150
cube 200

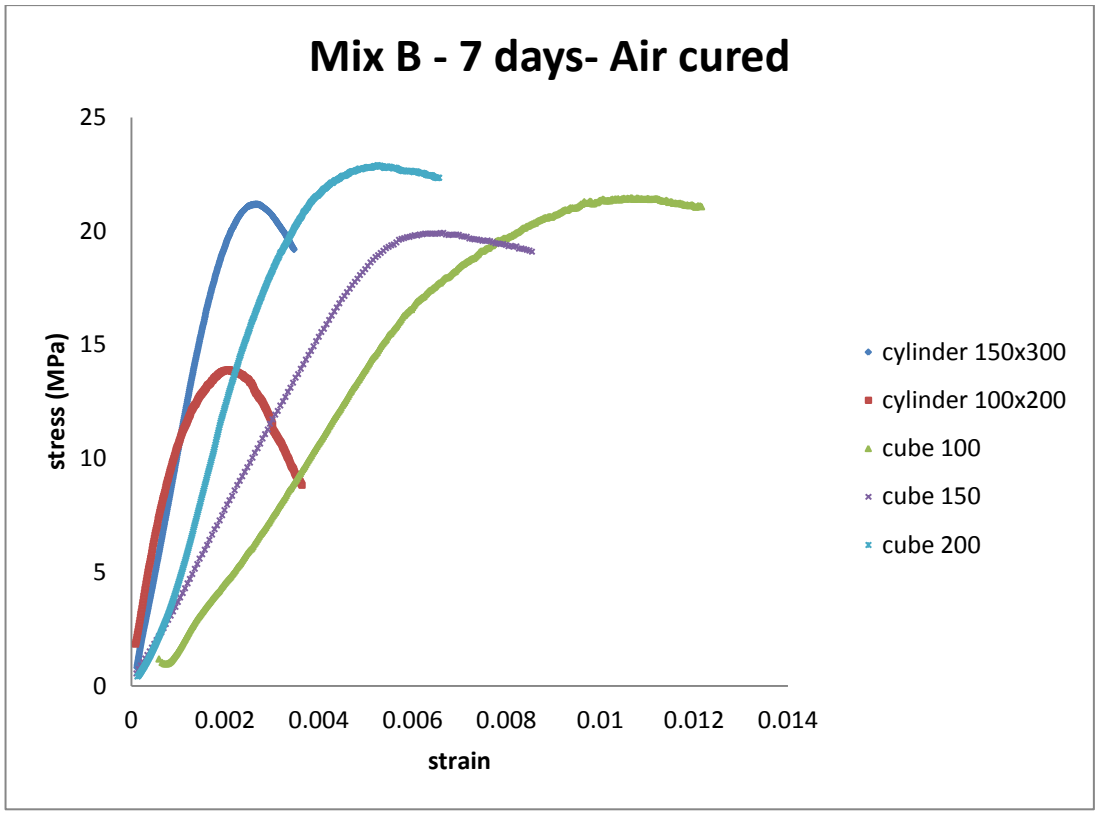
Mix B - 7 days- Air cured
stress (MPa)
25
20
15
10
5
0
0
0.002
0.004
0.006
0.008
0.01
0.012
0.014
strain
cylinder 150x300
cylinder 100x200
cube 100
cube 150
cube 200

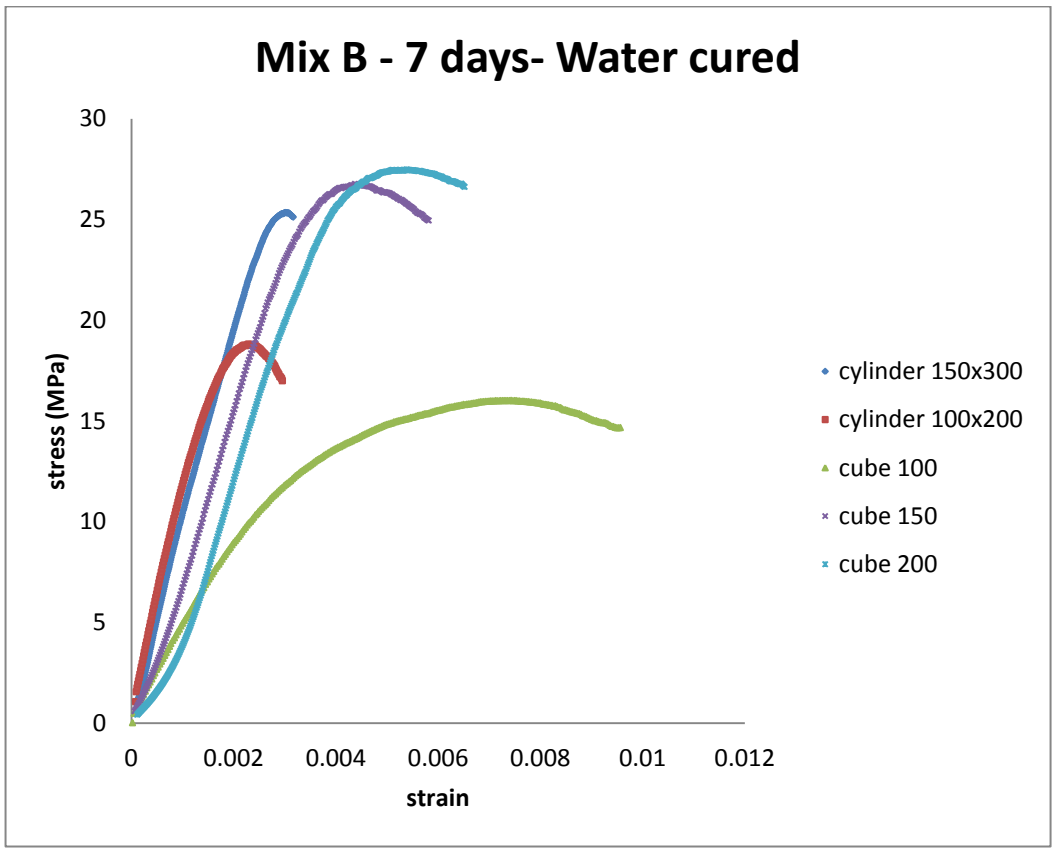
Mix B - 7 days- Water cured
stress (MPa)
30
25
20
15
10
5
0
0
0.002
0.004
0.006
0.008
0.01
0.012
strain
cylinder 150x300
cylinder 100x200
cube 100
cube 150
cube 200

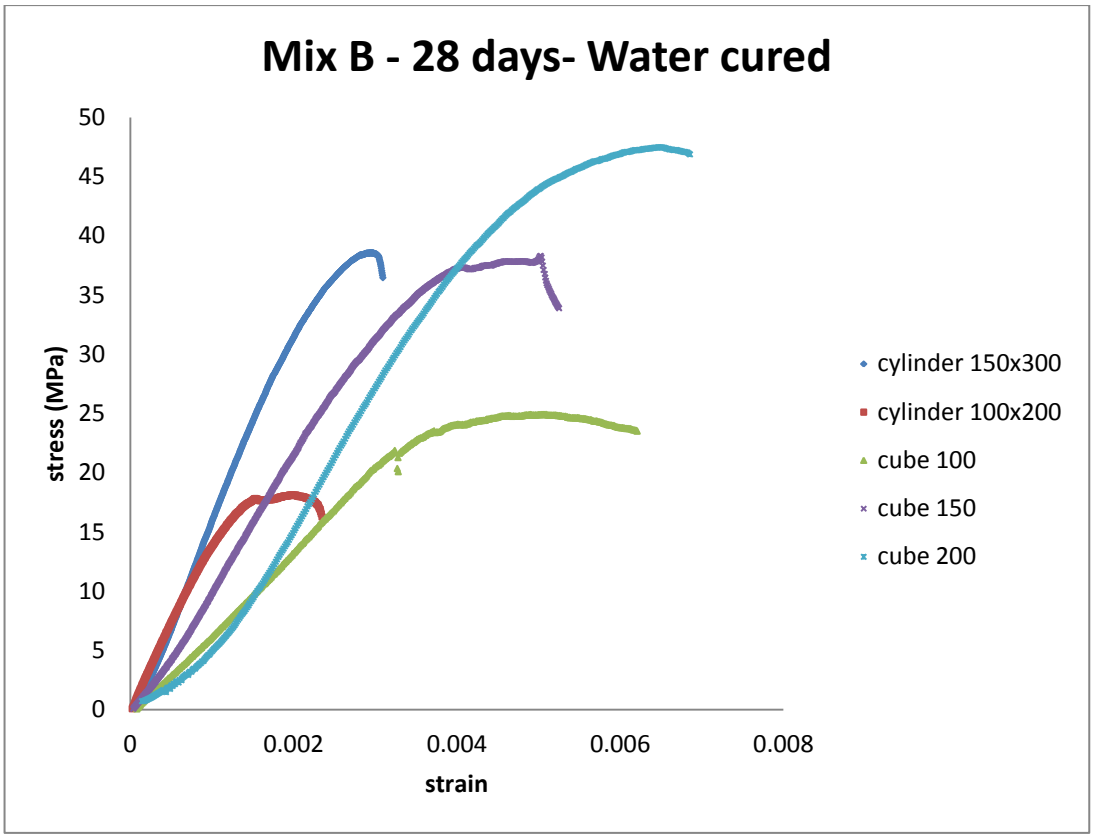
Mix B - 28 days- Water cured
stress (MPa)
50
45
40
35
30
25
20
15
10
5
0
0
0.002
0.004
0.006
0.008
strain
cylinder 150x300
cylinder 100x200
cube 100
cube 150
cube 200

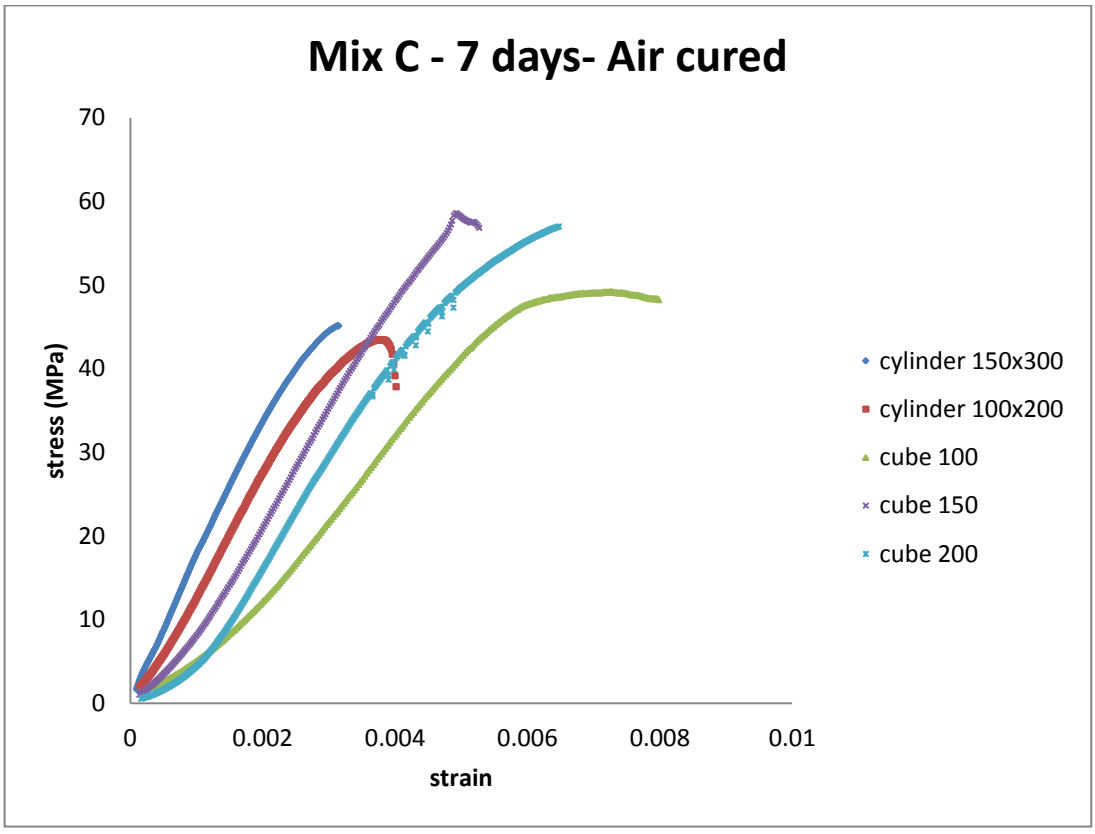
Mix C - 7 days- Air cured
stress (MPa)
70
60
50
40
30
20
10
0
0
0.002
0.004
0.006
0.008
0.01
strain
cylinder 150x300
cylinder 100x200
cube 100
cube 150
cube 200

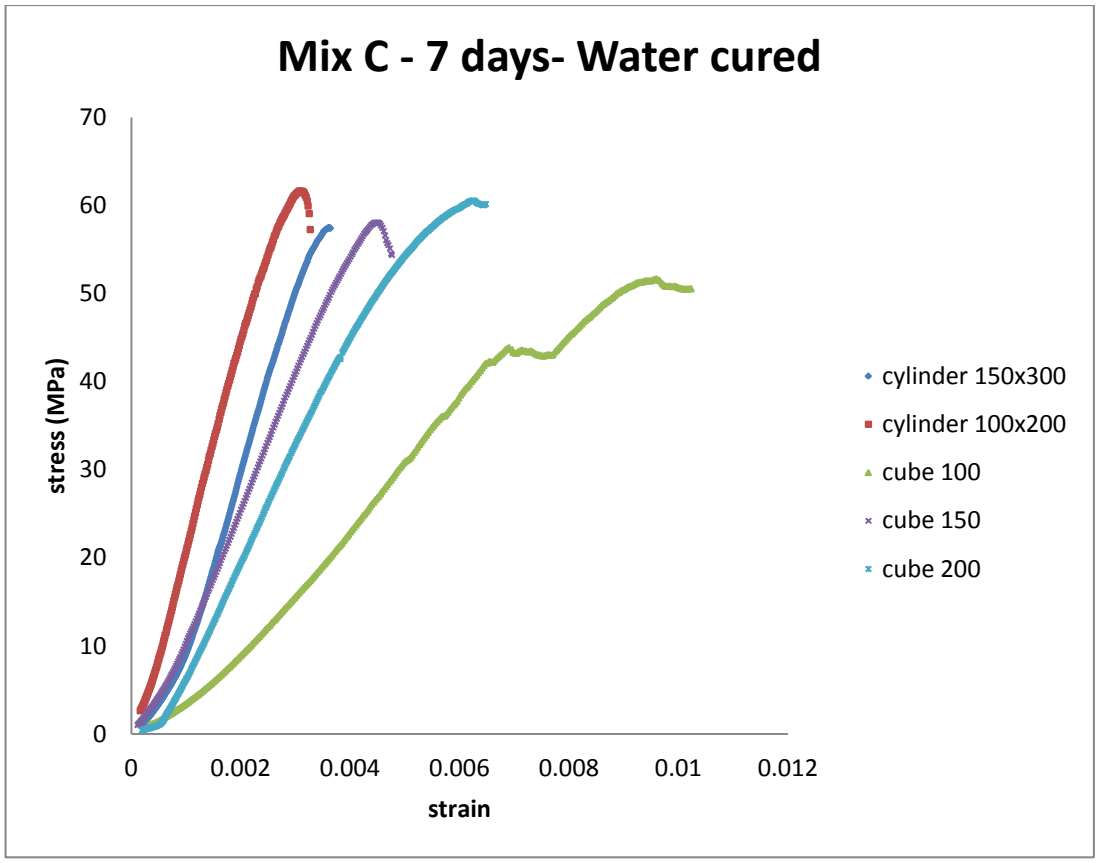
Mix C - 7 days- Water cured
stress (MPa)
70
60
50
40
30
20
10
0
0
0.002
0.004
0.006
0.008
0.01
0.012
strain
cylinder 150x300
cylinder 100x200
cube 100
cube 150
cube 200

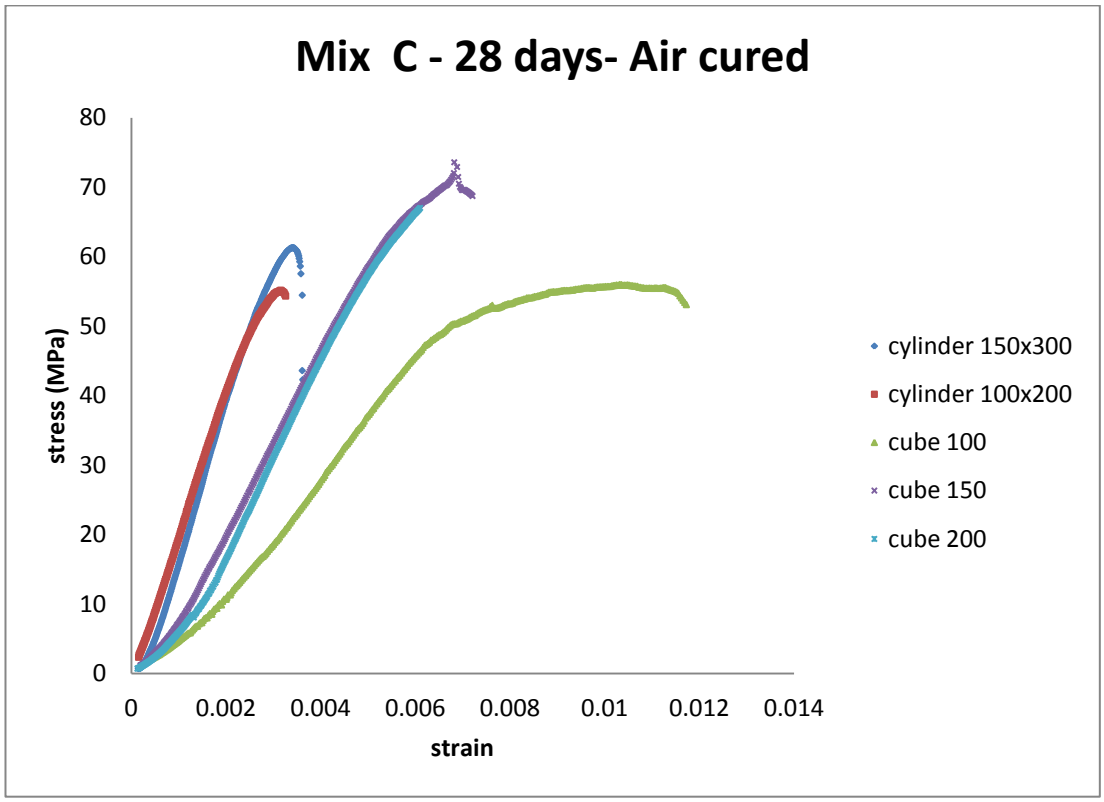
Mix C - 28 days- Air cured
stress (MPa)
80
70
60
50
40
30
20
10
0
0
0.002
0.004
0.006
0.008
0.01
0.012
0.014
strain
cylinder 150x300
cylinder 100x200
cube 100
cube 150
cube 200

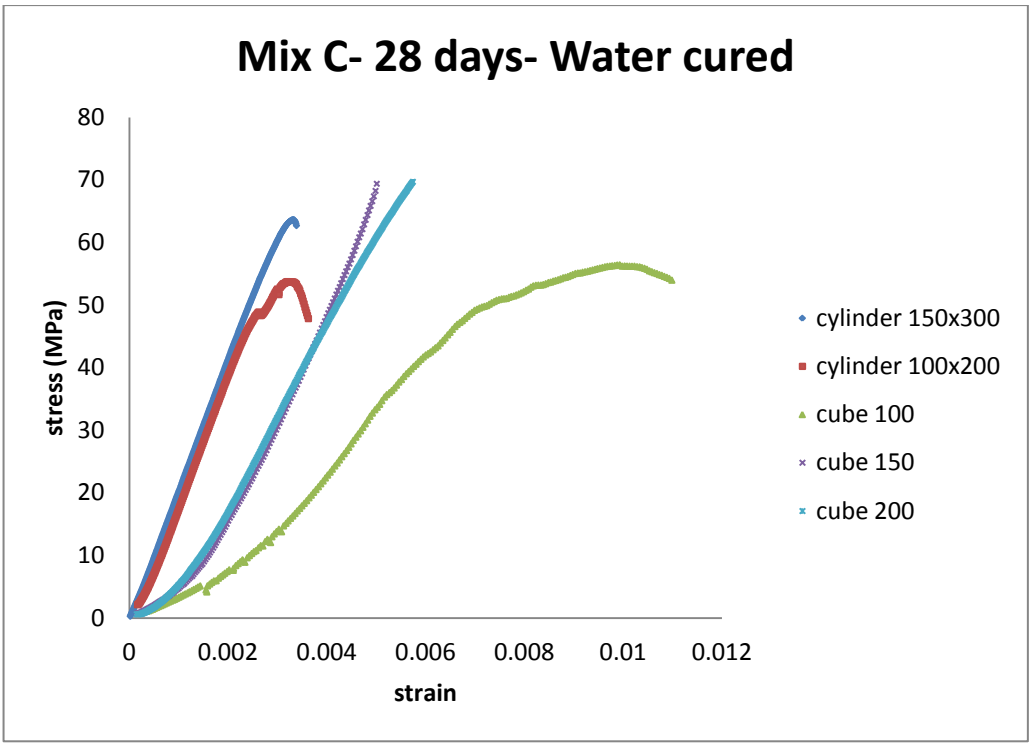
Mix C- 28 days- Water cured
stress (MPa)
80
70
60
50
40
30
20
10
0
0
0.002
0.004
0.006
0.008
0.01
0.012
strain
cylinder 150x300
cylinder 100x200
cube 100
cube 150
cube 200